Analysing Tumor Growth in *Drosophila*: Definig a Role for the Transcription factor Ets21C

Dissertation

zur

Erlangung der naturwissenschaftlichen Doktorwürde

(Dr. sc. nat.)

vorgelegt der

Mathematisch-naturwissenschaftlichen Fakultät

der

Universität Zürich

von

Janine Toggweiler

aus

Mönchaltorf (ZH)

Promotionskomitee

Prof. Dr. Konrad Basler (Leitung und Vorsitz der Dissertation)

Prof. Dr. Ian Frew

Prof. Dr. Stefan Luschnig

Zürich, 2016

Table of Contents

Zusammenfassung

Die Entwicklung von Krebs erfolgt schrittweise und beinhaltet das Zusammenspiel von verschiedenen Mutationen, die der Zelle erlauben Fähigkeiten zu erwerben, die man als Markenzeichen von Krebs bezeichnet: sie produziert ihre eigenen Wachstumsfaktoren, wird unempfindlich gegenüber wachstumshemmenden Signalen, kann dem Zelltod entkommen oder aus ihrem Ursprungsgewebe auswandern. Um herauszufinden, wie Zellen diese Markenzeichen erwerben, müssen *in vivo* Modelle entwickelt werden, welche die Krebsentwicklung widerspiegeln. Die Maus ist unumstritten das beste Modell um diese Frage zu untersuchen, jedoch ist es schwierig und sehr zeit- und arbeitsaufwendig krebsverursachende Gene zu erforschen. Einfachere Tiermodelle, wie *Drosophila*, können hier weiterhelfen und die Entdeckung von neuen, krebs-relevanten Genen beschleunigen.

Wird eine konstant aktive Form des Onkoproteins Ras (Ras^{V12}) im Epithelgewebe von *Drosophila* exprimiert und mit Mutationen im Tumorsuppressorgen *scribbled* (*scrib*) kombiniert, entstehen grosse, metastasierende Tumore, die gewisse Ähnlichkeiten mit menschlichen Krebsformen aufweisen. Vor kurzem wurde herausgefunden, dass diese Tumore von der Aktivität des c-Jun N-terminale Kinase (JNK) Signalwegs abhängen. Dieser aktiviert Matrixmetalloproteinasen (Mmp1) und Zytokine, welche das Krebswachstum begünstigen.

In unserem Labor ist eine veränderte Version dieses Ras^{V12} $scrib^{-/-}$ Modells entwickelt worden, die anstelle von Mutationen eine RNAi gegen *disc-large* (*dlg*) benützt. Mit diesem Modell haben wir 100 Gene mit RNAi getestet und zehn Gene identifiziert, die das Tumorwachstum hemmen, wenn man ihr Genprodukt erschöpft. In der vorliegenden Arbeit haben wir eines dieser Gene funktionell charakterisiert und angefangen ein zweites Kandidatengen zu analysieren. Zusätzlich haben wir getestet, ob der Tumor Nekrosis Faktor (TNF) Rezeptor Wengen (Wgn) das Wachstum von Ras^{V12} dlg^{RNAi} Tumoren beinflusst.

Der Hauptteil dieses Projektes befasst sich mit der Rolle des Transkriptionsfaktors Ets21C im Tumorwachstum. ETS Proteine sind eine grosse Familie von Transkriptionsfaktoren, die auch für gewisse menschliche Krebsformen wichtig sind. Wir zeigen, dass Ets21C sowohl für das

Krebswachstum benötigt wird, als auch ausreicht, um das Wachstum zu verstärken. Die Expression von Ets21C ist in neoplastischen Tumoren erhöht, was auf die Aktivität des JNK Signalwegs zurückzuführen ist. Ausserdem haben wir herausgefunden, dass Zielgene des JNK Signalwegs wie *Mmp1*, *Pvf1* oder *upd1* durch Ets21C induziert werden, möglicherweise durch Kooperation mit dem JNK Transkriptionsfaktor AP-1. Besonders hervorzuheben ist hier, dass die Aktivierung der Zielgene von der PNT und ETS Domaine von Ets21C abhängt. Vorläufige Daten deuten auch darauf hin, dass Ets21C in der regulatorischen Region von *Mmp1* bindet, was eine Rolle von Ets21C als nukleärer Effektor des JNK Signalwegs bestätigen würde.

Astrocytic leucin-rich repeat module (*alrm*) ist das zweite Kandidatengen, das wir angefangen haben zu charakterisieren. RNAi gegen *alrm* reduziert das Krebswachstum, beeinträchtigt jedoch normales Gewebe nicht. Um diese Erkenntnis zu bestätigen, haben wir ein mutantes Allel und unabhängige RNAi Linien von *alrm* hergestellt. Zusätzlich, haben wir einen Zusammenhang zwischen Alrm und der Aktivität des JNK Signalwegs gefunden.

Der letzte Teil dieser Arbeit beschreibt die Identifizierung von Grindelwald (Grnd), einem neuen *Drosophila* Tumor Nekrosis Faktor (TNF) Rezeptor. Wir haben zu dieser Studie einige Experimente beigesteuert und zeigen, dass die Aktivierung des JNK Signalwegs in neoplastischen Ras^{V12} dlg^{RNAi} Tumoren ausschliesslich von Grnd und nicht von Wengen (Wgn) abhängt. Wgn wurde ursprünglich als *Drosophila* TNF Rezeptor beschrieben, diese Daten konnten jedoch nie bestätigt werden.

Unsere Resultate haben neue Komponenten identifiziert, die wichtig für das Wachstum von neoplastischen Tumoren sind und tragen mechanistische Erkenntnisse zur Funktion des JNK Signalwegs bei.

Summary

The development of cancer is a multistep process, involving the cooperation of mutations that allow cells to acquire capabilities that are considered hallmarks of cancer, such as self-sufficiency in growth signals, insensitivity to anti-growth signals, evasion of apoptosis, limitless replicative potential, sustained angiogenesis, and tissue invasion and metastasis (Hanahan & Weinberg, 2000, 2011). To elucidate the steps involved in acquiring these hallmarks, in *vivo* models need to be developed that recapitulate tumorigenesis. Although the optimal model system is currently the mouse, simpler animal model systems, such as *Drosophila*, that mimic some of the characteristics of mammalian tumorigenesis provide a means to more rapidly uncover novel cancer-relevant genes in an *in vivo* setting (Brumby & Richardson, 2005).
In epithelial tissues in *Drosophila*, cooperation between the oncogenic protein Ras^{V12} and loss-of-function mutations in the conserved tumor suppressor gene *scribbled* (*scrib*) gives rise to metastatic tumors that display many of the characteristics observed in human cancers (Pagliarini, 2003; Brumby & Richardson, 2003). More recently it was found that the interaction between Ras^{V12} $scrib^{-/-}$ clones involves JNK signaling propagation and upregulation of Mmp1 and JAK/STAT-activating cytokines (Igaki *et al*, 2006; Wu *et al*, 2010).

Our laboratory has established a modified version of the Ras^{V12} $scrib^{-/-}$ model that used an RNAi that targets *dlg* (Willecke *et al*, 2011). Using this model we have screened 100 genes with RNAi and identified ten genes that suppressed tumor growth upon depletion of the gene product (Master Thesis J. Toggweiler). In the study presented here, we have functionally characterized one of these candidates and started to evaluate a second suppressor. In addition, we tested a role of the tumor necrosis factor (TNF) receptor Wengen (Wgn) in Ras^{V12} dlg^{RNAi} tumors.

The major part of this thesis describes the role of the transcription factor Ets21C in neoplastic growth. ETS proteins are a large family of transcription factors that are relevant for certain types of human cancers (Kar & Gutierrez-Hartmann, 2013). We show that Ets21C is necessary for neoplastic growth and sufficient to enhance tumor growth. Ets21C is upregulated in

neoplastic tumors as a consequence of JNK signaling activity. Furthermore, we find that downstream targets of the JNK pathway such as *Mmp1*, *Pvf1* or *upd1* are induced by Ets21C possibly via cooperation with the JNK transcription factor AP-1. Importantly, target gene induction depends on the PNT and ETS domain of Ets21C. Preliminary data also suggest binding of Ets21C in the Mmp1 regulatory region, which would further support a function for Ets21C as nuclear effector of the JNK pathway.

The second candidate that we started to evaluate is Astrocytic leucin-rich repeat module (Alrm). An RNAi targeting *alrm* reduced growth of Ras^{V12} dlg^{RNAi} tumors, but did not affect wild-type tissue. To confirm this finding, we have generated a mutant allele and independent RNAi lines of *alrm*. In addition, we assessed a role for Alrm in regulating the activity of the JNK pathway by monitoring *Mmp1* and *Ets21C* expression.

The third part of this thesis is a manuscript that has identified Grindelwald (Grnd), a new *Drosophila* tumor necrosis factor (TNF) receptor. We have contributed experiments to this study showing that neoplastic Ras^{V12} dlg^{RNAi} tumors depend on Grnd to activate the JNK pathway, but not on Wgn. Wgn was initially reported to be the *Drosophila* TNF receptor.

Our results uncovered novel players in regulating neoplastic tumor growth and added important mechanistic insights how JNK signaling is transduced and leads to the activation of distinct sets of target genes.

1 Introduction

1.1 Studying tumor growth in *Drosophila*

Tumor progression is a multistep process, which is caused by the accumulation of genetic alterations over time. Such mutations commonly perturb the signaling pathways that are responsible for the regulation of proliferation, cell death or tissue homeostasis. Based on this, six hallmarks have been proposed that are associated with malignant transformation: Self-sufficiency in growth, insensitivity to anti-growth signals, evasion of apoptosis, metastasis and invasion, sustained angiogenesis and limitless replicative potential (Hanahan & Weinberg, 2000). *Drosophila* has made seminal contributions to the understanding of certain aspects of tumorigenesis by helping reveal the function of oncogenes and tumor suppressor genes during normal development. For example, many components of the recently identified Salvador/Warts/Hippo (SWH) pathway have initially been found through genetic screens in flies. Inactivation of *warts (wts)* or *hippo (hpo)* causes hyperplastic growth of imaginal discs and adult organs, highlighting an crucial tumor suppressive role of this pathway (Udan *et al*, 2003; Justice *et al*, 1995). Orthologs of many other components have later also been identified in mammals and investigations in cell lines or mouse models point towards a similar role of the analogous human pathway in tumorigenesis (Harvey *et al*, 2013).

Cancer is an age-dependent disease and multiple hits are necessary to transform a healthy cell into a malignant derivative. Due its short lifespan *Drosophila* only rarely develops natural tumors and is not useful to study *de novo* tumorigenesis (Salomon & Jackson, 2008). However, the large collection of available genetic tools in flies provides an excellent resource to generate and investigate neoplastic tumors via defined genetic mutations. Binary expression systems such as the Gal4/UAS or LexA/LexO allow spatial and temporal control of gene expression; mitotic recombination enables the generation of genetic mosaics consisting of wild-type and mutant cell populations next to each other (Lee & Luo, 1999; Lai & Lee, 2006; Brand & Perrimon, 1993). Such a situation is reminiscent of the early development of tumors where a single cell acquires a mutation and has to survive within the remaining wild-type cells. A number of tumor models have therefore been established – in larval stages as well as in adult

organs – that rely on defined genetic modifications, which activate or shut-down specific signaling pathways that have been associated with cancer. These models have been used to either screen for new pathway components involved in tumor formation or for new chemical inhibitors that can block a specific form of tumors. Recently, *Drosophila* has also been utilized in whole animal screens to test small molecule inhibitors for efficacy and toxicity (Gladstone *et al*, 2012; Willoughby *et al*, 2012). Although the mouse is undeniably the optimal model for studying tumorigenesis, *Drosophila* provides a more rapid means for identifying *in vivo* relevant pathway components and pre-screening of drugs to sort out toxic compounds could help close the gap between cell culture and mouse models.
The following sections describe current *Drosophila* tumor models with a focus on imaginal disc based models, as those are most relevant for this thesis.

1.1.1 Imaginal disc based models

Imaginal discs are the primordia for the adult organs such as the wing, eye or leg and consist of epithelial cells arranged in a 2D sheet-like structure. Tumorous growth of imaginal discs can be classified into hyperplastic or neoplastic (Gateff, 1994). Hyperplastic growth occurs if epithelial cells expand beyond their normal limitations, but still retain apical-basal organization and the ability to differentiate. Overexpression of oncogenic Ras^{V12} or loss of *wts* or *phosphatase and tensine homolog* (*Pten*) produces a hyperplastic epithelium (Pagliarini, 2003; Justice *et al*, 1995; Goberdhan *et al*, 1999). Neoplastic growth denotes excessive proliferation of epithelial cells that have lost polarity and breach basement membranes. These cells grow into multi-layered tumors and are not able to differentiate. Neoplastic growth is achieved by a loss of a so called neoplastic tumor suppressor genes. The earliest tumor suppressor gene identified in flies was *lethal giant larvae* (*lgl*). Later it was found to regulate apico-basal polarity together with *scribbled* (*scrib*) and *discs-large* (*dlg*) (Gateff, 1978; Bilder, 2000). Homozygous mutant *lgl* larvae display overgrown imaginal discs and do not enter metamorphosis, but instead grow into giant larvae (Gateff, 1978). Other neoplastic tumor suppressor genes besides the polarity genes *scrib*, *dlg* or *lgl*, are required for endocytosis like *avalanche (avl)*, *Rab5* or *Vacuolar protein sorting 25* (*Vps25*) (Woods & Bryant, 1991; Bilder & Perrimon, 2000; Thompson *et al*, 2005; Gateff, 1978; Lu & Bilder, 2005).

1.1.1.1 Eye discs – cooperation of *Ras^{V12}* and *scrib$^{-/-}$*

The *Drosophila* eye imaginal disc and adult eye are an excellent tissue to carry out genetic screens aiming at investigating gene function. They have also been used to study tumor growth. Work of two groups has been seminal in this regard. Both describe the generation of tumor cells in otherwise wild-type tissue to study the cooperation between oncogenes and tumor suppressor genes and to identify additional components that modify tumor development (Brumby and Richardson, 2003; Pagliarini and Xu, 2003).

Pagliarini and Xu generated non-invasive tumors by inducing clones of cells that express an active form of the *Drosophila* Ras homolog (Ras85D^{G12V}), further referred to as *Ras^{V12}*. This leads to constitutive active Ras signaling, which results in overgrowth and benign tumors. As a next step they were interested whether additional genetic alterations were able to transform the non-invasive tumor cells into metastatic derivatives. Mutations in the neoplastic tumor suppressor gene *scrib* and concomitant activation of *Ras^{V12}* resulted in large primary tumors and groups of cells located at distant sites, mainly in the ventral nerve cord (VNC) and in the brain lobes, which suggested that the tumor cells had acquired the ability to metastasize. Furthermore, *Ras^{V12} scrib$^{-/-}$* tumors displayed lower expression levels of E-cadherin (E-cad) and showed a degradation of the basement membrane. Both are characteristics of metastatic mammalian tumors (Egeblad and Werb, 2002; Perl et al., 1998). Combining *scrib* mutant cells with other growth-promoting genes, such as *dMyc* or *dAkt*, lead to overgrowth, but no invasive capabilities. Thus, the metastasis-promoting effect of mutant *scrib* seems to specifically depend on its cooperation with *Ras^{V12}*.

Brumby and Richardson obtained similar results by generating *scrib$^{-/-}$* clones in eye imaginal discs and testing if secondary oncogenic mutations could rescue *scrib$^{-/-}$* cells from apoptosis by ectopically activating the major growth and pattering pathways, such as Wingless (Wg), epidermal growth factor receptor (EGFR) or Decapentaplegic (Dpp). *Scrib$^{-/-}$* cells are usually not tolerated by the neighbouring wild-type cells and eliminated by c-Jun N-terminal kinase (JNK) mediated cell death, ensuring tissue integrity and preventing uncontrolled growth. The strongest cooperation with *scrib$^{-/-}$* was seen with constitutive active forms of Ras or Notch: *Ras^{V12} scrib$^{-/-}$* or *Notch^{ACT} scrib$^{-/-}$* cells hyperproliferated, failed to differentiate, grew in three dimensions and fused with adjacent tissue (Brumby & Richardson, 2003)

The cooperative nature of *Ras^{V12}* and *scrib* mutations has subsequently been studied by many groups and produced valuable insights into the complex interplay of the two signaling pathways. *Ras^{V12} scrib$^{-/-}$* tumors express matrix metalloproteinase 1 (Mmp1) required for degrading extracellular matrix proteins, thus endowing tumor cells with invasive capabilities (Uhlirova & Bohmann, 2006). Mmp1 expression is regulated by the JNK pathway, the latter is activated as a consequence of loss of polarity (Uhlirova & Bohmann, 2006; Igaki *et al*, 2006) (Fig.1). Furthermore, JNK activity is responsible for the cell autonomous induction of Unpaired (Upd) cytokines, Upd1, Upd2 and Upd3, that substantially contribute to tumor growth by activating the JAK/STAT pathway (Wu *et al*, 2010). More recently, JNK signaling has also been proposed to regulate Pvf1 expression, thereby regulating the proliferation of hemocytes, the immune cells of *Drosophila* that are recruited to tumors (Parisi *et al*, 2014; Pastor-Pareja *et al*, 2008; Cordero *et al*, 2010). The flies innate immune system is thought to act as crucial anti-tumor defense; increased numbers of hemocytes restrict growth of *scrib$^{-/-}$* or *dlg$^{-/-}$* tumors by producing the Toll ligand Spätzle (Spz) and Eiger (Egr) proteins that induce an innate immune response in the larval fat body or cause cell death of tumor cell, respectively (Parisi *et al*, 2014) (Fig. 1, A). This shows important parallels to the human innate and adaptive immune responses that act as a first-line defense against emerging tumor cells (Swann & Smyth, 2007).

Recent efforts in our laboaratory have led to the establishment of a tumor model that is based on *Ras^{V12}* and an RNAi targeting *dlg*. This model gives rise to similar phenotypes as the *Ras^{V12} scrib$^{-/-}$* model, but facilitated screening of additional RNAi or overexpression lines in only one generation. Utilizing this system, we have uncovered that tumor cells are sensitive to reductions in PI3K pathway activity while normal cells are not (Willecke *et al*, 2011). The same model also led to the identification of the transcription factor Ets21C as a critical regulator of tumor growth, possibly by cooperating with the AP-1 transcription factor (this thesis, Toggweiler et al., in prep.) (Fig. 1, A). Ets21C has also been proposed to mediate oncogenic growth and invasion by Kühlshammer et al. along with the nuclear receptor Ftz transcription factor 1 (Ftz-F1) that could mediate Hippo signaling (Kulshammer *et al*, 2015). The involvement of the Hippo pathway in regulating *scrib$^{-/-}$* and *Ras^{V12} scrib$^{-/-}$* tumor growth has been demonstrated by several groups, but the how has been under debate. Sun and Irvine proposed that JNK signaling inhibits *wts*, leading to enhanced growth by elevating Yki activity whereas

Doggett et al. propose that loss of polarity impairs Hippo signaling via JNK independent mechanisms (Sun & Irvine, 2011; Doggett *et al*, 2011). Yet another publication reported that in *scrib*$^{-/-}$ cells *wts* is activated by JNK signaling and restricts tumor growth while in the presence of *Ras*^{V12}, JNK signaling enhances the activity of the Hippo effector Yorkie (Yki) by promoting the accumulation of filamentous actin (F-actin) (Enomoto *et al*, 2015). Clearly, changes in actin cytoskeletal dynamics regulate normal organ growth and tumor growth: Enhanced F-actin affects organ growth by upregulating Yki activity and loss of the actin cross-linker Cheerio (Cher) interferes with *Ras*^{V12} *scrib*$^{-/-}$ tumor growth (Fernández *et al*, 2011; Kulshammer & Uhlirova, 2013; Sansores-Garcia *et al*, 2011). Similar results have been subsequently obtained in mammalian cells, highlighting the power of *Drosophila* models to uncover mechanisms relevant to human tumors (Wada *et al*, 2011). Panel A in Figure 1 provides a simplified overview of the pathways and components that are active in *Ras*^{V12} *scrib*$^{-/-}$ cells.

Although used extensively for genetic screens, *Ras*^{V12} *scrib*$^{-/-}$ tumor models have only rarely been used for screening therapeutic compounds. In a pilot screen of 2000 compounds Willoughby et al. have identified the glutamine analogue acivicin as a potent inhibitor of tumor growth in *Drosophila* (Willoughby *et al*, 2012). Chemical screens have also provided valuable results in a *Drosophila* model of multiple endocrine neoplasia type 2 (MEN2), which is a hereditary form of thyroid cancer. Ret, the underlying tyrosine kinase that is active in MEN2 was targeted to the *Drosophila* eye, resulting in a "rough eye" phenotype due to enhanced proliferation and defects in differentiation. Signaling through the Ret kinase activates a broad spectra of pathways including Ras, Src, JNK and Hedgehog (Read et al., 2005) (Fig. 1, B). To test its usefulness for screening compound libraries, a small set of known therapeutics has been tested. Vandetanib (ZD6474) was validated as being efficient in blocking Ret dependent tumorigenesis (Vidal, 2005). Based on these results, the MEN2 model has been improved for drug screening and a whole library of polypharmacological compounds has been tested for efficacy and toxicity. AD57, one of the most promising candidates, has further been characterized and based on these results analogs have been developed that only block the kinases relevant for the MEN2 phenotype but spared mTor whose inhibition was associated with severe toxicity (Dar *et al*, 2012). Panel B of Figure 1 summarizes the pathways that are activated upon *Ret*^{MEN2} expression.

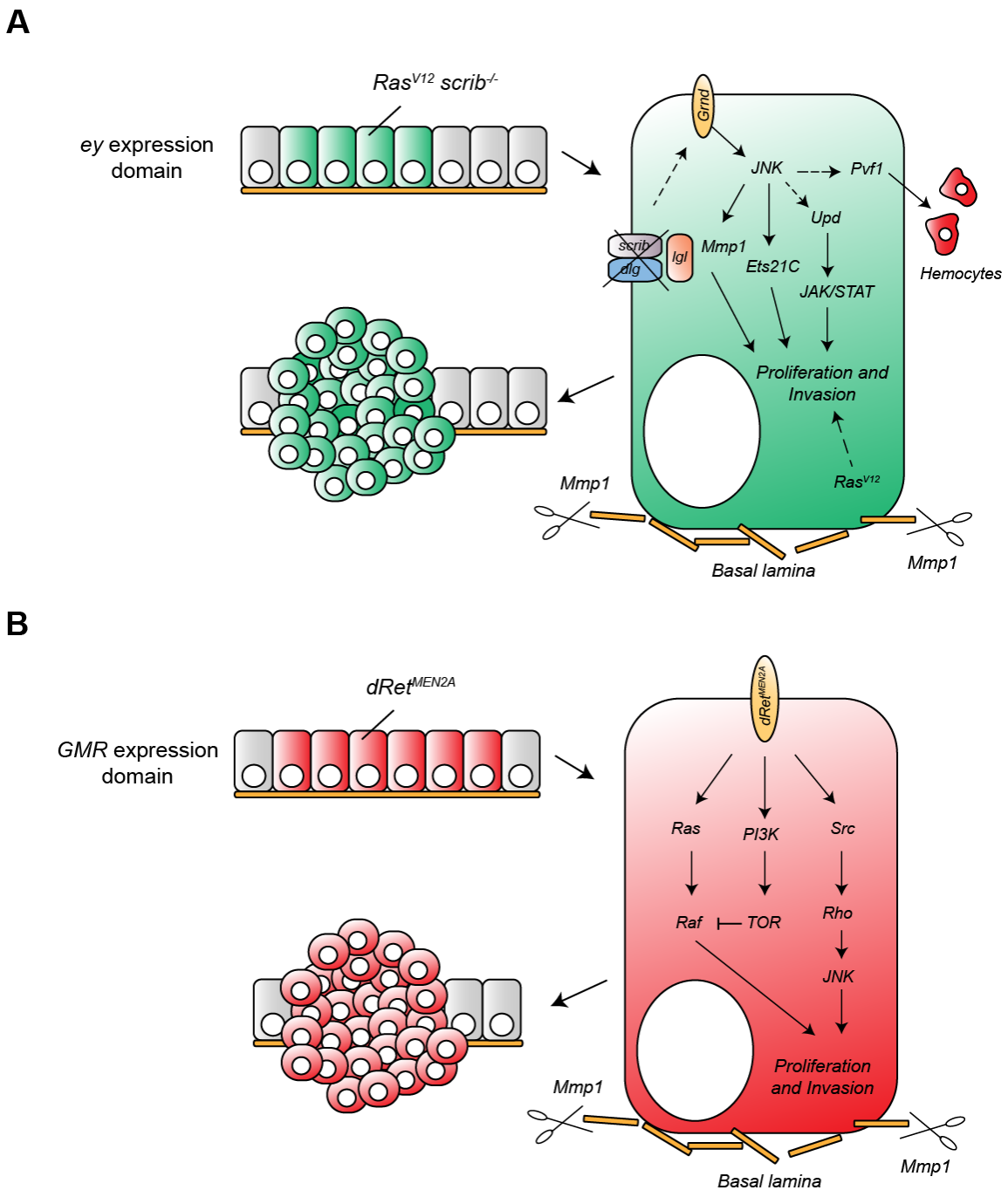

Figure 1: Schematic depiction of *Drosophila* eye disc based tumor models. (A) *Ras*^{V12} *scrib*$^{-/-}$ model: loss of *scrib* causes loss of polarity and activates the JNK pathway via the TNF receptor Grnd. JNK activity leads to the induction of downstream effectors such as Mmp1, Ets21C, Upd1 and Pvf1 that collectively contribute to tumorigenesis and invasion. (B) *Ret*^{MEN2} model: targeted expression of Ret in the GMR domain of eye imaginal disc activates several downstream signaling modules such as Ras, PI3K and Src that stimulate proliferation and invasive behavior.

1.1.1.2 Wing discs

Not only the *Drosophila* eye, but also the wing has been studied in great detail and yielded many pivotal findings on organ growth and patterning during development (Neto-Silva *et al*, 2009). It is therefore not surprising that the wing disc has been exploited to analyze tumor growth. The syntaxin Avalanche (Avl) functions in the early endocytic machinery and a loss of *avl* gives rise to neoplastic tumors due to an expansion of the apical domain, which leads to a disorganization of cell polarity (Lu & Bilder, 2005) (Fig. 2). This phenotype has been utilized by the Léopold group for a genome-wide RNAi screen for modifiers of neoplastic growth. Targeting an avl^{RNAi} to the developing wing induces a developmental delay of 2-3 days as a consequence of neoplastic tumor formation. An RNAi targeting the *Dilp8* gene, which encodes an insulin-like peptide, rescued the developmental delay, but not neoplastic growth. Further investigations revealed a key function for Dilp8 in coordinating growth with developmental timing, demonstrating that *Drosophila* tumor models are not only useful in deciphering mechanisms of tumor growth, but also yield other unexpected findings about fundamental biological processes (Colombani *et al*, 2012) (Fig. 2). Dilp8 was identified independently in yet another *Drosophila* tumor model. Concomitant activation of the Notch ligand Delta together with two neighboring epigenetic repressors *pipsqueak* (*psq*) and *longitudinals lacking* (*lola*) in eye discs leads to massive overgrowth and metastasis (Ferres-Marco *et al*, 2006). Microarrays revealed a strong enrichment of Dilp8 in tumors and subsequent analyses reached similar conclusions as the Léopold group (Garelli *et al*, 2012).

The genome-wide screen of the Léopold laboratory has revealed an additional interesting candidate gene, *grindelwald* (*grnd*) (Fig. 2). Loss of function of *grnd* rescued both, the developmental delay as well as neoplastic growth of avl^{RNAi} tumors. Grnd is a transmembrane protein, harboring a cysteine-rich domain (CRD) that is homologous to the vertebrate TNFRs. Grnd was therefore suspected to mediate TNF signaling in *Drosophila*. Indeed, $grnd^{RNAi}$ suppressed the small eye phenotype caused by targeted expression of the *Drosophila* TNF alpha homolog Egr to the *Drosophila* eye and was found to associate with TRAF2, the most upstream component of the JNK pathway. Furthermore, Ras^{V12} $scrib^{-/-}$ tumors were found to critically depend on Grnd function. In this context, Grnd seems to be activated independently of Egr, but through interaction with an apical polarity complex consisting of Crumbs (Crb),

Stardust (Std) and Patj, providing for the first time a link between defects in polarity and the activation of the JNK pathway (Andersen *et al*, 2015) (Fig. 2).

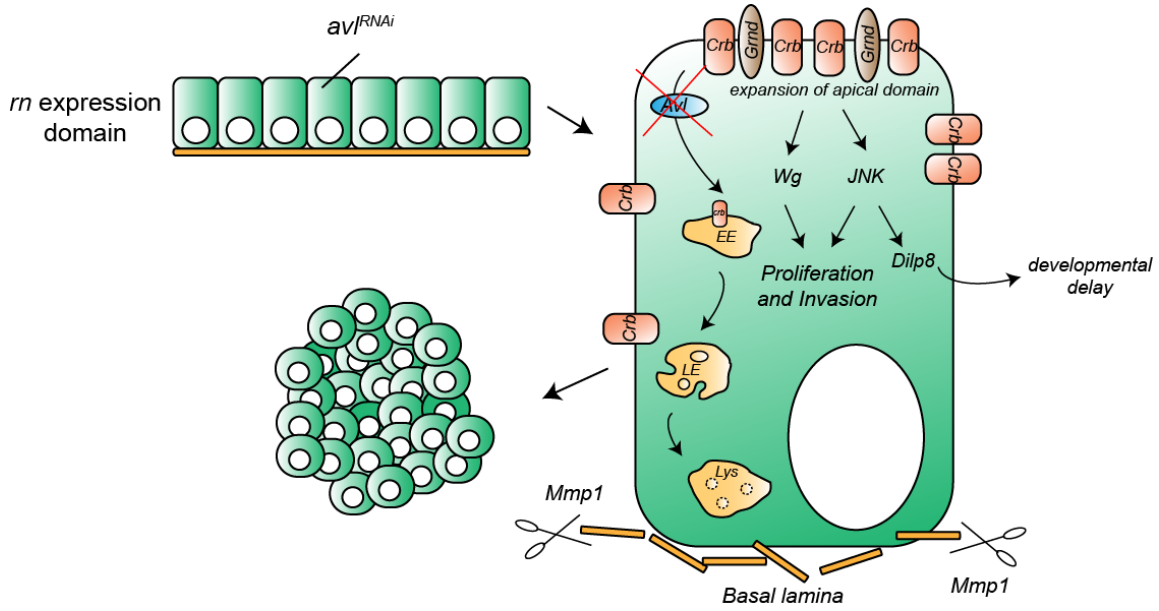

Figure 2: Schematic depiction of a *Drosophila* wing disc based model: Depletion of the syntaxin Avl in the rotund (rn) expression domain results in an expansion of the apical domain most likely due to defective endosomal degradation of apical determinants such as Crumbs (Crb). As a consequence, Wingless (Wg) and JNK signaling are activated and lead to overgrowth and invasion through degradation of the basement membrane. The activation of the JNK pathway also provokes a developmental delay by inducing the expression of the insulin-like peptide Dilp8. EE: early endosome, LE: late endosome, Lys: lysosome.

1.1.2 Details of our tumor model

Pagliarini and Xu, and Brumby and Richardson used the MARCM system to generate *Ras^{V12} scrib$^{-/-}$* tumors (Lee and Luo, 1999). To analyse the effect of additional genes on growth of *Ras^{V12} scrib$^{-/-}$* tumors with this system, two generations of fly crosses are necessary, which is not well suited for a large screen. As mentioned above, our laboratory has modified the genetic setup so that all the components needed to generate a neoplastic phenotype are present in one fly strain (Willecke *et al*, 2011). Additional transgenes such as RNAi lines or cDNA`s can easily be crossed to this tester stock and be analysed in one generation. The tester stock overexpressed *Ras^{V12}* and a dsRNA construct targeting *dlg*. To specifically create tumors in the eye discs, we expressed a Flp recombinase driven by the *eyeless* (*ey*) promoter, which flipped out a stop cassette between two FRT sites. This led to the expression of Gal4 driven by the *actin5c* (*act*) promoter. Gal4 drives *UAS-Ras^{V12}*, *UAS-dlg^{RNAi}* and *UAS-GFP* which was used to visualize the tumor tissue (Fig. 3, A). We used *UAS-dlg^{RNAi}* because there was no suitable RNAi line available for *scrib*. As reported for the original tumor models, the tumor-carrying larvae showed a developmental delay and were often not able to pupariate, but continued to grow for up to 10 days after egg laying (AEL) and died as giant larva (Brumby and Richardson, 2003; Pagliarini and Xu, 2003). Animals that managed to pupariate died as pupae and never reached adulthood. In order to maintain the tester stock, Gal4 had to be prevented from activating *Ras^{V12}* and *dlg^{RNAi}*. The stock therefore has been balanced with a chromosome that carries Gal80, the transcriptional repressor of Gal4, under the control of the *tubulin* (*tub*) promoter.

1.2 The ETS family of transcription factors

The main part of this thesis describes the characterization of the *Drosophila* ETS protein, Ets21C. The following sections will therefore provide a general overview on the ETS transcription factor family, describe the family members in *Drosophila* and discuss what was known about their relevance in cancer.

1.2.1 Structure and function of human ETS proteins

The ETS family is a family of transcription factors unique to Metazoans. ETS stands for "E-twenty-six", since the founding member of the family, *Ets-1*, was identified as an oncogene (*v-Ets*) transduced by the avian eurythroblastosis virus E26 (Leprince *et al*, 1983; Nunn *et al*, 1983). The ETS family is represented with 27 members in humans, with 26 in the mouse, with ten in *Caenorabtitis elegans (C.elegans)* and with nine in *Drosophila* (Kar & Gutierrez-Hartmann, 2013). ETS proteins function as the nuclear effectors of multiple signaling pathways, thereby regulating a variety of processes. The activity of many ETS proteins is regulated by post-translational modifications including phosphorylation, acetylation and sumoylation. The most prominent modification is phosphorylation by mitogen activated protein kinases (MAPKs); these can either control the downstream activity, subcellular localization or protein partners of ETS factors (Yordy & Muise-Helmericks, 2000).

1.2.1.1 The ETS domain

The DNA binding domain, called the ETS-domain, is the common characteristic shared by all proteins that belong to this family of transcription factors. The ETS-domain is a variant of the winged helix-turn-helix-structure with three alpha-helices and four anti-parallel beta-sheets and binds to a core 5' - GGA(A/T) - 3' DNA sequence (Hollenhorst *et al*, 2011). Despite binding to similar sequences on the DNA, ETS proteins are involved in many different biological processes including regulation of cell proliferation, inhibition of apoptosis, promotion of differentiation, regulation of neuronal functions, cell migration and angiogenesis and they therefore regulate a corresponding number of target genes. Binding specificity and diversity are

likely achieved by collaborating with other transcription factors and/or co-regulatory proteins, or by restricted expression to a certain tissue (Hollenhorst *et al*, 2011). There is some redundancy in function as assessed by genetic knockouts and genome-wide studies on promoter occupancy (Zhang *et al*, 2009; Hollenhorst *et al*, 2007). In addition, many ETS proteins are expressed ubiquitously in several cell types. In some cases, up to 25 family members can be co-expressed in the same cell type (Hollenhorst *et al*, 2004; Galang *et al*, 2004).

The ETS-domain proteins are classified in 11 families (ETS, ERG, ELG, ELF, ESE, ERF, ETV, PEA3, SPI, TCF and PDEF) based on sequence similarity and the presence of further functional domains (Fig. 3) (Kar & Gutierrez-Hartmann, 2013). The majority of ETS proteins act as activators, only members of the ERF and ETV subfamilies repress transcription. A few other members, such as ELK-1 and NET, can do both, depending on the specific context and the interaction with other proteins (Sharrocks, 2001). NET, for example, switches from a repressive to an activator function upon activation by Ras (Maira *et al*, 1996).

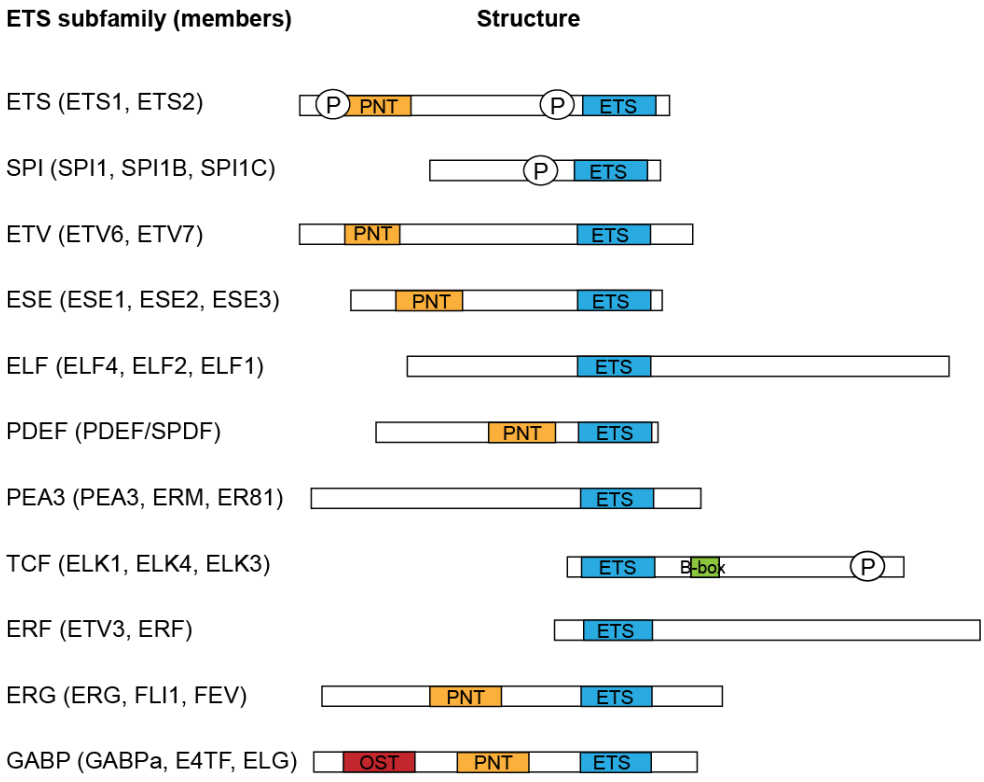

Figure 3: Schematic structures of the human ETS subfamilies**.** Blue: the characteristic ETS DNA binding domain shared by all members. Orange: Pointed (PNT) domain found in about one-third of ETS factors. Green: B-box of the TCF family. Red: OST domain of the GABP family. P: known phosphorylation sites (adapted from Hollenhorst et al., 2011 and Kar & Gutierrez-Hartmann, 2013).

1.2.1.2 The PNT domain

In about one-third of ETS proteins (ETS, ETV, ERG families plus GABPα and SPDEF) a second functional domain is present, termed the Pointed (PNT) domain according to the name of the *Drosophila* ETS protein, in which it was first identified (Klämbt, 1993). The PNT domain is approximately 80 residues long and has a similar organization as the sterile alpha motif (SAM) domain that is known to engage in protein-protein or protein-RNA interactions (Qiao & Bowie, 2005). PNT domains have several functions:

(1) as MAP kinase docking sites: the transcriptional activity of several ETS proteins (for example ETS-1 and ETS-2, as well as the *Drosophila* ortholog Pnt-P2) is regulated by mitogen-activated protein (MAP) kinase phosphorylation (Wasylyk *et al*, 1997). The PNT domain enhances binding of the ETS protein to the kinase thereby facilitating signaling. It is thought that docking of the PNT domain to the kinase enhances substrate specificity and the effectiveness of phosphorylation (Sharrocks *et al*, 2000).

(2) as a platform for interactions with other proteins: PNT domains not only serve as MAP kinase docking sites, but can also mediate the interaction with other proteins. In the case of ETS-2 the PNT domain is responsible for binding to the C-terminal domain of CREB-binding protein (Qiao & Bowie, 2005).

(3) for self association: ETV-6 or its *Drosophila* homolog Aop form helical polymers via their PNT domains (Kim *et al*, 2001; Qiao *et al*, 2004). A dimer presumably facilitates DNA binding, but a longer polymer might also enable the recruitment of other protein partners. Other ETS proteins acquire a dimeric configuration as well, but typically not via the PNT but via their ETS domains (Cooper *et al*, 2014).

1.2.2 The *Drosophila* ETS family

Drosophila melanogaster possesses eight ETS genes: *pnt, anterior open (aop), Ets21C, Ecdyson induced protein 74EF (E74), Ets96B, Ets98B, Ets65A and Ets97D*. *pnt, aop, E74* and *Ets97D* have been characterized based on mutant alleles whereas *Ets98B, Ets65A* and *Ets21C* were cloned and sequenced based on fragments amplified with degenerated primers homologous to a region of the ETS domain of *ETS-1* that is highly conserved (Chen *et al*, 1992; Pribyl *et al*, 1991, 1988; Lai & Rubin, 1992). The final *Drosophila* ETS protein, Ets96B, was identified through a BLAST search using the ETS domain of human ETS-1, PU-1 or SPI-1. With the exception of *pnt* and *aop*, all *Drosophila* ETS genes were named or renamed according to their chromosomal position (Hsu & Schulz, 2000).

Pnt and Aop play important roles in *Drosophila* eye development where they act as nuclear effectors of the Ras/MAP kinase pathway and provide an excellent example of the interplay between active and repressive functions of ETS proteins. In the absence of MAP kinase pathway activity, Aop sits on the DNA by default and represses the expression of genes needed for photoreceptor cell determination. Pnt and Aop are both phosphorylated by the MAP kinase Rolled (Rl) leading to the activation of Pnt and to the export of Aop from the nucleus (Brunner *et al*, 1994; O'Neill *et al*, 1994; Rebay & Rubin, 1995). The interplay between Pnt and Aop is not only important during eye development, but also to pattern the ventral ectoderm, for the migration of tracheal cells, and to activate the TGFβ homolog Decapentaplegic (Dpp) during dorsal closure (Metzger & Krasnow, 1999; Gabay *et al*, 1996; Noselli, 1998).

In addition to *pnt* and *aop*, *E74* and *Ets97D* also have been characterized by mutational studies. *E74* is important during metamorphosis and is spliced into two isoforms; *E74A* and *E74B*. *E74B* mutants are unable to form normal pupae, they die either as early pupae or prepupae. In contrast, many *E74A* mutants survive the period as prepupaes and die before emerging from their cocoon (Fletcher & Thummel, 1995). E74 has also been reported to regulate apoptosis during metamorphosis by activating the apoptosis inducer Hid in the respective tissues (Jiang *et al*, 2000).
Ets97D is required for the correct localization of *oskar* and *gurken* mRNA in the *Drosophila* oocyte and also for the migration of follicle cells. With the continuous enlargement of the

oocyte, the follicle cells migrate posteriorly until they surround the oocyte. This process is crucial to ensure proper development of the embryo. Ets97D has been implicated in these processes as its absence leads to small eggs and abnormal formation of the egg chamber (Schulz *et al*, 1993; Gajewski & Schulz, 1995)

Functions for the remaining *Drosophila* ETS genes have mainly been deduced from expression patterns. *Ets98B* is broadly expressed in embryos, especially in the premigratory primordial germ cells (PGC), but lost in the migratory and postmigratory PGCs. In addition, the gene is expressed in oocyte nuclei and larval tissues (Hsouna *et al*, 2004). Ets21C and Ets65A are both expressed throughout development. Around stage 12 and 14 of embryogenesis, their expression becomes restricted to the nervous system and they have therefore been hypothesized to play a role in the development of the central nervous system (CNS) (Chen *et al*, 1992). In addition, Ets21C has been implicated in regulating defense responses against pathogens, as Ets21C expression is induced upon activation of an immune response and *Ets21C* mutants also exhibit a higher load of bacteria (Boutros *et al*, 2002; Chambers *et al*, 2012; Radyuk *et al*, 2010). For Ets96B neither expression nor experimental data is available that would allow conclusions to be drawn about its function.

Table 1: Overview of *Drosophila* ETS genes (modified from Hsu and Schulz, 2000).

Gene	Chromosomal position	Human homolog	Function
pnt	3R 94E10-94E13	ETS-1	Eye development, oogenesis, tracheal cell migration
aop	2L 22D1	ETV6	Eye development, tracheal cell migration, dorsal closure
E74	3L 74D4-74E2	ELF2	Metamorphosis, wing development? [2]
Ets97D	3R 97D7	GABPα	Oogenesis, wing development? [2]
Ets65A	3L 65A6	FLI-1	CNS development [1]
Ets98B	3R 98B2	PDEF/ESF	Germ cell development[1], wing development? [2]
Ets21C	2L 21E2	ERG	JNK signaling, neoplastic tumor growth
Ets96B	3R 96A22	ER81	Unknown

[1] Deduced from expression patterns (Chen *et al*, 1992). [2] Conclusions based on our own data described in Appendix 4.1.

1.2.3 ETS transcription factors and cancer

Due to their crucial role as effectors of many signaling pathways, particularly the MAP kinase pathways, it is not unexpected that a dysfunction of ETS proteins can contribute to the development of cancer. ETS protein mediated transformation can occur via several mechanisms; here we will only briefly describe the two most common mechanisms: Overexpression of ETS proteins and *ETS* gene fusions.

1.2.3.1 Overexpression of ETS proteins

ETS proteins are overexpressed in several solid cancers including breast, prostate, lung and colon as well as in leukemias. Breast cancers frequently show an upregulation of the ETS proteins, ESE-1, PEA3, ETS-1, ETS-2, ERM or ER81 and this is usually associated with a poor prognosis and metastasis as they regulate the expression of a number of genes that support tumorigenesis such as *MMP* genes, *VEGF, BCL2* or *HER2* (Seth & Watson, 2005; Turner *et al*, 2007). Expression of PEA3 subfamily members (PEA3, ERM, ER81) correlates with HER2 expression in 25-30% of HER2-positive breast cancers. PEA3 expression is controlled by HER2 via MAPK pathway activation and in turn stimulates HER2 expression via a positive feedback loop (Benz *et al*, 1997; Scott *et al*, 1994). Similar to PEA3, overexpression of ETS-1 promotes metastasis and invasiveness of breast cancer by affecting the expression of *urokinase (uPA), MMP1, MMP3* or *vimentin* (Dittmer, 2003).

Advanced stage prostate cancer is another type of solid cancer that is associated with either overexpression of ETS factors such as ETS-1, ETS-2, FLI-1, ERG, ESE-2, ELF-1 or ETV-1, or downregulation of other ETS protein like PEA-3, PDEF or ESE-3 (Alipov *et al*, 2005; Cangemi *et al*, 2008; Gu *et al*, 2007; Rostad *et al*, 2007). It is not well understood why ETS proteins are differentially regulated in this cancer.

Besides solid cancers, ERG is upregulated in acute myeloid leukemia (AML) and associated with a poor prognosis (Baldus *et al*, 2004; Marcucci *et al*, 2005). Until a correlation between ERG and WNT1 expression was recently found, only little was known about downstream targets of ERG that would promote leukemogenesis. ERG and WNT1 are co-expressed in 80% of AML cases analyzed and a knockdown of *ERG* lead to a downregulation of *WNT1* transcripts (Mochmann *et al*, 2011).

1.2.3.2 ETS fusion proteins

Another mechanism of ETS dependent oncogenesis involves ETS gene fusions; this frequently occurs in prostate cancers, Ewing`s sarcoma and leukemias. In prostate cancers, *5` TMPRSS2* can be fused to *ERG*, *ER81* or *PEA3*. The *TMPRSS:ERG* fusion is the most abundant one, found in 50% of prostate cancers. *TMPRSS* is an androgen-responsive gene and the fusion to ETS genes results in androgen-dependent activation of ETS target genes that support cellular transformation and invasive characteristics such as MYC misexpression (Sun *et al*, 2008; Tomlins *et al*, 2008)

Another type of cancer that is often associated with ETS gene translocations are Ewing`s sarcomas. In the majority of cases, 5`*EWS* is fused to the 3` end of *FLI1*, resulting in a much stronger transactivator than FLI1 itself (Riggi & Stamenkovic, 2007). *NROB1/DAX1* is a direct transcriptional target of EWS-FLI1 and an important mediator of oncogenesis as a depletion of DAX1 in *EWS-FLI1* cells lines results in growth arrest (Kinsey *et al*, 2009; García-Aragoncillo *et al*, 2008). The tumor suppressor *FOXO1* is directly repressed by EWS-FLI1, and probably also contributes to tumor formation (Kar & Gutierrez-Hartmann, 2013). Often, pathogenesis of EWS-FLI1 depends on cooperativity with other transcription factors that have binding sites close to those of EWS-FLI (Kim *et al*, 2006).

The third type of cancer that often harbors ETS genes translocations are leukemias. A single ETS gene, *TEL*, is engaged in more than 40 different types of translocations found in hematological cancers. Common fusion partners are *AML1*, or kinases such *PDGFRB*, *TRK*, *ABL* or *JAK2*

(Romana *et al*, 1995; Golub *et al*, 1994, 1996; Papadopoulos *et al*, 1995; Lacronique *et al*, 1997). If the fusion partner is a tyrosine kinase, oligomerization of the PNT domain of TEL causes a constitutive activation of the kinases, which promotes transformation and pathogenesis (Kar & Gutierrez-Hartmann, 2013). In case of AML1, the TEL-AML1 fusion protein acquires an exclusively repressive function and prevents differentiation (Hiebert *et al*, 1996).

1.3 Aims of the project

The project presented here is based on previous work performed in our laboratory (Master Thesis J. Toggweiler). Ras^{V12} dlg^{RNAi} tumors were transcriptionally profiled with microarrays to compare the gene expression levels of wild-type and Ras^{V12} dlg^{RNAi} cells. We identified over 500 misregulated genes. Based on their fold change we selected 100 of the upregulated genes and tested if a depletion of the gene product by RNAi modified the tumor phenotype. As the tumors express GFP we could easily score tumor size by looking at GFP expression under a fluorescent binocular. In this way, we narrowed down the selected candidates to ten genes that strongly suppressed growth of Ras^{V12} dlg^{RNAi} tumors upon depletion of the gene product. We further validated these results by quantifying tumor size more accurately and confirmed the upregulation of these genes in Ras^{V12} dlg^{RNAi} cells with quantitative real-time PCR (qRT-PCR). Interestingly, eight of the ten suppressors did not show a phenotype in wild-type eye discs suggesting that their growth regulatory effects are specific for the tumor.

As aim of this thesis we wanted to carry out a detailed functional characterization of two of the identified suppressors. We chose two candidates that showed a strong suppression of tumor growth, but had no effect on wild-type eye imaginal discs: Ets21C and astrocytic leucin-rich repeat molecule (Alrm). Ets21C is a member of the *Drosophila* ETS family of transcription factor in *Drosophila* and was considered interesting due to the relevance of ETS proteins in cancer (see section 1.2.3). The second candidate has not been characterized extensively. In the following sections, we will present our characterization of these two genes, including our work to understand how they regulate tumor growth. A last section will present a study about Grindelwald (Grnd), a newly identified *Drosophila* tumor necrosis factor receptor (TNFR) homolog, to which we contributed.

2 Results and Discussion

This thesis investigates growth regulatory mechanisms in Ras^{V12} dlg^{RNAi} tumors. We identified and characterized new components that contribute to tumor growth.

Section 2.1 is the main part of this thesis and comprises a study addressing the role of Ets21C in Ras^{V12} dlg^{RNAi} tumors. A depletion of Ets21C significantly decreased growth of Ras^{V12} dlg^{RNAi} tumors whereas overexpression of Ets21C increased tumor growth. Ets21C expression is elevated in tumors and is regulated by the JNK pathway. Moreover, Ets21C activates JNK pathway target genes that induce and sustain tumor growth, possibly via interaction with the transcription factor AP-1. Additional subsections describe supplemental experiments that address the following topics: effects of an Ets21C depletion or overexpression on Ras^{V12} or dlg^{RNAi} tumors; occupancy of *Mmp1* regulatory regions by Ets21C; requirement of a potential phosphorylation site for Ets21C function; structure function analysis of Ets21C; mutagenesis of AP-1 sites in the regulatory region of *Ets21C*.

Section 2.2 delineates experiments directed at elucidating the role of *alrm*, in neoplastic tumors. Alrm is specifically upregulated in Ras^{V12} dlg^{RNAi} tumors and a depletion of Alrm suppresses tumor growth. Furthermore, we started to investigate a connection between Alrm and the JNK pathway as we had evidence that Alrm might interact with an adaptor protein that links the JNK pathway receptor to further downstream components. An additional subsection provides an outlook of future experiments to dissect the role of Alrm in neoplastic tumors.

Section 2.3 presents a publication that describes the discovery of Grnd as the receptor for the *Drosophila* TNF-α homolog Egr: Egr activates the JNK pathway via Grnd. Furthermore, Grnd associates with apical polarity determinants, providing a link between loss of polarity and neoplastic tumor growth.

2.1 Ets21C regulates neoplastic growth by cooperating with AP-1

The following study focused on functionally characterizing the role of the *Drosophila* ETS transcription factor, Ets21C, in tumor growth. RNAi mediated depletion of *Ets21C* strongly suppressed Ras^{V12} dlg^{RNAi} dependent tumor growth. The expression or activity of human ETS proteins is frequently deregulated in several types of cancers and therefore elucidating the role of Ets21C in Ras^{V12} dlg^{RNAi} tumors could provide new insights into the mechanisms of ETS factor mediated transformation. In subsequent experiments, we have generated a mutant allele of *Ets21C* and confirmed the results obtained with the RNAi. As the molecular function of Ets21C was not well defined, we worked to identify the pathway that regulates Ets21C expression as well as target genes that are induced upon Ets21C. Our current working model is that Ets21C associates with the AP-1 transcription factor to activate target genes required for tumor growth.

Toggweiler Janine, Willecke Maria and Basler Konrad
Ets21C regulates neoplastic growth by cooperating with AP-1.

Manuscript in preparation

The transcription factor Ets21C drives tumor growth by cooperating with AP-1

Janine Toggweiler[1], Maria Willecke[1] and Konrad Basler[1*]

[1] Institute of Molecular Life Sciences, University of Zurich, Zurich, Switzerland

[*] Corresponding author: konrad.basler@imls.uzh.ch

Running title: Co-regulation of tumor growth by Ets21C and AP-1

KEY WORDS

Ets21C; Drosophila; tumor; JNK; AP-1

ABSTRACT

The JNK pathway is crucial for coordinating and transducing cellular responses to stress. Belonging to the MAPK family, its role is conserved across species. While upstream factors of the pathway are well established, the transcriptional control of target genes is less well understood. Neoplastic tumors in *Drosophila* heavily depend on JNK signaling to induce target genes that are essential for tumor growth and invasion. In this study we identified the transcription factor Ets21C as a pivotal regulator of tumor growth: depletion strongly suppressed growth while ectopic expression of Ets21C increased tumor size. In addition, we find that Ets21C expression is elevated as a consequence of JNK signaling activity. In turn, the JNK pathway transcription factor AP-1 requires Ets21C to induce target genes that drive tumor growth. Furthermore, we demonstrate that the Ets21C DNA-binding domain and the Pointed domain are essential for Ets21C function. Our data reveal Ets21C as a novel player in regulating the transcriptional program of the JNK pathway and thus improve our understanding of the mechanisms that govern tumor growth.

INTRODUCTION

Cells have to constantly adapt to changes in their environment. This is achieved via sophisticated intracellular signaling pathways that integrate and amplify signals from various extracellular stimuli to regulate cellular processes such as proliferation, apoptosis or differentiation. The Jun N-terminal kinase (JNK) pathway is a subgroup of the mitogen-activated protein (MAP) kinase signaling pathways and is responsible for activating the apoptotic machinery in response to inflammatory cytokines or environmental stress such as UV radiation, heat or reactive oxygen species (Weston & Davis, 2007). Defects in JNK signaling are associated with several pathologies such as neurological disorders, type 2 diabetes or cancer. Mammals possess three *Jnk* genes, *Jnk1*, *Jnk2* and *Jnk3*, all of which can be spliced into different isoforms (Davies & Tournier, 2012). In contrast, *Drosophila* has only one JNK and thus represents a simpler system, which facilitates genetic analyses and the identification of pathway components. In flies, stress cues also lead to JNK pathway activation. One such cue is Eiger (Egr), the *Drosophila* tumor necrosis factor (TNF) homolog (Moreno *et al*, 2002; Igaki *et al*, 2002). Binding of Egr to the TNF receptor Grindelwald (Grnd) recruits several adaptor proteins that lead to the phosphorylation of TGF-β activated kinase 1 (TAK1) (Andersen *et al*, 2015; Takatsu *et al*, 2000). Consequently, dTAK1 activates the JNKK Hemipterous (Hep) that activates the JNK Basket (Bsk) (Riesgo-Escovar *et al*, 1996; Sluss *et al*, 1996; Glise *et al*, 1995). Finally, Bsk phosphorylates the transcription factors Jun and Fos (Jra and Kayak in *Drosophila*), which dimerize to form the activator protein 1 (AP-1) complex that induces transcription of target genes (Kockel *et al*, 2001). *puckered* (*puc*) is one of these target genes and encodes a negative regulator of the JNK pathway that dephosphorylates Bsk (Martín-Blanco *et al*, 1998). While the upstream components of the JNK pathway in *Drosophila* are well known, it is less clear how different target genes are activated in different contexts and if AP-1 requires co-factors for such transcriptional activation.

Neoplastic tumors serve as a valuable system in *Drosophila* to study the JNK pathway as their cells exhibit JNK signaling activity without undergoing apoptosis (Igaki *et al*, 2006; Uhlirova & Bohmann, 2006; Andersen *et al*, 2015). These tumors are generated by concomitantly activating Ras signaling (Ras^{V12}) and inactivating *scribbled* (*scrib*): if *Drosophila* eye imaginal discs are genetically manipulated in such way, large tumors form that invade neighboring

tissues such as the ventral nerve cord (VNC) and the brain lobes (Brumby & Richardson, 2003; Pagliarini, 2003). Scrib is required to establish and maintain apical-basal polarity and forms a complex with two other proteins, Discs-large (Dlg) and Lethal giant larvae (Lgl) (Bilder & Perrimon, 2000; Bilder, 2000). If *scrib*$^{-/-}$ cells grow as clones among wild-type cells, however, they are eliminated from the tissue via JNK signaling (Igaki *et al*, 2006). Loss of polarity is thought to activate the JNK pathway through association of apical polarity determinants with the TNF receptor Grnd (Andersen *et al*, 2015). The activation of Ras in *scrib*$^{-/-}$ cells renders them resistant to cell death, as Ras activity favors proliferation and cell survival, resulting in cells that continue to proliferate in an uncontrolled manner (Brumby & Richardson, 2003). In this context, activation of the JNK pathway induces the expression of Matrix metalloproteinase 1 (Mmp1), which leads to the degradation of extracellular matrix proteins, thereby allowing tumor cells to become mobile and to migrate out of their tissue of origin (Uhlirova and Bohmann, 2006). JNK signaling also upregulates the expression of the cytokines Unpaired1 (Upd1), Unpaired2 (Upd2) and Unpaired3 (Upd3). Upd1 and Upd2 stimulate cell growth and proliferation by activating JAK/STAT signaling (Wu et al., 2010).

In this study we used a modified version of the above described *Ras*^{V12} *scrib*$^{-/-}$ tumor model to identify factors that are required for tumor growth. We identified the transcription factor Ets21C as a crucial regulator of tumor growth: depletion of Ets21C strongly suppressed tumor growth while ectopic expression increased tumor size. Ets21C expression was found to be elevated in tumor cells and this upregulation is a consequence of JNK signaling activity. In turn, Ets21C associates with AP-1 and stimulates the expression of downstream effectors that increase tumor growth.

RESULTS

Ras^{V12} dlg^{RNAi} tumors require Ets21C for growth

To identify genes that regulate growth of *Ras^{V12} scrib$^{-/-}$* tumors, we used a modified assay that employs a dsRNA targeting *dlg* instead of mutations in *scrib*. This system can accommodate all genetic components necessary to cause a neoplastic phenotype in one fly stock and makes it possible to test the effect of additional transgenes (RNAi, or cDNA constructs) in a one generation cross (Willecke *et al*, 2011). To identify new components that regulate tumor growth, we tested a subset of genes that were upregulated in *Ras^{V12} dlg^{RNAi}* tumors by RNAi and screened for modifications of the tumor phenotype. We identified an RNAi targeting the *Ets21C* (*CG2914*) transcript as a strong suppressor of tumor growth (Fig. 1). Tumors depleted of Ets21C are reduced to half the size of control tumors, which in turn lead to an increased fraction of larvae that succeeded to pupariate (Fig. 1, A, B and K). Typically, only a subset of larvae bearing control tumors manage to pupariate while most die as larvae (Fig. 1, L). Depleting tumors for Ets21C results in an increased 'pupae to dead larvae' ratio (Fig. 1, L). To exclude the possibility that the growth suppressing effects are caused by off-target activities of the RNAi transgene, we created a null allele of the *Ets21C* gene by inducing a deletion that removed a major part of the gene (Fig. 1, G and H). As the deletion is homozygous lethal, we used the MARCM system to generate clones homozygous mutant for *Ets21C* and expressing *Ras^{V12}* and *dlg^{RNAi}*. Similar to the effects of the *Ets21C^{RNAi}*, deleting *Ets21C* leads to a reduction of tumor size and to a significant restoration of disc morphology (Fig. 1, G and H).

As removal of Ets21C exhibited tumor growth suppressing effects, we wondered whether higher levels of Ets21C would promote growth of *Ras^{V12} dlg^{RNAi}* tumors. Co-expression of HA-tagged Ets21C (Ets21C^{HA}) together with *Ras^{V12}* and *dlg^{RNAi}* did indeed increase tumor size and shifted the lethality point to earlier stages, i.e. more animals died as larvae (Fig.1, A, C, K and L).

Complementary to our data from eye imaginal discs, we found that changes in Ets21C levels also affected the growth of wing disc tumors (Sup. Fig.1, B-C). In this assay, we targeted expression of the respective transgenes to the posterior compartment of the wing disc by means

of an *engrailed-Gal4* driver (Willecke *et al*, 2011). Ras^{V12} dlg^{RNAi} expression leads to overgrowth of the posterior compartment resulting in a much larger wing disc and in lethality of the animal (Sup. Fig. 1, A and B). Co-expression of $Ets21C^{RNAi}$ partially restricted overgrowth of the wing disc whereas expression of the $Ets21C^{HA}$ protein further enlarged the posterior compartment at the expense of the anterior part (Sup. Fig. 1, B-D). In sum, these results demonstrate that Ets21C regulates growth of Ras^{V12} dlg^{RNAi} tumors in both eye and wing disc tissue.

To assess whether Ets21C generally affects growth or only exhibits an effect on tumor cells, we depleted or overexpressed Ets21C in wild-type cells (Fig. 1, D-F). Interestingly, the effect on proliferation of wild-type cells was different compared to tumors. Wild-type eye discs expressing $Ets21C^{RNAi}$ were slightly enlarged (Fig. 1, D and E), but developed into morphologically normal adult eyes (Sup. Fig. 2, D and E). In addition, *Ets21C* mutant clones did not behave differently from wild-type clones (Fig. 1, I and J). In contrast, overexpression of Ets21C leads to loss of imaginal disc tissue and triggered apoptosis as evidenced by the presence of active Caspase 3 (Cas3) (Fig. 1, D and F, Sup. Fig. 2, A-C). Consistent with this effect, the adult eye and head were smaller than wild-type (Sup. Fig 2, D and F). This phenotype was partially rescued by co-expression of *Drosophila* inhibitor of apoptosis protein 1 (DIAP1) (Sup. Fig. 2, G). Taken together, these results suggest that depletion of Ets21C exhibits a high degree of tumor-specificity, while overexpression causes an effect in wild-type animals that is opposite to that observed in tumor backgrounds.

Depletion of other ETS proteins does not negatively influence tumor growth

Ets21C belongs to the family of ETS (E-twenty six) transcription factors, which is unique to metazoans and represented by eight members in *Drosophila*. The *Drosophila* ETS proteins have been implicated in various processes such a oogenesis, metamorphosis, eye development and cell migration (Hsu & Schulz, 2000). The best characterized *Drosophila* ETS proteins are Pointed (Pnt) and Anterior open (Aop). Pnt is a transcriptional activator downstream of the Ras/MAPK pathway and Aop acts as repressor of MAPK target genes. Upon MAPK pathway activation, Aop is phosphorylated and inactivated, which releases target genes from repression. Concomitantly, Pnt is phosphorylated and activated by MAPK and stimulates transcrip-

tion of target genes (Brunner *et al*, 1994; O'Neill *et al*, 1994; Rebay & Rubin, 1995). In mammals, different ETS family members are known to interact with each other or with co-regulatory protein partners to control gene expression (Oikawa & Yamada, 2003). We reasoned that depleting Ets21C could abrogate a vital association with another *Drosophila* ETS protein and thereby elicit the observed tumor suppressing effect. Particularly Pnt or Aop would be good candidates to serve as Etc21C partners, as they act downstream of Ras signaling (Brunner *et al*, 1994; O'Neill *et al*, 1994). In order to test this assumption, we analyzed the effect of knocking-down *pnt* and *aop* in the tumor background. All RNAi constructs efficiently downregulated the expression of their corresponding genes (*Ets21C*, *pnt* or *aop*, Fig. 2, F). In contrast to *Ets21C*, however, downregulation of *pnt* or *aop* expression did not cause growth suppressing effects on tumors (Fig. 2, A- E). Tumors expressing an RNAi targeting *pnt* were even increased in size (Fig. 2, A, C and E).

We also tested the role of the other five *Drosophila* ETS genes in tumor growth, *Ets97D*, *Ets98B*, *Ets65A*, *Ets96B* and *E74*. None of these genes affected tumor growth upon depletion (Sup. Fig. 3, A-G). This was not unexpected as *Ets98B*, *Ets65A* and *Ets96B* are expressed at very low levels in Ras^{V12} dlg^{RNAi} tumors and *Ets97D* and *E74* have been implicated in different processes (Sup. Fig. 3, H7) (Hsu & Schulz, 2000). From these results, we conclude that Ets21C is the only *Drosophila* ETS protein required for growth of Ras^{V12} dlg^{RNAi} tumors.

Ets21C expression depends on the JNK pathway

Growth of Ras^{V12} dlg^{RNAi} tumors is regulated by downstream effects of Ras^{V12}, which can lead to MAPK or PI3K activation, and loss of polarity, which results in JNK pathway activation (Igaki *et al*, 2006; Willecke *et al*, 2011). Transcriptome profiles of Ras^{V12} dlg^{RNAi} tumors have revealed an upregulation of *Ets21C*; we reasoned that its expression could be regulated either by the MAPK/PI3K or by the JNK pathway. To test this, we co-expressed different JNK pathway components with Ras^{V12} and examined *Ets21C* expression levels (Fig. 3, A). First, we co-expressed Ras^{V12} and Egr, the *Drosophila* TNF-α homolog and a strong activator of the JNK pathway, in eye imaginal discs and measured *Ets21C* expression levels by qPCR. Strikingly, we observed a 30-fold upregulation of *Ets21C* transcript levels in Ras^{V12} *UAS-egr* tumors, a response even stronger than that observed in Ras^{V12} dlg^{RNAi} tumors (Fig. 3, B). Ex-

pression of the *Mmp1* gene, an established JNK pathway target (Uhlirova & Bohmann, 2006), was also strongly induced (Fig. 3, C). Next we combined Ras^{V12} with core JNK components acting downstream of Egr: the *Drosophila* JNK Basket (Bsk) and the JNKK Hemipterous (Hep). Bsk and Hep expression also induced expression of *Ets21C* and *Mmp1* (Fig. 3, D and E). To complement these findings, we also blocked JNK signaling in Ras^{V12} dlg^{RNAi} tumors using RNAi targeting the JNK transcription factors Jun or Fos and monitored *Ets21C* expression. Consistent with our previous data, *Ets21C* and *Mmp1* levels decreased upon removal of Jun or Fos (Fig. 3, F-I). We therefore conclude that Ets21C expression in neoplastic tumors is dependent on the JNK pathway.

Since Ras is constitutively active in all the experimental conditions we exploited, it leaves open the possibility that Ras signaling, via MAPK or PI3K activation, is required in conjunction with JNK pathway activity for the observed *Ets21C* upregulation. To test this, we activated the JNK pathway in wild-type eye discs by expressing Egr in the Glass-Multimer-Reporter (GMR) expression domain and measured *Ets21C* transcript levels by qPCR. Similar to our observations in the tumor background, *Ets21C* as well as the control target *Mmp1* are strongly induced upon Egr expression in the absence of a Ras^{V12}. Therefore, JNK pathway activity is sufficient to induce *Ets21C* expression independent of elevated Ras activity (Fig. 3, J and K).

Ets21C influences the expression of JNK pathway targets

Having established that *Ets21C* expression is regulated by the JNK pathway, we wanted to investigate, which genes are activated downstream of Ets21C in the tumor context. To this end, we analyzed and compared the transcriptomes of Ras^{V12} dlg^{RNAi} tumors co-expressing either $Ets21C^{RNAi}$ or $Ets21C^{HA}$. We identified 24 genes that were significantly downregulated upon Ets21C depletion and upregulated if Ets21C was overexpressed (Sup. Fig. 4, A). Among these genes was *Mmp1*, a known JNK pathway target (Uhlirova & Bohmann, 2006). Depletion of Ets21C in Ras^{V12} dlg^{RNAi} tumors decreased *Mmp1* expression whereas overexpression of Ets21C increased *Mmp1* levels (Fig. 4, A). In agreement with our qPCR results, we found that Mmp1 expression is reduced at the protein level if Ets21C is depleted in Ras^{V12} dlg^{RNAi} tumors (Fig. 4, B).

In addition to *Mmp1*, two genes that are downstream of JNK signaling were also found differentially expressed in the microarray analysis: *upd1*, and *PDGF and VEGF related factor 1(Pvf1*) (Sup. Fig. 4, A). However, in contrast to *Mmp1*, it is not known whether *upd1* or *Pvf1* activation through the JNK pathway is direct or indirect. *upd1* encodes a cytokine that activates the JAK/STAT pathway. It has previously been found to be upregulated in Ras^{V12} $scrib^{-/-}$ tumors in a JNK-dependent manner and to be essential for tumor growth (Wu *et al*, 2010). Pvf1 is one of the *Drosophila* orthologs of mammalian vascular endothelial growth factors (VEGFs) and platelet derived growth factors (PDGFs) and known to drive hemocyte proliferation in neoplastic tumors (Parisi *et al*, 2014). qPCR analysis confirmed the differential expression of *upd1* and *Pvf1* upon altering Ets21C levels (Fig. 4, C). Moreover, we found that other Upd- and PDGF/VEGF-like factors (Upd2, Upd3, Pvf2 and Pvf3) were also significantly upregulated in tumors overexpressing Ets21C (Sup. Fig. 4, B). Thus, our results show that Ets21C regulates the expression of various critical targets of the JNK pathway, targets that explain, at least in part, the effects Ets21C exerts on tumor growth.

We next asked if the ability of Ets21C to induce *Mmp1*, *Pvf1* and *upd1* expression was dependent on the Ras^{V12} dlg^{RNAi} background or if it was a general function of Ets21C. In order to test this, we measured transcript levels of *Mmp1*, *Pvf1* and *upd1* in wild-type eye discs overexpressing *Ets21C* and in discs that co-expressed Ras^{V12} and *Ets21C*. As in Ras^{V12} dlg^{RNAi} tumors, expression of Ets21C in Ras^{V12} tumors or wild-type eye discs lead to an induction of *Mmp1* and *Pvf1* transcripts and to a lesser extent also *upd1* transcripts (Fig. 4, D and E). This indicates that Ets21C is able to activate these target genes in a physiological context.

The ETS and PNT domains are essential for Ets21C function

ETS proteins share as their unifying domain an ETS DNA binding motif, a variant of the winged helix-turn-helix motif that not only mediates binding to the DNA, but can also mediate protein-protein interactions (Sharrocks, 2001). Besides the DNA binding domain, about one third of ETS proteins encompasses the Pointed (PNT) domain that has originally been identified in the *Drosophila* ETS protein Pnt (Klämbt, 1993). PNT domains have been shown to govern homo-oligomerization, hetero-dimerization as well as transcriptional repression (Qiao & Bowie, 2005). A SMART alignment for Ets21C revealed that, besides the common

ETS DNA binding domain, Ets21C also harbors a PNT domain (Schultz *et al*, 1998). In order to gain insights into which part of Ets21C accounts for its effects on tumor growth, we generated protein variants that lack either the ETS or the PNT domain and tested their effects on Ras^{V12} dlg^{RNAi} tumors (Fig. 6, A-E). Deleting the DNA binding domain ($Ets21C^{\Delta Ets}$) abrogated the tumor growth enhancing effect that we observed with full length Ets21C. It even caused a slight dominant-negative effect as tumors expressing $Ets21C^{\Delta Ets}$ were smaller than control tumors (Fig. 6, B, C and E). Ets21C without the PNT domain behaved like $Ets21C^{\Delta Ets}$: these tumors were also smaller than control tumors (Fig. 6, D). In addition, we performed qPCR on RNA isolated from tumor cells expressing the protein variants and monitored the expression of the Ets21C targets *Mmp1*, *Pvf1* and *upd1*. Consistent with the effects on tumor growth, expression of *Mmp1*, *Pvf1* and *upd1* did not increase upon expression of $Ets21C^{\Delta Ets}$ or $Ets21C^{\Delta Pnt}$ and remained at the same levels as in control tumors or were even slightly decreased (Fig. 6, F and G).

Taken together, our results demonstrate that the function of Ets21C depends on both, the ETS and the PNT domains.

Effects of Ets21C depend on JNK signaling

Given the requirement of the DNA binding domain for Ets21C function and taking into account that the genes induced by Ets21C are known to be targets of the JNK pathway, we sought to clarify the relationship between Ets21C and JNK signaling regarding target gene induction. Ets21C could act either downstream of AP-1 or together with AP-1. For *Pvf1* and *upd1* it is not known whether they are directly or indirectly activated by the JNK pathway. *Mmp1* is a direct target as its expression is mediated by AP-1 binding sites in its regulatory region; we hypothesized that Ets21C and AP-1 may co-operatively activate target gene expression (Uhlirova & Bohmann, 2006). To investigate this possibility, we first checked whether Ets21C outputs genetically depend on the JNK pathway. To this end, we co-expressed a dominant-negative form of Bsk (Bsk^{DN}), the *Drosophila* Jun kinase, together with Ras^{V12}, dlg^{RNAi} and $Ets21C^{HA}$ and monitored *Mmp1*, *Pvf1* and *upd1* expression. Blocking the JNK pathway abrogated expression of all three genes regardless of whether or not $Ets21C^{HA}$ was overexpressed (Fig. 6, A). This change was also reflected in a dramatic reduction of tumor size upon Bsk^{DN} expression. We observed a similar effect when we inhibited JNK signal-

ing at the level of the two AP-1 transcription factors, Jun and Fos: depletion of both together reverted the expression levels of *Mmp1*, *Pvf1* and *upd1* induced by $Ets21C^{HA}$ to those found without Ets21C overexpression (Fig. 6, B). These results show that Ets21C-dependent up-regulation of *Mmp1*, *Pvf1* and *upd1* requires JNK signaling activity. Importantly, *Pvf1* and *upd1* upregulation is not an indirect downstream consequence of JNK signaling mediated by Ets21C. Hence we conclude that Ets21C likely co-operates with AP-1 to mediate maximal target gene expression.

To gain further insight into the mechanism underlying this cooperation we performed co-immunoprecipitation experiments with Ets21C and/or Jun or Fos proteins to test for a physical interaction between the three proteins. It is well documented that Jun and Fos bind to each other, but it is not known to which extent they depend on additional co-factors to drive target gene expression. We found that N-terminally HA-tagged Ets21C precipitates C-terminally FLAG-tagged Jun or Fos from *Drosophila* Kc167 cell lysates (Fig. 6, C). While Jun and Fos were readily detectable, we did not find GFP in the precipitates, which emphasizes the specificity of the interaction. Thus, our genetic and biochemical data suggest that the function of Ets21C depends on a direct cooperation with AP-1.

DISCUSSION

In this study, we used a genetic approach to identify novel genes that regulate growth of Ras^{V12} dlg^{RNAi} tumors. We identified the transcription factor Ets21C as a regulator of tumor growth and found its gene to be a target of the JNK pathway. Moreover, we uncovered a novel role for Ets21C as a potential co-factor of AP-1; together, these DNA-binding factors drive the expression of specific target genes that induce and sustain growth and invasiveness of Ras^{V12} dlg^{RNAi} tumors.

Neoplastic tumors depend on Ets21C function

The human ETS gene family comprises 28 genes that affect a wide range of cellular processes such as proliferation, apoptosis, differentiation, migration and invasion. Defective or hyperactive ETS proteins substantially contribute to several diseases, among them cancer (Kar & Gutierrez-Hartmann, 2013). Here, we demonstrate that Ras^{V12} dlg^{RNAi} tumors require Ets21C function: tumors depleted for Ets21C remained small and showed a reduced expression of key factors that drive tumor malignancy. Overexpression of Ets21C increased tumor size and target gene expression, underscoring that Ets21C is not only required for tumor growth, but also capable of enhancing tumor malignancy. Studies on human ETS factors corroborate these findings as the closest human orthologs of Ets21C, *ETS-related gene* (*ERG*) and *Friend leukemia virus-induced erythroleukemia 1* (*FLI-1*) have been linked to tumorigenesis as well (Chen *et al*, 1992). *ERG* is fused to *Transmembrane protease, serine 2* (*TMPRSS*) in 50% of prostate cancers, which results in androgen mediated activation of *ERG*. Another type of cancer in which fusion of *ERG* is frequently observed is Ewing sarcoma, a soft tissue cancer occurring in children. In these tumors, *ERG* and *FLI-1* can be fused to the *EWS* gene turning the resulting products into more potent transactivators than ERG or FLI-1 on their own. Besides chromosomal translocations, ERG is overexpressed in acute myeloid leukemia (AML) and is associated with a poor prognosis, whereas higher FLI-1 expression has been detected in triple negative breast cancer or in metastatic melanoma (Li *et al*, 2014; Kar & Gutierrez-Hartmann, 2013).

Ets21C is a context-independent target of the JNK pathway

While Ras^{V12} dlg^{RNAi} tumors depleted for Ets21C are smaller than control tumors, wild-type tissue is not affected by the loss of Ets21C. This suggests that Ets21C function might only be required if a tissue has to cope with stress such as increased growth and epithelial disorganization in Ras^{V12} dlg^{RNAi} tumors, but is otherwise dispensable. Such a role for Ets21C is supported by previous reports that analyzed *Ets21C* mutant flies challenged with pathogens. Chambers et al. (2012) demonstrated that *Ets21C* mutants are more susceptible to infection with certain pathogens, either due to a reduced tolerance or to a higher bacterial load (Chambers *et al*, 2012; Ayres *et al*, 2008). Additional studies identified *Ets21C* transcripts among the immediate early response genes activated in immune challenged cells or flies. Importantly, this activation depends on the JNK pathway as it is blocked in *tak1* or *hep* mutants, but not in cells mutant for the Immune deficiency (IMD) pathway components *relish (rel)* and *kenny (key)* (Boutros *et al*, 2002; Johansson *et al*, 2005; Radyuk *et al*, 2010).

Loss of epithelial polarity caused by a depletion of *dlg* activates the JNK pathway that critically affects tumor growth. Since we found elevated *Ets21C* transcript levels in Ras^{V12} dlg^{RNAi} tumors we tested whether *Ets21C* expression was induced as a consequence of JNK signaling. Indeed, *Ets21C* is highly upregulated if we directly activate the JNK pathway in Ras^{V12} tumors by co-expressing Egr. Conversely, *Ets21C* expression is prevented in Ras^{V12} dlg^{RNAi} tumors if we block the formation of the JNK transcription factor AP-1 by removing one of its components, Jun or Fos. In addition, we found that *Ets21C* is induced in response to JNK signaling in a wild-type background implying that *Ets21C* expression also depends on JNK pathway activity in a non-neoplasia context.

Although *Ets21C* is activated by the JNK pathway in both tumor and wild-type tissues, its effects vary greatly. Ectopic expression in tumors increases growth, while it causes cell death in a wild-type background. This paradoxical result can be explained with the presence or absence of Ras^{V12} and the role of Ets21C in the JNK pathway. Previous studies have shown that polarity deficient cells are eliminated from the tissue in a JNK-dependent manner (Brumby & Richardson, 2003). Removal of these cells is, however, prevented if Ras^{V12} is present (Brumby & Richardson, 2003; Pagliarini, 2003). In a Ras^{V12} background the same mechanism

likely protects Ets21C expressing cells from undergoing apoptosis and unleashes its potential in driving tumor growth.

Importantly, while this manuscript was in preparation, Külshammer et al. (2015) published related findings, which also suggest that Ets21C functions downstream of the JNK pathway, and acts as an oncogene in cooperation with Ras; we consider this as an independent validation of certain aspects of our study (Kulshammer *et al*, 2015).

Ets21C cooperates with AP-1 in inducing tumor growth

A unifying feature of ETS transcription factors is their DNA binding domain that recognizes a core sequence 5'-GGA(A/T)-3'. With all ETS proteins sharing the same core binding motif, specificity for target gene activation must be governed by protein sequences flanking the ETS domain, but also by cooperation with other transcription factors and co-activators (Cooper *et al*, 2014). Protein-protein interactions can occur directly on the DNA via the ETS domains, or via the PNT domains, a second functional domain present in about 30% of ETS proteins. Our analyses on Ets21C demonstrate that both, the ETS and the PNT domain are relevant for Ets21C function. Protein variants lacking the ETS or the PNT domain do not increase tumor growth if co-expressed with Ras^{V12} dlg^{RNAi} nor do they upregulate *Mmp1*, *Pvf1* and *upd1* expression.

Mmp1, Pvf1 and upd1 expression has previously been shown to be induced by the JNK pathway and to be essential for tumor growth and invasion (Uhlirova & Bohmann, 2006; Wu *et al*, 2010; Parisi *et al*, 2014). Based on this data, we wondered if and how Ets21C regulates transcriptional outputs of the JNK pathway. (1) Ets21C could interact with Jun and/or Fos. (2) Ets21C could activate or interact with an unknown factor that feeds back on the JNK pathway. We show here that in Ras^{V12} dlg^{RNAi} tumors the effects of Ets21C fully depend on an active JNK pathway. If the latter is blocked by co-expressing Bsk^{DN} with Ras^{V12} dlg^{RNAi} and $Ets21C^{HA}$, tumors remain small and there is no induction of the target genes *Mmp1*, *Pvf1* or *upd1*. These results support both possibilities (1 and 2), but exclude an autonomous function of Ets21C. A physical interaction between Ets21C and Jun and Fos has previously been proposed based on large scale mass-spectroscopy data (Rhee *et al*, 2014). Here, we show in cul-

tured cells that HA-tagged Ets21C binds FLAG-tagged Jun or Fos, suggesting that the three proteins interact to regulate target gene expression. Such a model is further supported by studies in mammalian systems that have shown a physical interaction between AP-1 and the Ets21C ortholog ERG, or other ETS proteins (Bassuk & Leiden, 1995; Camuzeaux *et al*, 2005; Basuyaux *et al*, 1997).

Based on our data we propose a two-step model on how JNK signaling regulates tumor growth: in an early wave of pathway activity AP-1 induces the expression of targets such as cell death genes, *puc*, *Ets21C* and likely additional targets that remain elusive. In a wild-type background, this leads to apoptosis as demonstrated by numerous studies (Moreno *et al*, 2002; Luo *et al*, 2007; Brumby & Richardson, 2003; Takatsu *et al*, 2000). Neoplastic tumors, however, are protected against cell death through the presence of Ras^{V12}, which allows the induction of a second tier of targets, such as *Mmp1*, *Pvf1* and *upd1*. Importantly, these targets not only depend on AP-1 activity, but also on Ets21C as their expression is reduced in tumors depleted for Ets21C (Fig. 6, D). So far we can, however, not distinguish whether Ets21C only enhances and sustains AP-1 dependent target gene expression or whether it is required for their initial activation. In conclusion, our results provide a novel mechanistic explanation for the role of Ets21C in tumorigenesis.

MATERIALS & METHODS

Fly stocks and genetics

To test for an effect on tumor growth, UAS-RNAi lines or UAS-cDNAs were crossed to females of the following tester fly stock: *eyFlp; UAS-Ras^{V12}, UAS-dlg$^{RNAi(VDRC41134)}$, UAS-GFP/CyO, tub-Gal80^{BL9491}; act>CD2>Gal4, UAS-GFP^{S65T}*. To express the transgenes in a wild-type background, the following flies were used: *eyFlp; sp/CyO; act>CD2>Gal4, UAS-GFP^{S65T}*. To generate tumors that express *Ras^{V12}* only, we used: *eyFlp; act>y^{+}>Gal4, UAS-GFP/CyO, tub-Gal80^{BL9491}; UAS-Ras^{V12}/TM6b* flies. *yw* flies were used for control crosses. To generate MARCM clones, *eyFlp; FRT40, tub-Gal80/SM5; tub-Gal4, UAS-GFP/TM6b* females were crossed to *yw; FRT40; MKRS/TM6b* or *yw; FRT40, ΔEts21C^{21}/SM5; +/TM6b* or *yw; FRT40; UAS-Ras^{V12}, UAS-dlg$^{RNAi(BL34854)}$/TM6b* or *yw; FRT40, ΔEts21C^{21}/SM5; UAS-Ras^{V12}, UAS-dlg$^{RNAi(BL34854)}$/TM6b* males. Flies and larvae were reared and kept at 25°C. Other RNAi lines from the Vienna Drosophila RNAi library (VDRC) used were: *UAS-Ets21C$^{RNAi(51225)}$*, *UAS-Ets65A$^{RNAi(15354)}$*, *UAS-dJun$^{RNAi(107997)}$*, *UAS-rempA$^{RNAi(31575)}$*, *UAS-rempA$^{RNAi(103424)}$*. From the DGRC Trip^{RNAi}: *UAS-Fos$^{RNAi(BL33379)}$*, *UAS-Pnt$^{RNAi(BL35038)}$*, *UAS-Aop$^{RNAi(BL35404)}$*, *UAS-Ets97D$^{RNAi(35749)}$*, *UAS-Ets98B$^{RNAi(36811)}$*, *UAS-Ets96B$^{RNAi(BL31935)}$*, *UAS-E74$^{RNAi(BL29353)}$*. The following fly stocks used for overexpression experiments were from FlyORF: *UAS-Ets21C$^{HA(F000624)}$*, *UAS-Jra$^{HA(F000089)}$*, *UAS-kay$^{HA(F001841)}$*. Other fly stocks used were: *UAS-egr* (Moreno et al. 2002), *UAS-hep^{BL9308}*, *UAS-bsk^{BL9310}*, *UAS-Diap1* (from G. Halder), *GMR-Gal4* (Hay *et al*, 1994).

To generate tumors in the posterior compartment of wings discs, *yw; UAS-Ras^{V12}, UAS-dlg$^{RNAi(VDRC41134)}$/SM5; +/TM6b* or *yw; UAS-Ras^{V12}, UAS-dlg$^{RNAi(VDRC41134)}$, UAS-Ets21C$^{RNAi(VDRC51225)}$* or *yw; UAS-Ras^{V12}, UAS-dlg$^{RNAi(VDRC41134)}$/SM5; Ets21C$^{HA(F000624)}$/TM6b* males were crossed to females of the following genotype: *yw; en-Gal4, Gal80ts, UAS-CD8-GFP/CyO; MKRS/TM6b* females. *yw* flies were used as control. The progeny was kept at 18°C for 120 h and then transferred to 29°C for 48h.

Quantification of tumor volume

Tumor bearing larvae were dissected 6-7 days after egg laying (AEL). For confocal imaging and quantifications, larvae were fixed according to standard protocols and tumors were

mounted in VectaShield (Vector Laboratories). To minimize squeezing of tumors by the cover slip, one layer of double scotch tape was placed between cover slip and glass slide. Image stacks were treshholded for GFP and analyzed with Icy to calculate the tumor volume (de Chaumont *et al*, 2012). When GFP intensities were quantified from whole larvae, tresholding in ImageJ was used to detect and measure GFP signal only in the head parts of the animals.

Cloning and generation of transgenes

Truncated proteins: A plasmid with the open-reading frame of the *Ets21C* A isoform was obtained from FlyORF. To produce the Ets21C protein variants, overlapping PCRs were performed to either delete aminoacids 134-214 (ΔPnt) or 254-339 (ΔEts). The truncated protein versions were cloned into pUAST.attB via Acc65I and XbaI cut sites that had been attached in the PCR. With the same cloning strategy, a wild-type version of Ets21C without HA-tag was cloned as well to exclude any adverse effects of the HA tag. All constructs were inserted via the ΦC31 integrase system into landing site *ZH-86Fb* (Bischof *et al*, 2007).
Expression vectors for cell culture: fos or *Ets21C* cDNA was amplified by PCR and inserted into the triple HA-containing vector pMZ55 via NheI and XbaI sites. The fragments were then subcloned along with the HA-tag into pUAST via Acc65I and XbaI sites.

Generation of the *Ets21C* deletion

Ets21C was removed with an *in trans* recombination of flanking PiggyBac (PBac) elements according to the strategy of Parks et al. (Parks *et al*, 2004). PBac elements *WH Ets21C*^{f03639} and *RB rempA*^{e02928} were combined with *hsp70-flp* on the X-chromosome and then brought together in trans. *hsFlp; Ets21C*^{f03639}*/ rempA*^{e02928} progeny were heat-shocked two days AEL for 1h at 37°C. The heat-shock was repeated the next two days. Single adult males were crossed to balancer stocks and the progeny was tested by PCR for recombination with one primer binding to the remaining part of *WH Ets21C*^{f03639} going in direction of the RB element and another primer binding to the flanking region of the RB element going in direction of the WH element. A product is only yielded if recombination was successful as the region between the primer binding sites is otherwise too long. The recombination also removed a part of the neighboring gene *rempA* (*CG11838*). However, mutant clones do not show any obvious phe-

notypes (Fig. 1, I and J) and expression of an RNAi targeting *rempA* in Ras^{V12} dlg^{RNAi} cells did not have an effect on tumor growth (Sup. Fig. 4, C).

Immunofluorescence

Fixation and immunostainings of *Drosophila* eye imaginal discs and tumors were performed according to standard protocols. Primary antibodies used in this study were: anti-Mmp1 (1/200, 3B8D12, Developmental studies hybridoma bank (DSHB)) and anti-DE-cadherin (1/200, DCAD2, DSHB). Alexa fluor 594 (1/500, Molecular Probes) was used as label for the secondary antibody. Imaginal discs were mounted in VectaShield (Vector Laboratories). Images were taken with a Zeiss Lsm710 confocal microscope and processed with ImageJ and Adobe Photoshop.

RNA isolation and real-time PCR

For RNA isolations, larvae were dissected in Ringers plus 0.05% Tween-20 and tumors were collected in an 1.5 ml Eppendorf tube. Tumors were centrifuged for 10 min at 4°C and pellets were snap freezed in liquid nitrogen, stored at -80°C or processed further. For each experiment total RNA was isolated from 30 tumors or 45 wild-type eye discs with the indicated genotypes using the NucleoSpin RNA kit (Machery Nagel). Following an additional Dnase digest for 1h at 37°C (DNA-free™ kit, Ambion), 500 ng of total RNA was used for cDNA synthesis with the transcriptor High Fidelity cDNA Synthesis Kit (Roche) using oligo-dT primers. Quantitative PCR reactions were performed in triplicates using the MESA Green qPCR Mastermix Plus for SYBR Assay (Eurogentec) and an ABI Prism SDS 7900 HT (Applied Biosystems). All mesurements of transcript levels were normalized to *actin-5C*, *alpha-tubulin* and *TATA box binding protein (TBP)*. Primers were designed with Roche Universal Probe Library or with Primer3plus. When ever possible an intron-spanning assay was chosen. Primers used were: Ets21C: F: caacgacgacgaaccaaat, R: gttcgcgttggacgaatc, Mmp1: F: gaaggctcggacaacgagt, R: gtcgttggactggtgatcg, Pvf1: F: aagccggaacaccattgac, R: catgatgctgcgcttaaagt, Upd: F: gcacactgatttcgatacgg, R: ctgccgtggtgctgtttt, actin: F: gcccatctacgagggttatgc, R: aatcgcgaccagccagatc, alpha-tubulin at 84C: F: gccagatgccgtctgacaa, R: ag-

tctcgctgaagaaggtgttga, TATA binding protein: F: cgcgcatcatccaaaagc, R: gccgaccatgtttt-gaatcttaa

Microarrays

Total RNA was isolated and Dnase digested as described above from tumors with the following genotypes: *eyFlp; UAS-Ras^{V12}, UAS-dlg^{RNAi}/+; act<CD2<Gal4, UAS-GFP/+* or *eyFlp; UAS-Ras^{V12}, UAS-dlg^{RNAi}/UAS-Ets21C^{RNAi}; act<CD2<Gal4, UAS-GFP/+*or *eyFlp; UAS-Ras^{V12}, UAS-dlg^{RNAi}/sp or CyO; act<CD2<Gal4, UAS-GFP/UAS-Ets21C^{HA}*. RNA was sent to the Genomics platform in Geneva (http://www.ige3.unige.ch/genomics-platform.php) for further processing and hybridization to Affymetrix GeneChip arrays for *Drosophila*. Microarray data are available in the ArrayExpress database (www.ebi.ac.uk/arrayexpress) under accession number E-MTAB-4315.

***Drosophila* cell culture and transfections**

Kc167 cells were cultured in M3+PYRE medium supplemented with 5% FBS and 1% penicillin/streptomycin at 25°C. Cells were transfected with expression vectors using FuGene®HD (Promega) according to the manufacturers protocol.

Immunoprecipitation and western blotting

Kc167 cells (2 x 10^6 cells per well) were seeded into a 6-well plate and transfected with the indicated expression vectors. *UAS-GFP* was used as control for transfection efficiency and to keep the total amount of DNA transfected constant. Cells were harvested 48 h post-transfection and lysed in lysis buffer containing 20mM Tris-HCl pH 7.5, 1.5mM $MgCl_2$, 75mM NaCl, 1mM EGTA, 5% Glycerol, 0.25% Nonidet P-40 and protease inhibitors (Complete Mini, Roche). Following 5 min of sonication with a Bioruptor, the cell suspension was centrifuged at full speed at 4°C and supernatants were mixed with 30µl of Protein A sepharose beads (GE Healthcare) and 1µg of HA antibody (sc-805, Santa Cruz) and allowed to rotate for 4 h at 4°C. Beads were collected (2500 x g, 3 min at 4°C), washed 2 x with lysis buffer and stored at -20°C until further processing.

For western blot analysis, protein complexes were eluted from the beads, denatured and resolved on 4-12% NuPAGE Bis-Tris gels (Invitrogen) and transferred to a PVDF membrane (Amersham Hybond-P, GE Healthcare). After blocking with 5% milk, the membrane was incubated with either anti-FLAG M2 (mouse, 1/2000, Sigma) antibody followed by secondary goat anti-mouse antibodies conjugated with horseradish peroxidase (1/5000, Jackson Laboratories). Signals were detected with Western Bright Quantum detection reagent (Advansta). After stripping (Re-Blot Plus Strong Solution, Millipore), membranes were blocked and incubated with anti-HA (mouse, 1/2000, HA.11, Covance) antibody.

ACKNOWLEGEMENTS

We would like to thank G. Hausmann and C. Cantù for discussions and comments on the manuscript, E. Escher for DNA sequencing, M. Moser for assistance with qPCRs and M. Debrunner for embryo injections. Further, we thank G. Halder, the VDRC, Harvard Medical School, FlyORF and the Bloomington stock center for fly stocks and the Developmental Studies Hybridoma Bank for antibodies. This work was supported by a Krebsliga grant to K.B., a Marie Heim-Vögtlin grant to M.W., the Swiss National Science Foundation, and the Kanton of Zurich.

AUTHOR CONTRIBUTIONS

J.T., M.W. and K.B. designed the experiments. J.T. carried out the experiments and analyzed the data. J.T., M.W. and K.B. wrote the paper.

CONFLICT OF INTEREST

The authors declare no conflict of interest.

REFERENCES

Andersen DS, Colombani J, Palmerini V, Chakrabandhu K, Boone E, Röthlisberger M, Toggweiler J, Basler K, Mapelli M, Hueber A-O & Léopold P (2015) The Drosophila TNF receptor Grindelwald couples loss of cell polarity and neoplastic growth. *Nature* **522:** 482–486

Ayres JS, Freitag N & Schneider DS (2008) Identification of Drosophila mutants altering defense of and endurance to Listeria monocytogenes infection. *Genetics* **178:** 1807–1815

Bassuk a G & Leiden JM (1995) A direct physical association between ETS and AP-1 transcription factors in normal human T cells. *Immunity* **3:** 223–37

Basuyaux JP, Ferreira E, Stéhelin D & Butticè G (1997) The Ets transcription factors interact with each other and with the c-Fos/c-Jun complex via distinct protein domains in a DNA-dependent and -independent manner. *J. Biol. Chem.* **272:** 26188–95

Bilder D (2000) Cooperative Regulation of Cell Polarity and Growth by Drosophila Tumor Suppressors. *Science (80-.).* **289:** 113–116

Bilder D & Perrimon N (2000) Localization of apical epithelial determinants by the basolateral PDZ protein Scribble. *Nature* **403:** 676–80

Bischof J, Maeda RK, Hediger M, Karch F & Basler K (2007) An optimized transgenesis system for Drosophila using germ-line-specific phiC31 integrases. *Proc. Natl. Acad. Sci. U. S. A.* **104:** 3312–7

Boutros M, Agaisse H & Perrimon N (2002) Sequential activation of signaling pathways during innate immune responses in Drosophila. *Dev. Cell* **3:** 711–22

Brumby AM & Richardson HE (2003) scribble mutants cooperate with oncogenic Ras or Notch to cause neoplastic overgrowth in Drosophila. *EMBO J.* **22:** 5769–79

Brunner D, Dücker K, Oellers N, Hafen E, Scholzi H & Klambt C (1994) The ETS domain protein Pointed-P2 is a target of MAP kinase in the Sevenless signal transduction pathway. *Nature* **370:** 386–389

Camuzeaux B, Spriet C, Héliot L, Coll J & Duterque-Coquillaud M (2005) Imaging Erg and Jun transcription factor interaction in living cells using fluorescence resonance energy transfer analyses. *Biochem. Biophys. Res. Commun.* **332:** 1107–1114

Chambers MC, Lightfield KL & Schneider DS (2012) How the fly balances its ability to combat different pathogens. *PLoS Pathog.* **8:** e1002970

De Chaumont F, Dallongeville S, Chenouard N, Hervé N, Pop S, Provoost T, Meas-Yedid V, Pankajakshan P, Lecomte T, Le Montagner Y, Lagache T, Dufour A & Olivo-Marin J-C (2012) Icy: an open bioimage informatics platform for extended reproducible research. *Nat. Methods* **9:** 690–696

Chen T, Bunting M, Karim FD & Thummel CS (1992) Isolation and characterization of five Drosophila genes that encode an ets-related DNA binding domain. *Dev. Biol.* **151:** 176–91

Cooper CDO, Newman J a & Gileadi O (2014) Recent advances in the structural molecular biology of Ets transcription factors: interactions, interfaces and inhibition. *Biochem. Soc. Trans.* **42:** 130–8

Davies C & Tournier C (2012) Exploring the function of the JNK (c-Jun N-terminal kinase) signaling pathway in physiological and pathological processes to design novel therapeutic strategies. *Biochem. Soc. Trans.* **40:** 85–89

Glise B, Bourbon H & Noselli S (1995) hemipterous encodes a novel drosophila MAP kinase kinase, required for epithelial cell sheet movement. *Cell* **83:** 451–461

Hay B a, Wolff T & Rubin GM (1994) Expression of baculovirus P35 prevents cell death in Drosophila. *Development* **120:** 2121–2129

Hsu T & Schulz R a (2000) Sequence and functional properties of Ets genes in the model organism Drosophila. *Oncogene* **19:** 6409–16

Igaki T, Kanda H, Yamamoto-Goto Y, Kanuka H, Kuranaga E, Aigaki T & Miura M (2002) Eiger, a TNF superfamily ligand that triggers the Drosophila JNK pathway. *EMBO J.* **21:** 3009–18

Igaki T, Pagliarini R a & Xu T (2006) Loss of cell polarity drives tumor growth and invasion through JNK activation in Drosophila. *Curr. Biol.* **16:** 1139–46

Johansson KC, Metzendorf C & Söderhäll K (2005) Microarray analysis of immune challenged Drosophila hemocytes. *Exp. Cell Res.* **305:** 145–55

Kar A & Gutierrez-Hartmann A (2013) Molecular mechanisms of ETS transcription factor-mediated tumorigenesis. *Crit. Rev. Biochem. Mol. Biol.* **48:** 522–543

Klämbt C (1993) The Drosophila gene pointed encodes two ETS-like proteins which are involved in the development of the midline glial cells. *Development* **117:** 163–176

Kockel L, Homsy JG & Bohmann D (2001) Drosophila AP-1: lessons from an invertebrate. *Oncogene* **20:** 2347–64

Kulshammer E, Mundorf J, Kilinc M, Frommolt P, Wagle P & Uhlirova M (2015) Interplay among Drosophila transcription factors Ets21c, Fos and Ftz-F1 drives JNK-mediated tumor malignancy. *Dis. Model. Mech.* **8:** 1279–1293

Li Y, Luo H, Liu T, Zacksenhaus E & Ben-David Y (2014) The ets transcription factor Fli-1 in development, cancer and disease. *Oncogene***:** 1–10

Luo X, Puig O, Hyun J, Bohmann D & Jasper H (2007) Foxo and Fos regulate the decision between cell death and survival in response to UV irradiation. *EMBO J.* **26:** 380–90

Martín-Blanco E, Gampel A, Ring J, Virdee K, Kirov N, Tolkovsky AM & Martinez-Arias A (1998) puckered encodes a phosphatase that mediates a feedback loop regulating JNK activity during dorsal closure in Drosophila. *Genes Dev.* **12:** 557–670

Moreno E, Yan M & Basler K (2002) Evolution of TNF signaling mechanisms: JNK-dependent apoptosis triggered by Eiger, the Drosophila homolog of the TNF superfamily. *Curr. Biol.* **12:** 1263–8

O'Neill EM, Rebay I, Tjian R & Rubin GM (1994) The activities of two Ets-related transcription factors required for Drosophila eye development are modulated by the Ras/MAPK pathway. *Cell* **78:** 137–147

Oikawa T & Yamada T (2003) Molecular biology of the Ets family of transcription factors. *Gene* **303:** 11–34

Pagliarini R a (2003) A Genetic Screen in Drosophila for Metastatic Behavior. *Science (80-.).* **302:** 1227–1231

Parisi F, Stefanatos RK, Strathdee K, Yu Y & Vidal M (2014) Transformed epithelia trigger non-tissue-autonomous tumor suppressor response by adipocytes via activation of Toll and Eiger/TNF signaling. *Cell Rep.* **6:** 855–67

Parks AL, Cook KR, Belvin M, Dompe N a, Fawcett R, Huppert K, Tan LR, Winter CG, Bogart KP, Deal JE, Deal-Herr ME, Grant D, Marcinko M, Miyazaki WY, Robertson S, Shaw KJ, Tabios M, Vysotskaia V, Zhao L, Andrade RS, et al (2004) Systematic generation of high-resolution deletion coverage of the Drosophila melanogaster genome. *Nat. Genet.* **36:** 288–92

Qiao F & Bowie JU (2005) The Many Faces of SAM. *Sci. Signal.* **2005:** re7–re7

Radyuk SN, Michalak K, Klichko VI, Benes J & Orr WC (2010) Peroxiredoxin 5 modulates immune response in Drosophila. *Biochim. Biophys. Acta* **1800:** 1153–63

Rebay I & Rubin GM (1995) Yan functions as a general inhibitor of differentiation and is negatively regulated by activation of the Ras1/MAPK pathway. *Cell* **81:** 857–866

Rhee DY, Cho D-Y, Zhai B, Slattery M, Ma L, Mintseris J, Wong CY, White KP, Celniker SE, Przytycka TM, Gygi SP, Obar R a & Artavanis-Tsakonas S (2014) Transcription factor networks in Drosophila melanogaster. *Cell Rep.* **8:** 2031–43

Riesgo-Escovar JR, Jenni M, Fritz a & Hafen E (1996) The Drosophila Jun-N-terminal kinase is required for cell morphogenisis but not for DJun-dependent cell fate specification in the eye. *Genes Dev.* **10:** 2759–2768

Schultz J, Milpetz F, Bork P & Ponting CP (1998) SMART, a simple modular architecture research tool: identification of signaling domains. *Proc. Natl. Acad. Sci. U. S. A.* **95:** 5857–5864

Sharrocks a D (2001) The ETS-domain transcription factor family. *Nat. Rev. Mol. Cell Biol.* **2:** 827–37

Sluss HK, Han Z, Barrett T, Goberdhan DC, Wilson C, Davis RJ & Ip YT (1996) A JNK signal transduction pathway that mediates morphogenesis and an immune response in Drosophila. *Genes Dev* **10:** 2745–2758

Takatsu Y, Nakamura M, Stapleton M, Danos MC, Matsumoto K, O'Connor MB, Shibuya H & Ueno N (2000) TAK1 participates in c-Jun N-terminal kinase signaling during Drosophila development. *Mol. Cell. Biol.* **20:** 3015–3026

Uhlirova M & Bohmann D (2006) JNK- and Fos-regulated Mmp1 expression cooperates with Ras to induce invasive tumors in Drosophila. *EMBO J.* **25:** 5294–304

Weston CR & Davis RJ (2007) The JNK signal transduction pathway. *Curr. Opin. Cell Biol.* **19:** 142–9

Willecke M, Toggweiler J & Basler K (2011) Loss of PI3K blocks cell-cycle progression in a Drosophila tumor model. *Oncogene* **30:** 4067–74

Wu M, Pastor-Pareja JC & Xu T (2010) Interaction between Ras(V12) and scribbled clones induces tumour growth and invasion. *Nature* **463:** 545–8

FIGURE LEGENDS

Figure 1: *Ras^{V12} dlg^{RNAi}* tumors are sensitive to changes in Ets21C expression. Confocal images of (A-C) imaginal disc tumors and (D-F) wild-type imaginal discs expressing different UAS-transgenes under the control of eye specific Gal4: Flp recombinase is driven by the *eye-less* (*ey*) promoter, and causes activation of the act>y^{+}>Gal4 transgene. Recombined cells are marked by expression of a *UAS-GFP* transgene (green). In (D-F) DNA is stained with DAPI (blue). The discs co-express the following transgenes: (A) *Ras^{V12}*, *dlg^{RNAi}*, (B) *Ras^{V12}*, *dlg^{RNAi}*, *Ets21C^{RNAi}*, (C) *Ras^{V12}*, *dlg^{RNAi}*, *Ets21C^{HA}*, (D) none, (E) *Ets21C^{RNAi}*, (F) *Ets21C^{HA}*. Discs (G-I) contain *ey-FLP* induced MARCM clones (Lee & Luo, 1999) that are positively labeled with GFP (green). Additionally, discs are stained for E-cadherin (E-cad) to visualize cell outlines (magenta). (G) *Ras^{V12} dlg^{RNAi}* expressed in wild-type clones, (H) *Ras^{V12} dlg^{RNAi}* expressed in clones homozygous mutant for *Ets21C*, (I) wild-type clones, (J) clones homozygous mutant for *Ets21C*. (K) Quantification of tumor volume for the genotypes indicated (Mann-Whitney test **** $p<0.0001$) Error bars indicate SD. (L) Ratio between number of pupae and larvae for the genotypes indicated. Depleting Ets21C increased the number of pupae compared to control tumors whereas overexpressing Ets21C lead to a decrease of larvae undergoing puparation. (A) and (C) are composites of several images to display the whole tumor size. Scale bars: (A-F) 200µm, (G-J) 100µm.

Figure 2: Knockdown of *pnt* or *aop* does not affect tumor growth

(A-D) Images of whole larvae carrying *Ras^{V12} dlg^{RNAi}* tumors in eye discs depleted for Ets21C, Pnt or Aop. Tumor cells are marked by the expression of a GFP transgene (green). Tumors express the following additional transgenes: (A) none, (B) *Ets21C^{RNAi}* (C) *pnt^{RNAi}*, (D) *aop^{RNAi}*. (E) Quantification of fluorescence intensity. Larvae were 6-7 days old (t- test **** p-value < 0.0001, * p-value <0.05, ns p-value = 0.65). (F-H) qRT-PCRs for *Ets21C*, *pnt* or *aop* to assess the efficiency of RNA knockdown. Error bars indicate SD.

Figure 3: The JNK pathway regulates Ets21C expression

(A) Schematic overview of relevant components of the JNK signaling pathway. (B) (D), (F) and (G): qRT-PCR quantification of *Ets21C* mRNA from dissected tumors with the indicated

genotypes. (C), (E), (H) and (I): qRT-PCR for *Mmp1* mRNA from dissected tumors with the indicated genotypes. Ets21C is strongly upregulated in response to Eiger (B) or the JNK pathway components Hep and Bsk (D). Upregulation of *Ets21C* in Ras^{V12} dlg^{RNAi} tumors is blocked if Jun (F) or Fos (G) is removed. Similar results were observed for the established JNK pathway target *Mmp1* (C), (E), (H) and (I). (K) and (L) qRT-PCRs for *Ets21C* or *Mmp1* of eye discs that express Egr in the *GMR* expression domain indicating that the *Ets21C* and *Mmp1* genes are also activated by the JNK pathway in a wild-type situation. Error bars indicate SD.

Figure 4: Ets21C influences the expression of JNK pathway targets

(A) Levels of *Mmp1* transcripts were reduced upon Ets21C depletion and increased if Ets21C was overexpressed in Ras^{V12} dlg^{RNAi} (*RDi*) tumors. (B) Confocal images of Ras^{V12} dlg^{RNAi} tumors with the indicated genotypes. Tumor cells express GFP and are stained for Mmp1 (red) and DAPI (blue). Mmp1 protein levels change in a similar way as *Mmp1* transcripts upon Ets21C depletion or overexpression. (C) qRT-PCRs to detect *Pvf1* and *upd1* transcripts of dissected tumors with the indicated genotypes. *Pvf1* and *upd1* are differentially expressed upon changes in Ets21C levels (D) and (E) *Mmp1*, *Pvf1* and *upd1* transcripts were also upregulated in Ras^{V12} tumors (D) or wild-type eye discs (E) overexpressing Ets21C. Scale bar: 100μm. Error bars indicate SD.

Figure 5: The DNA binding and PNT domains are essential for Ets21C function

(A) Schematic overview of the wild-type Ets21C protein structure and the truncated versions generated. (B-E) Confocal images of Ras^{V12} dlg^{RNAi} (*RDi*) tumors expressing different UAS-transgene versions of Ets21C under the control of a FLP-inducible Gal4 driver. Flp recombinase is under the control of the *eyeless* promoter that is active in eye discs. Flp recombined cells are marked by expression of a *UAS-GFP* transgene (green). (B) Control, (C) $Ets21C^{wt}$, (D) $Ets21C^{\Delta Pnt}$ and (E) $Ets21C^{\Delta Ets}$. Ets21C protein variants lacking the DNA binding domain (ΔEts) (F) or the PNT domain (ΔPnt) (G) were no longer able to induce *Mmp1*, *Pvf1* and *upd1* expression. Error bars indicate SD. (B) and (C) are composites of several images to display the whole tumor size. Scale bar: 100μm.

Figure 6: Ets21C cooperates with the JNK pathway to activate target genes

(A) Blocking the JNK pathway by expressing Bsk^{DN} in Ras^{V12} dlg^{RNAi} (*RDi*) tumors that overexpress Ets21C abrogates the induction of *Mmp1*, *Pvf1* and *upd1* expression. (B) A similar effect is observed if the JNK pathway is blocked by knocking down *Jun* and *Fos*. Error bars indicate SD. (C) Ets21C physically interacts with Jun (second lane) or Fos (third lane). Kc167 cells were transfected with the transgenes indicated, together with *tub-Gal4* and *dTak1* to activate the JNK pathway. Anti-HA immunoprecipiates were immunoblotted first with anti-FLAG or anti-GFP antibodies (part of the blot below 35kDa). GFP was used as a negative control. After stripping, the same blot was incubated with anti-HA antibodies. (D) Model of Ets21C action: Ets21C is expressed in response to JNK pathway activation as a consequence of loss of polarity. Once Ets21C is expressed, it associates with AP-1 and together they drive the expression of target genes critical for tumor growth and invasion.

Fig. S1: Ets21C phenotypes are recapitulated in wing disc tumors

(A-C) Third instar wing discs expressing different transgenes in the posterior compartment by means of *en-Gal4*. Discs are stained for E-cad (blue) and co-express GFP (green) and the following transgenes: (A) Ras^{V12}, dlg^{RNAi} , (B) Ras^{V12}, dlg^{RNAi}, $Ets21C^{RNAi}$, (C) Ras^{V12}, dlg^{RNAi}, $Ets21C^{HA}$. Similar to eye discs, wing disc tumors are suppressed upon *Ets21C* knockdown, but enhanced if Ets21C is overexpressed. Scale bar: 100μm.

Fig. S2: Ets21C causes apoptosis in a wild-type background

(A-C) Confocal images of wild-type eye imaginal discs expressing GFP (green) and stained for DAPI (blue) and cleaved Caspase 3 (Cas3, red) (A`-C`). (A) Control eye disc, (B) Disc expressing $Ets21C^{HA}$, (C) close-up of the boxed region in (B). (D-F) Images of adult eyes expressing the indicated transgenes. Ets21C induces apoptosis as evident by an increase in Cas3 activation (B and C). This phenotype is partially rescued by co-expression of Diap1 (F). Scale bar: 100μm.

Fig. S3: A knockdown of other ETS family members does not affect tumor growth

(A-F) Images of whole larvae carrying Ras^{V12} dlg^{RNAi} tumors in eye discs depleted for *Ets97D*, *Ets98B*, *Ets96B*, *Ets65A* or *E74*. Tumor cells are marked by the expression of a GFP transgene (green). (G) Quantification of fluorescence intensity. Larvae were 6-7 days old (t-

test, ns: non-significant). (H) Expression levels of *Drosophila* ETS family members in Ras^{V12} dlg^{RNAi} tumors. Data were obtained from three independent microarrays. Error bars indicate SD.

Fig. S4: Gene expression change upon Ets21C overexpression or depletion.

(A) 24 genes that are significantly (fold change $\geq$2) upregulated upon Ets21C overexpression and downregulated with $Ets21C^{RNAi}$ in Ras^{V12} dlg^{RNAi} tumors (*RDi*). (B) Differential expression of additional Pvfs and Upd cytokine genes upon changes in Ets21C levels. (C) RNAi targeting *rempA* does not affect tumor growth. Images of whole larvae are shown carrying either control Ras^{V12} dlg^{RNAi} tumors or tumors depleted for RempA.

Figure 1

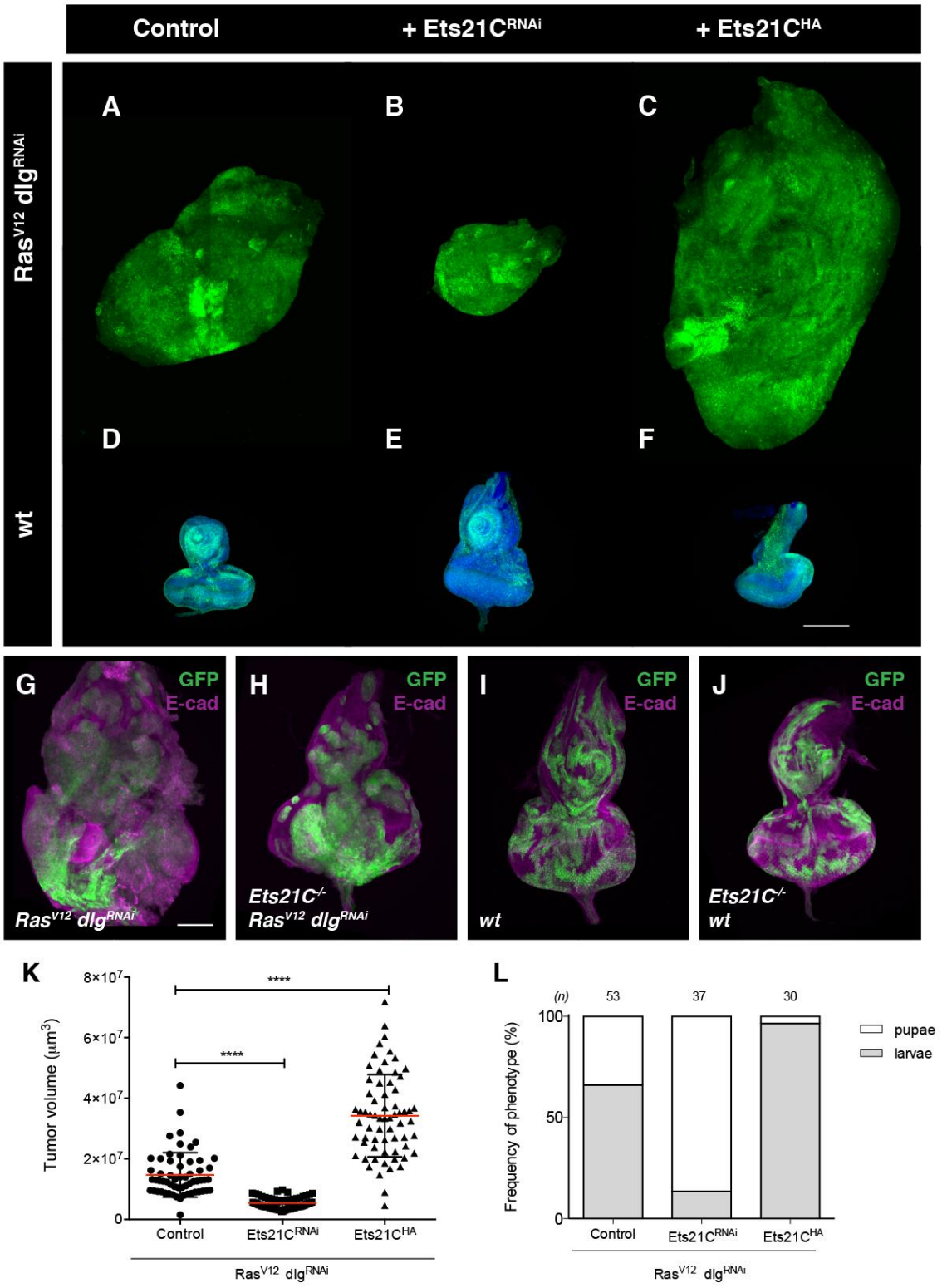
Control
+ Ets21C^RNAi
+ Ets21C^HA
Ras^V12 dlg^RNAi
wt
A
B
C
D
E
F
G
H
I
J
GFP
E-cad
Ras^V12 dlg^RNAi
Ets21C-/- Ras^V12 dlg^RNAi
wt
Ets21C-/- wt
K
Tumor volume (µm3)
8×10^7
6×10^7
4×10^7
2×10^7
0
****
****
Control
Ets21C^RNAi
Ets21C^HA
Ras^V12 dlg^RNAi
L
(n)
53
37
30
Frequency of phenotype (%)
100
50
0
pupae
larvae
Control
Ets21C^RNAi
Ets21C^HA
Ras^V12 dlg^RNAi

Figure 2

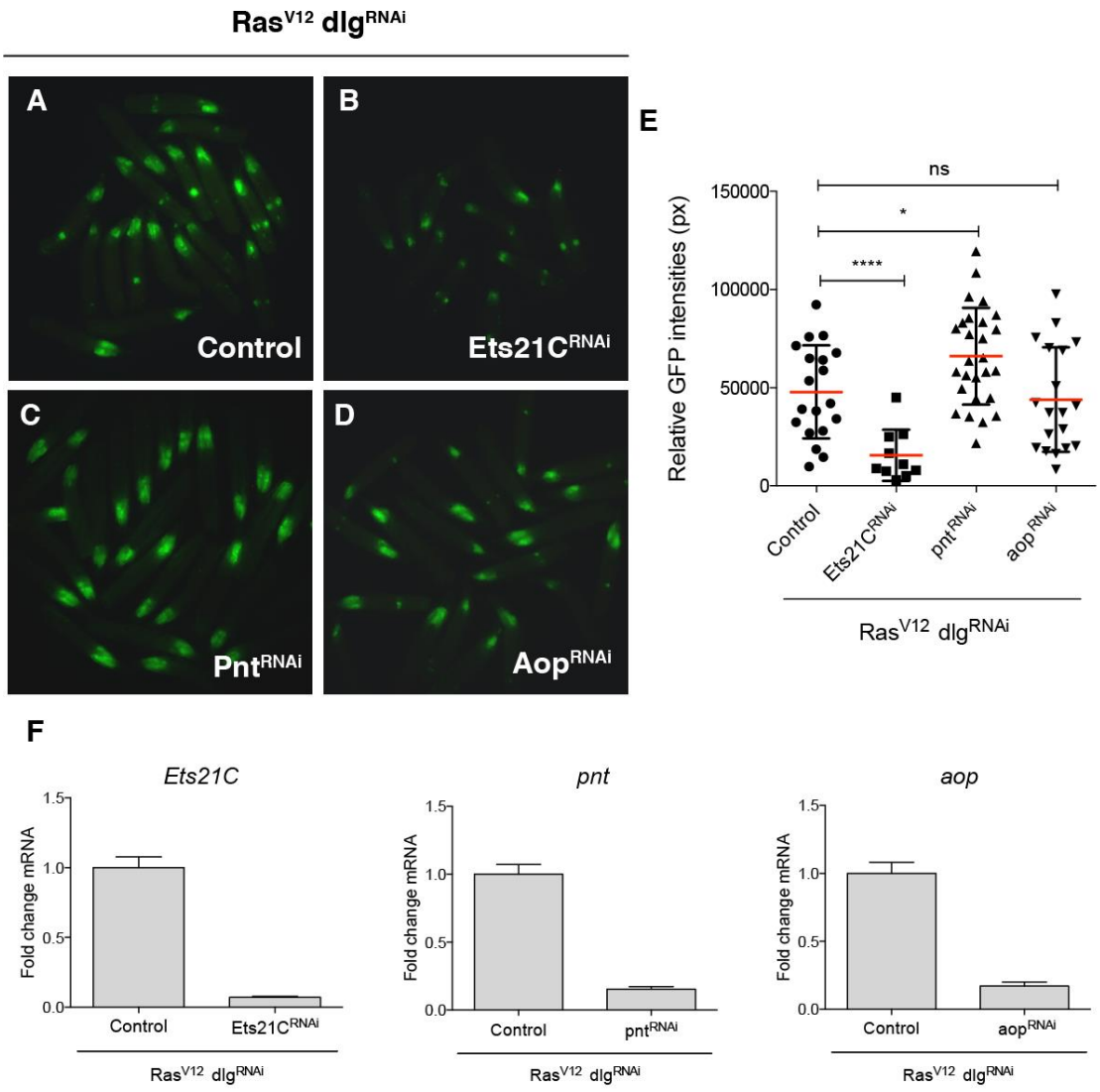
Ras^{V12} dlg^{RNAi}
A
Control
B
Ets21C^{RNAi}
C
Pnt^{RNAi}
D
Aop^{RNAi}
E
Relative GFP intensities (px)
150000
100000
50000
0
ns
*
****
Control
Ets21C^{RNAi}
pnt^{RNAi}
aop^{RNAi}
Ras^{V12} dlg^{RNAi}
F
Ets21C
pnt
aop
Fold change mRNA
1.5
1.0
0.5
0.0
Control
Ets21C^{RNAi}
pnt^{RNAi}
aop^{RNAi}
Ras^{V12} dlg^{RNAi}

Figure 3

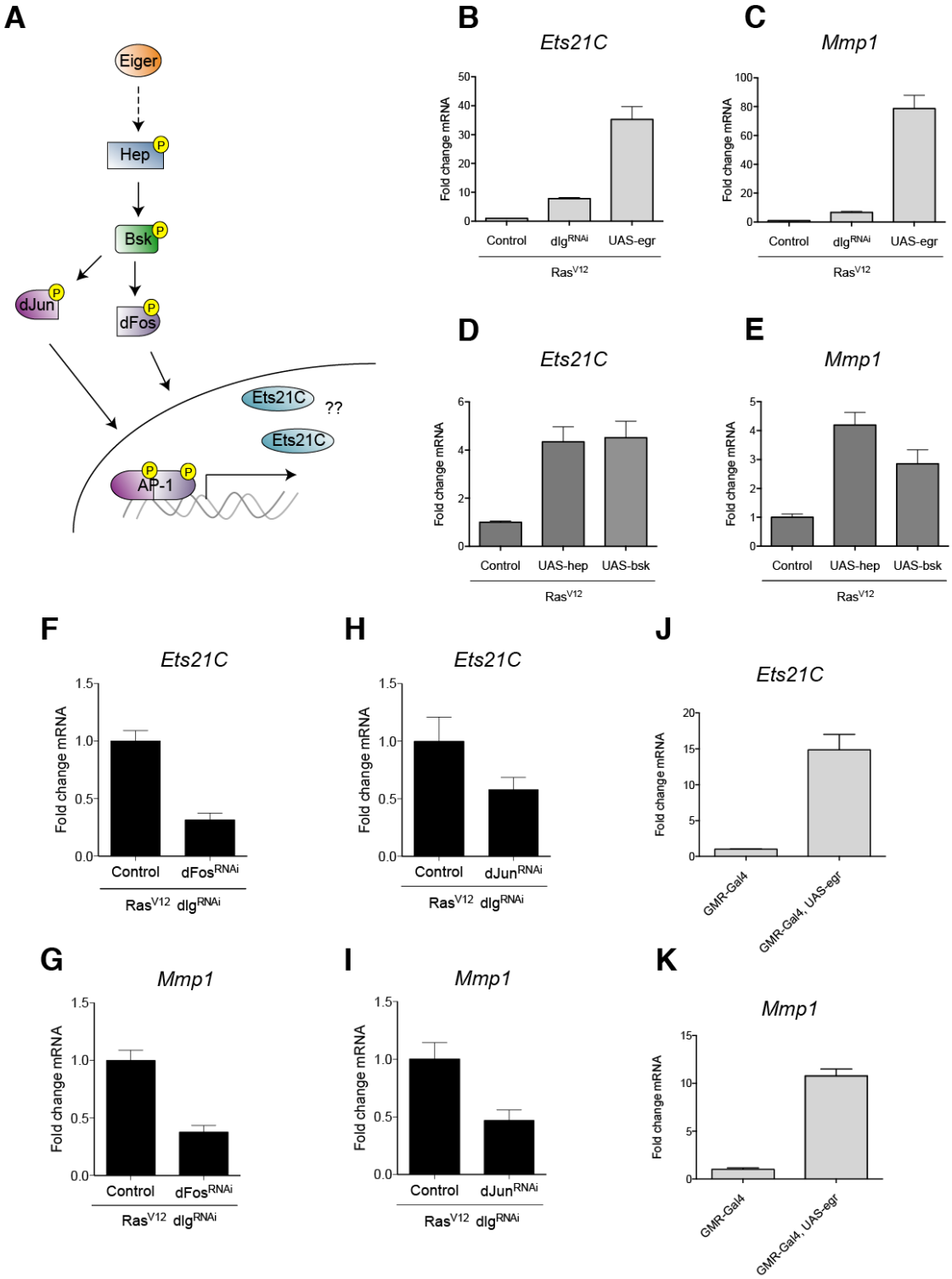
A
Eiger
Hep
Bsk
dJun
dFos
Ets21C
??
Ets21C
AP-1
B
Ets21C
Fold change mRNA
Control
dlgRNAi
UAS-egr
RasV12
C
Mmp1
Fold change mRNA
Control
dlgRNAi
UAS-egr
RasV12
D
Ets21C
Fold change mRNA
Control
UAS-hep
UAS-bsk
RasV12
E
Mmp1
Fold change mRNA
Control
UAS-hep
UAS-bsk
RasV12
F
Ets21C
Fold change mRNA
Control
dFosRNAi
RasV12 dlgRNAi
H
Ets21C
Fold change mRNA
Control
dJunRNAi
RasV12 dlgRNAi
J
Ets21C
Fold change mRNA
GMR-Gal4
GMR-Gal4, UAS-egr
G
Mmp1
Fold change mRNA
Control
dFosRNAi
RasV12 dlgRNAi
I
Mmp1
Fold change mRNA
Control
dJunRNAi
RasV12 dlgRNAi
K
Mmp1
Fold change mRNA
GMR-Gal4
GMR-Gal4, UAS-egr

Figure 4

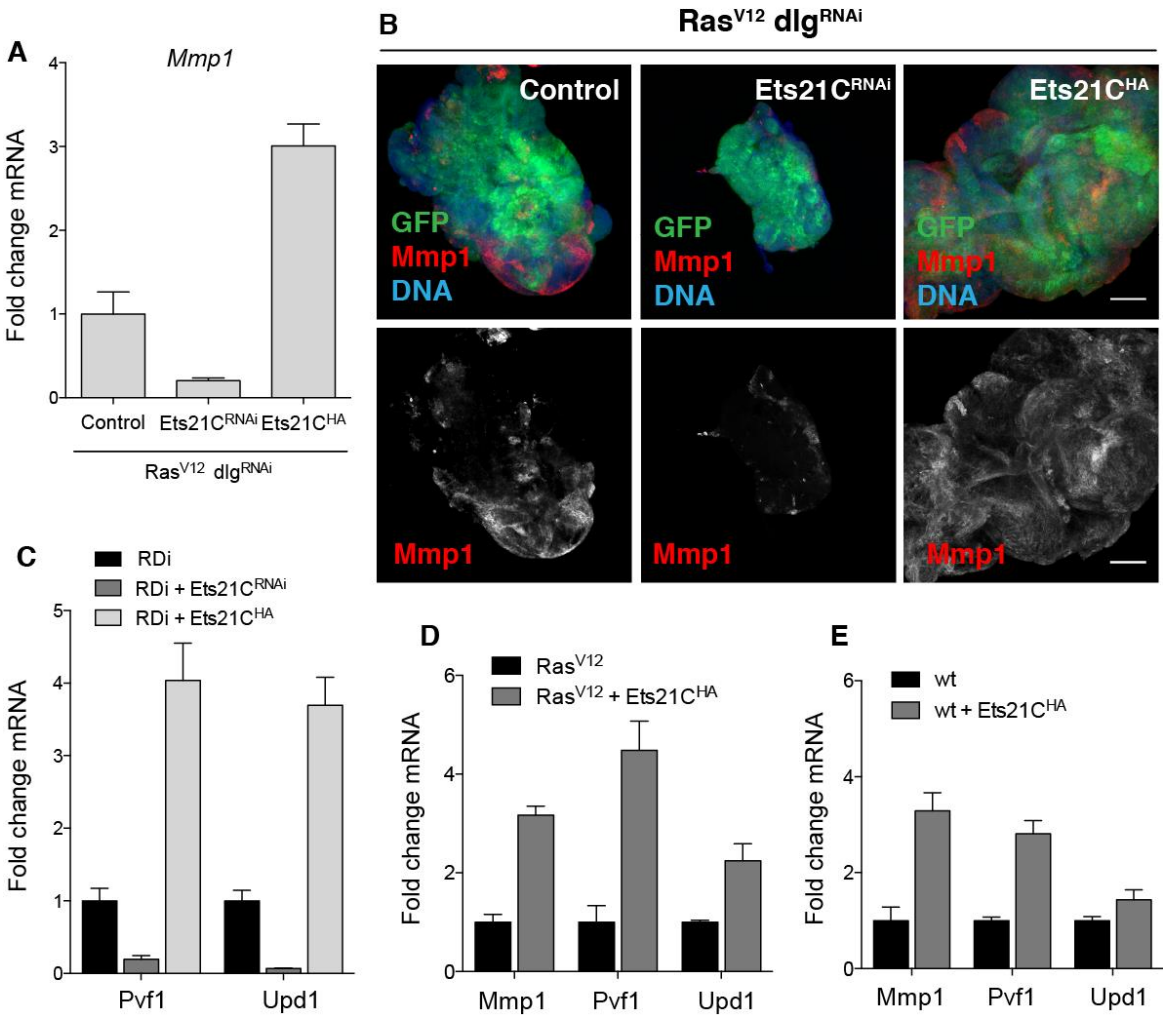
A
Mmp1
Fold change mRNA
Control
Ets21C^RNAi
Ets21C^HA
Ras^V12 dlg^RNAi
B
Ras^V12 dlg^RNAi
Control
Ets21C^RNAi
Ets21C^HA
GFP
Mmp1
DNA
Mmp1
C
RDi
RDi + Ets21C^RNAi
RDi + Ets21C^HA
Fold change mRNA
Pvf1
Upd1
D
Ras^V12
Ras^V12 + Ets21C^HA
Fold change mRNA
Mmp1
Pvf1
Upd1
E
wt
wt + Ets21C^HA
Fold change mRNA
Mmp1
Pvf1
Upd1

Figure 5

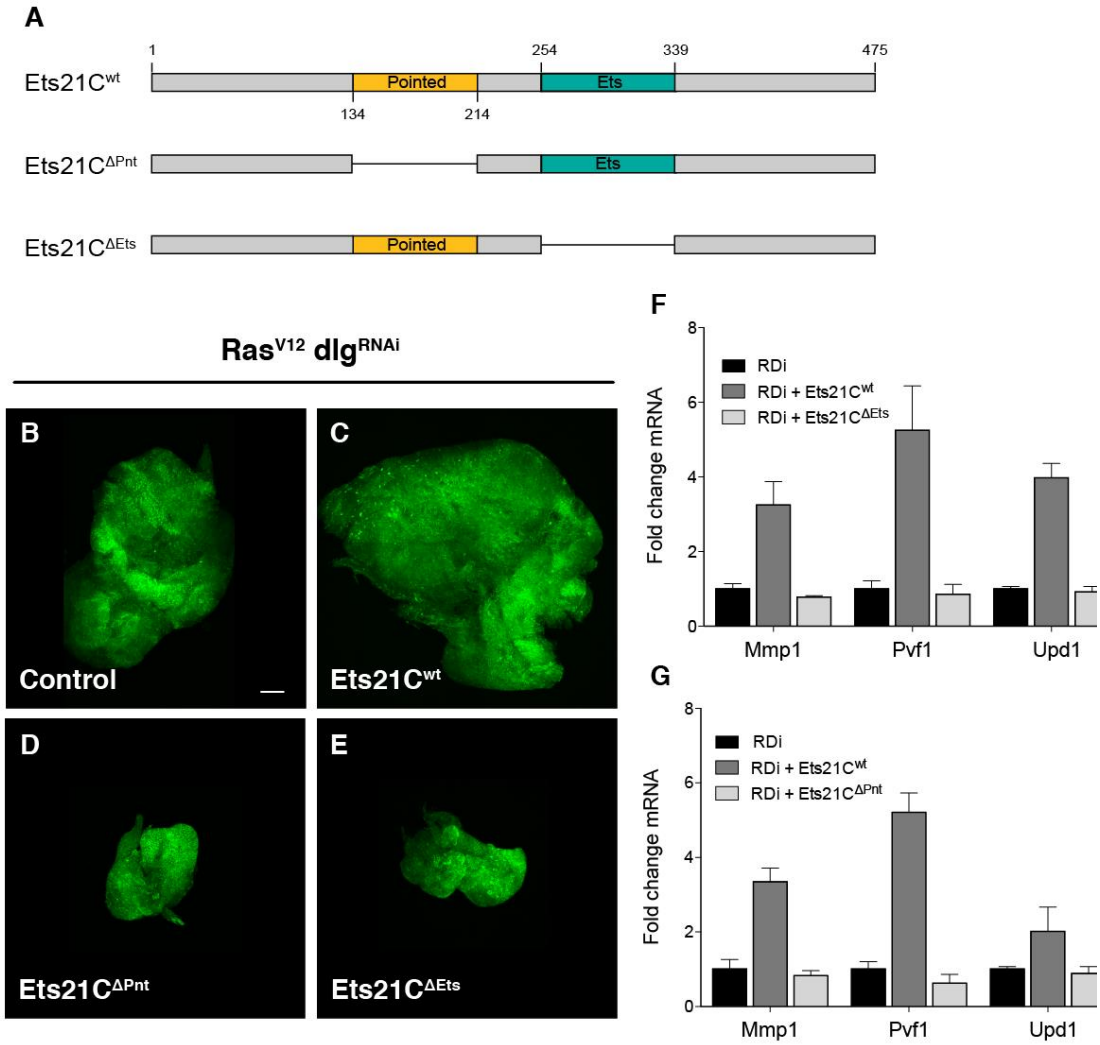
A
1
254
339
475
Ets21C^wt
Pointed
Ets
134
214
Ets21C^ΔPnt
Ets
Ets21C^ΔEts
Pointed
Ras^V12 dlg^RNAi
B
Control
C
Ets21C^wt
D
Ets21C^ΔPnt
E
Ets21C^ΔEts
F
RDi
RDi + Ets21C^wt
RDi + Ets21C^ΔEts
Fold change mRNA
Mmp1
Pvf1
Upd1
G
RDi
RDi + Ets21C^wt
RDi + Ets21C^ΔPnt
Fold change mRNA
Mmp1
Pvf1
Upd1

Figure 6

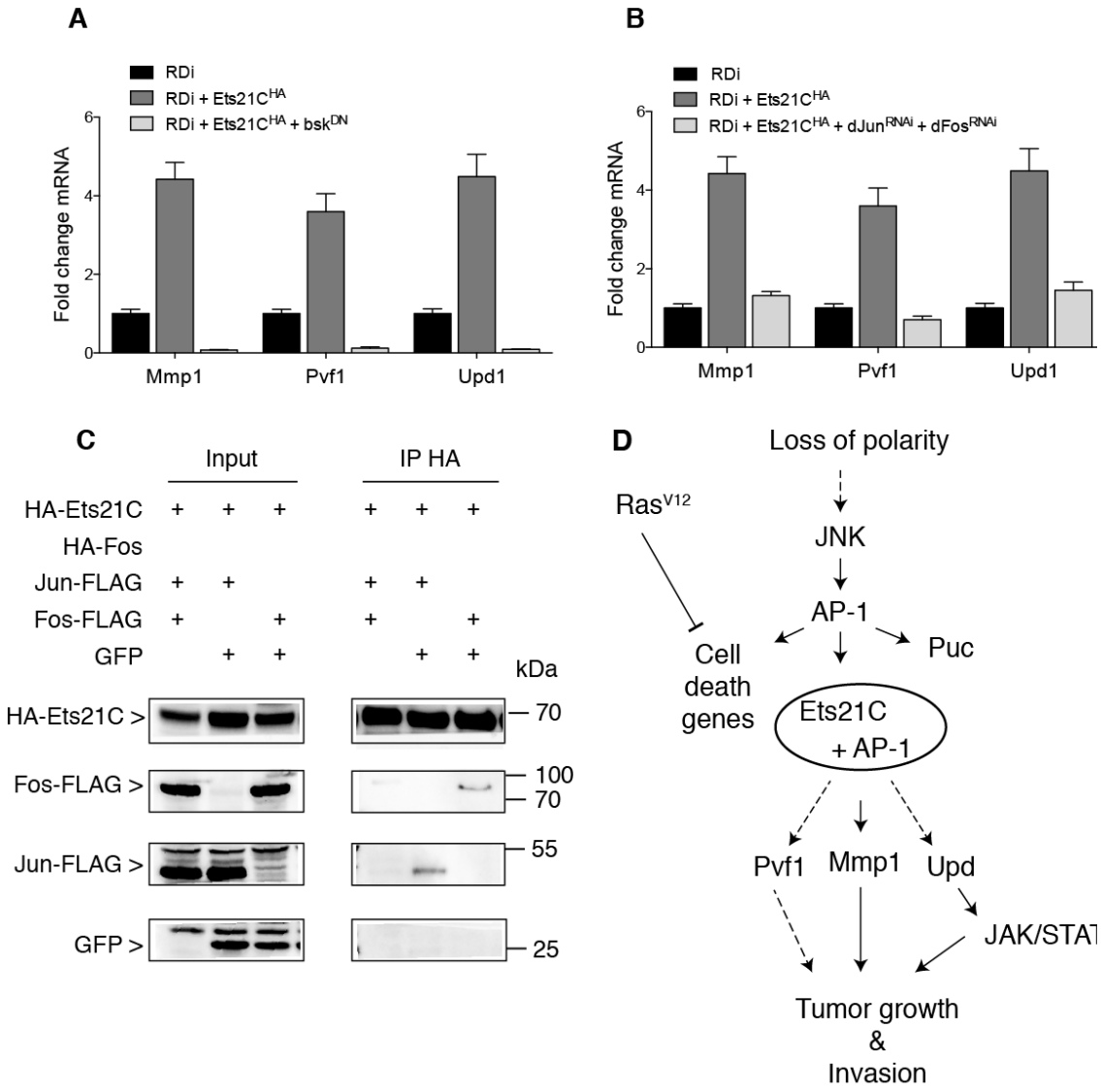
A
RDi
RDi + Ets21C^HA
RDi + Ets21C^HA + bsk^DN
Fold change mRNA
Mmp1
Pvf1
Upd1
B
RDi
RDi + Ets21C^HA
RDi + Ets21C^HA + dJun^RNAi + dFos^RNAi
Fold change mRNA
Mmp1
Pvf1
Upd1
C
Input
IP HA
HA-Ets21C + + + + + +
HA-Fos
Jun-FLAG + + + +
Fos-FLAG + + + +
GFP + + + +
kDa
HA-Ets21C >
Fos-FLAG >
Jun-FLAG >
GFP >
70
100
70
55
25
D
Loss of polarity
Ras^V12
JNK
AP-1
Puc
Cell death genes
Ets21C + AP-1
Pvf1
Mmp1
Upd
JAK/STAT
Tumor growth & Invasion

Supplementary Figure 1

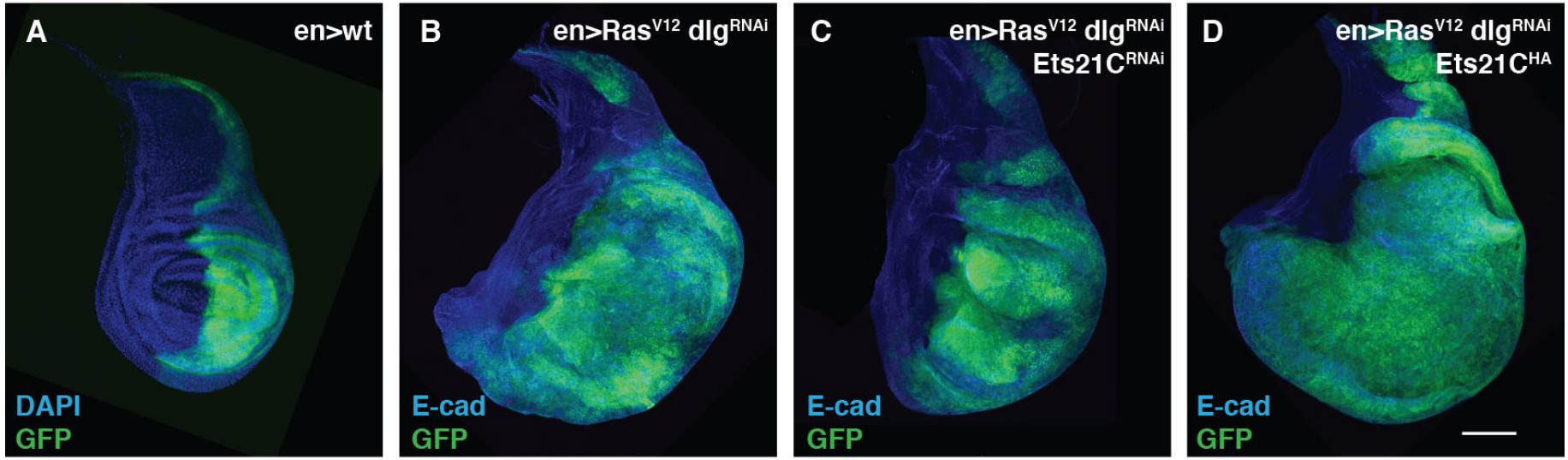

Supplementary Figure 2

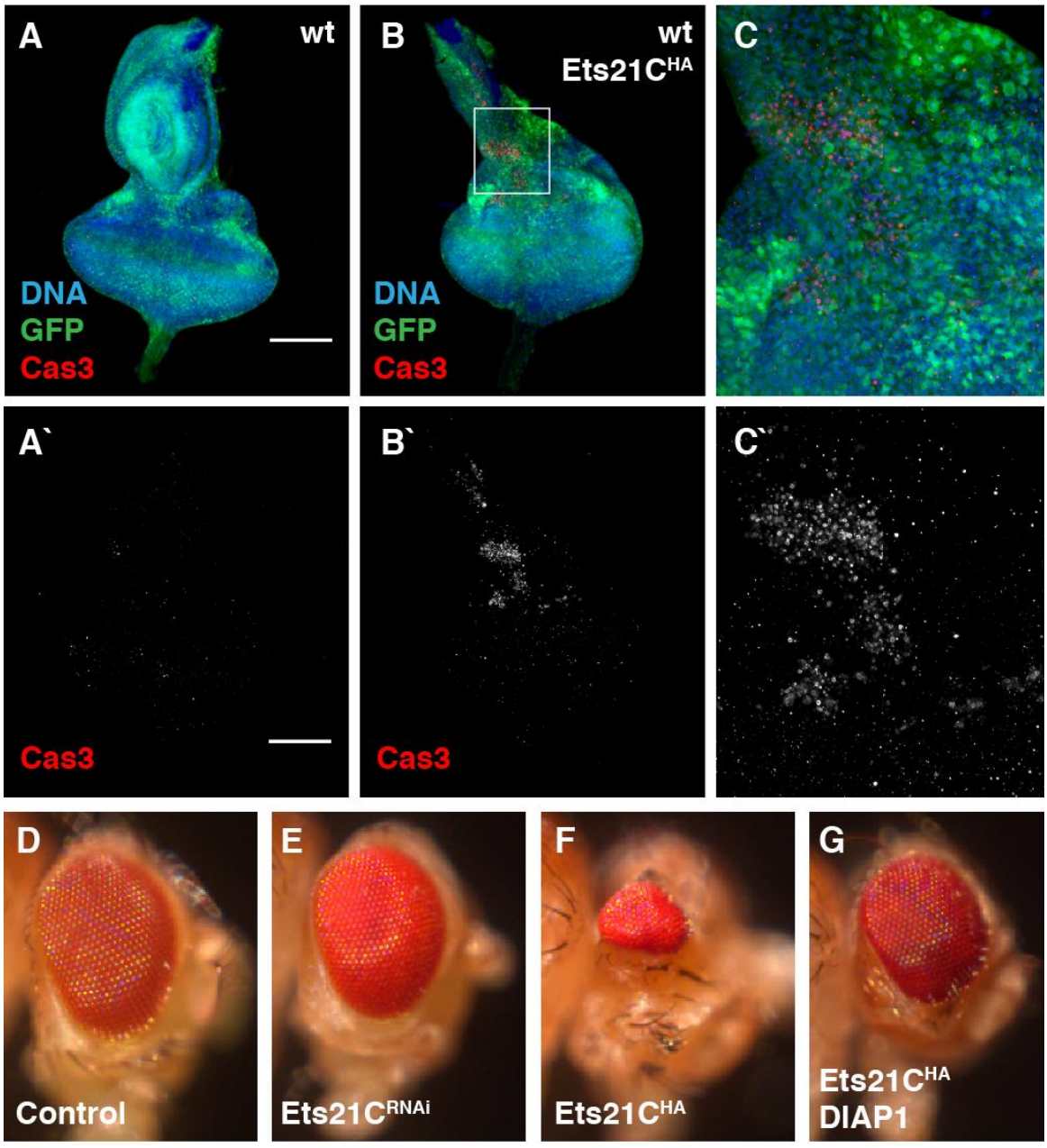

Supplementary Figure 3

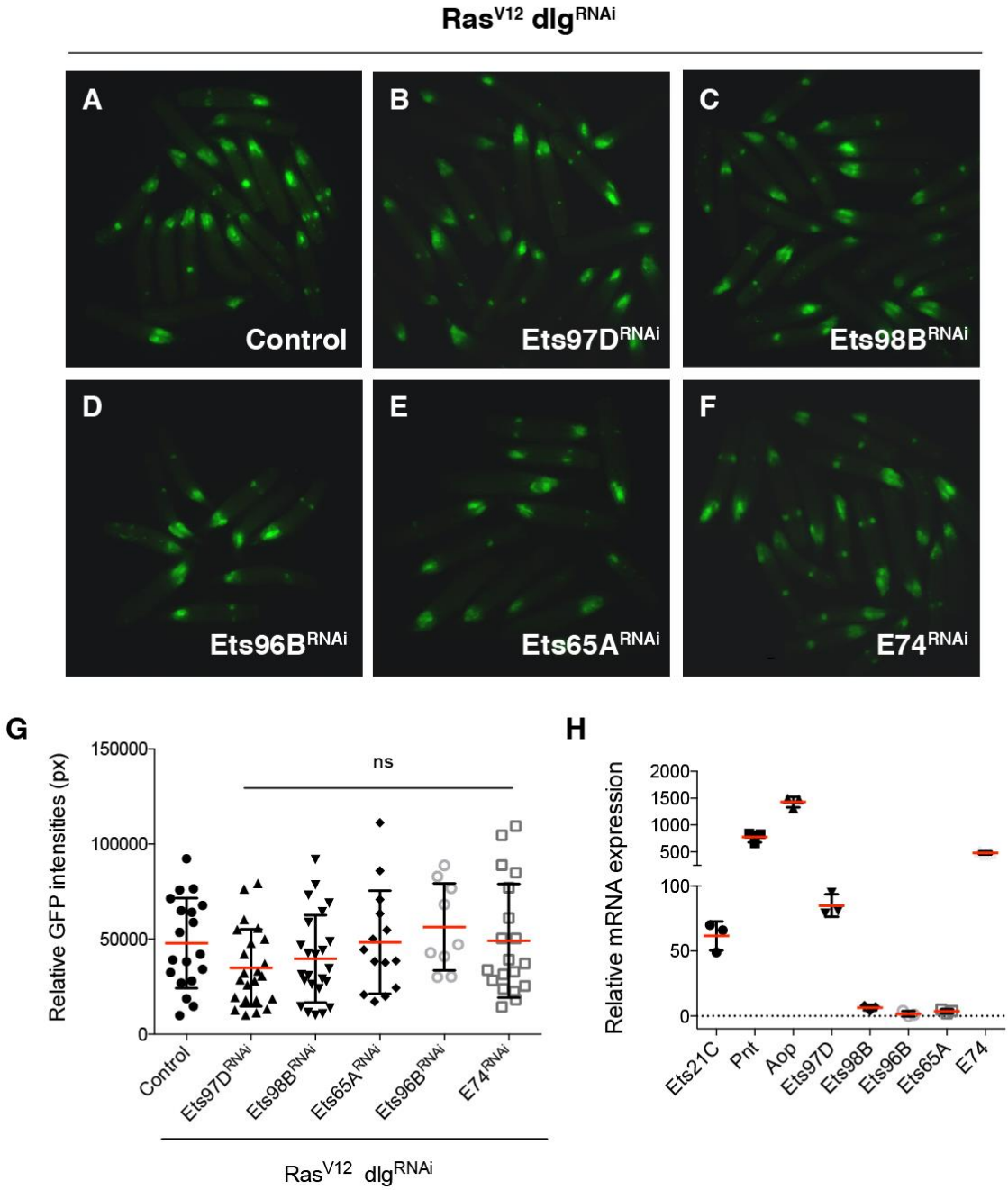

Supplementary Figure 4

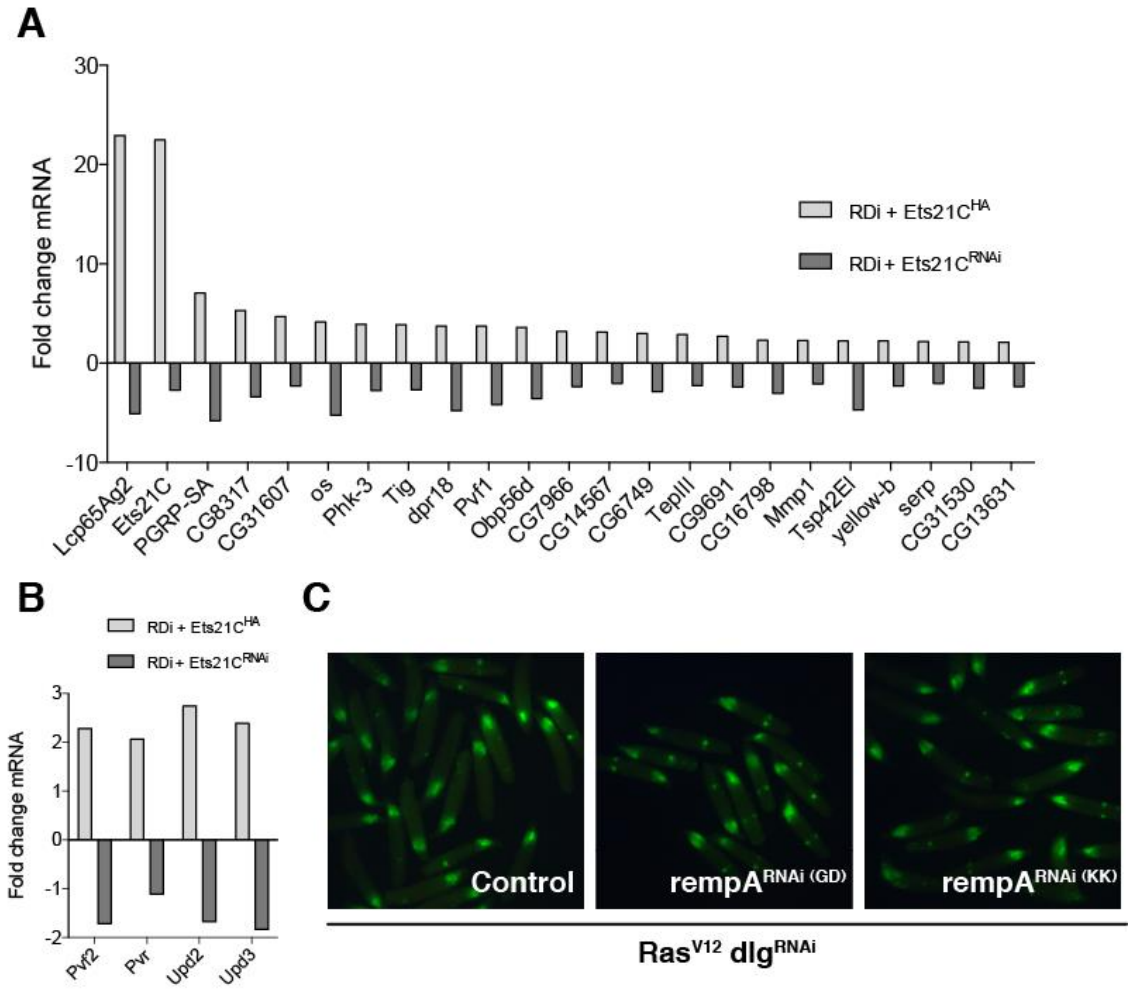

2.1.1 Ets21C is able to partially substitute for the loss of polarity in tumors

To further investigate the role of Ets21C in neoplastic tumors, we asked whether modifications of Ets21C levels had an impact on discs expressing only Ras^{V12} or dlg^{RNAi}. To test this, we generated Ras^{V12} or dlg^{RNAi} expressing tumors with the same system as for the Ras^{V12} dlg^{RNAi} tumors. Ras^{V12} tumors overgrew to a similar extent as Ras^{V12} dlg^{RNAi} tumors, but they stayed as a two dimensional layer in contrast to Ras^{V12} dlg^{RNAi} tumors that grow in three dimensions (Fig. 4, A). Eye discs expressing a dlg^{RNAi} develop into small neoplastic tumors that resemble *dlg* mutant eye discs (Fig. 4, D) (Bilder, 2000). Interestingly, co-expression of Ras^{V12} and $Ets21C^{HA}$ induced three dimensional growth and a slight increase in tumor size, but not to the same extent as the combination of Ras^{V12} and dlg^{RNAi} (Fig. 4, C). Depletion of Ets21C did not have any obvious effects on Ras^{V12} tumors (Fig. 4, B). Yet, combined with the dlg^{RNAi}, $Ets21C^{RNAi}$ seemed to partially restore shape and structure of the eye disc (Fig. 4, E, arrow). In contrast, overexpression of Ets21C together with the dlg^{RNAi} strongly reduced the size of dlg^{RNAi} tumors, reminiscent of its effects in a wild-type background (Fig. 4, F and Fig. 1, F). Taken together, these results suggest that Ets21C is partly sufficient to induce neoplastic growth in combination with Ras^{V12} and that its depletion it is able to ameliorate the phenotype of dlg^{RNAi} tumors. Particularly the effect on dlg^{RNAi} tumors is interesting and further supports our hypothesis that Ets21C is required to drive JNK pathway outputs. However, for a more detailed confirmation, we would need to generate dlg^{RNAi} tumors in an *Ets21C* mutant background and test if tumor development can be blocked from the onset.

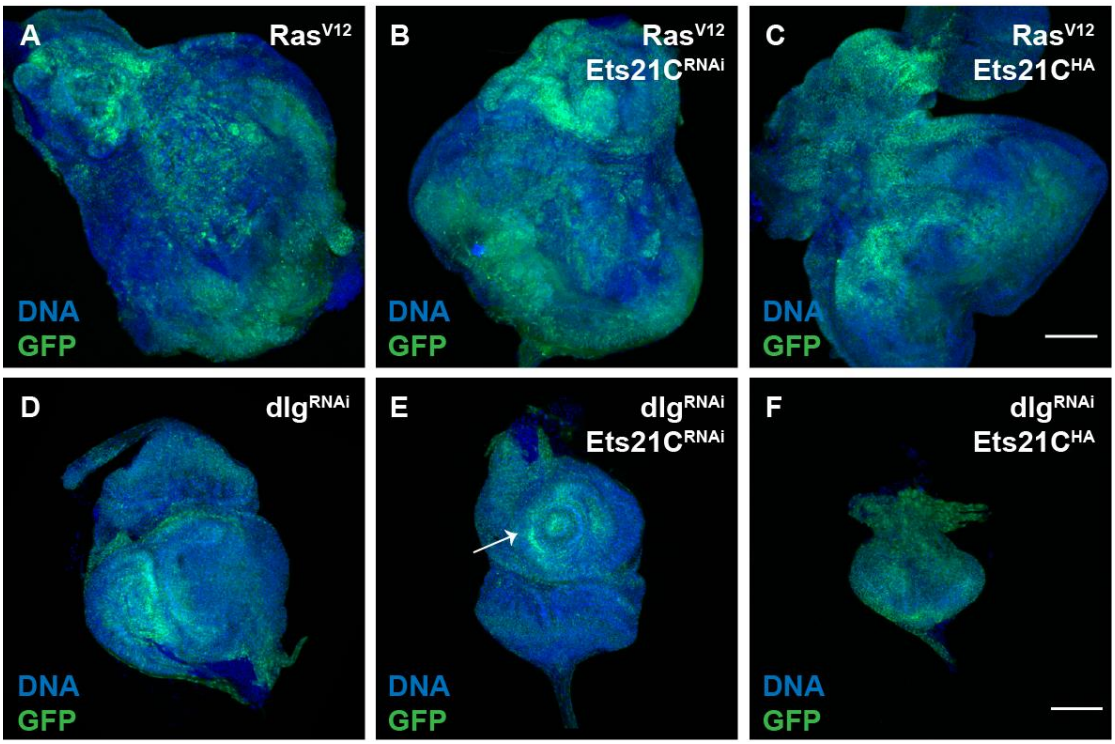

Figure 4: Effects of Ets21C depletion and overexpression on *Ras^{V12}* and *dlg^{RNAi}* tumors. (A) - (C) Confocal images of control *Ras^{V12}* tumors (A) or *Ras^{V12}* tumors expressing *Ets21C^{RNAi}* (B) or *Ets21C^{HA}* (C). Ets21C^{HA} seems to enhance growth of *Ras^{V12}* tumors. (D) – (F) Confocal images of control *dlg^{RNAi}* tumors (D) or tumors co-expressing *Ets21C^{RNAi}* (E) or *Ets21C^{HA}* (F). Tumors express GFP (green) and are stained for DAPI (blue). A depletion of Ets21C partially inhibits the effects of the *dlg^{RNAi}* as more wild-type looking structures re-appear (arrow). In contrast, overexpression of Ets21C results in much smaller *dlg^{RNAi}* tumors. Scale bar: 100 µm.

2.1.2 Ets21C occupies ETS binding sites in the Mmp1 promoter

We have shown that Ets21C induces the expression of *Mmp1* and other target genes downstream of the JNK pathway. Furthermore, we could demonstrate that the DNA binding domain of Ets21C is required for target gene induction and that Ets21C can physically interact with the JNK transcription factor AP-1, making it likely that Ets21C directly activates these targets. In order to demonstrate binding of Ets21C to the regulatory regions of *Mmp1*, we performed chromatin-immunoprecipitations (ChIP) of *Ras^{V12} dlg^{RNAi}* tumors that co-expressed *Ets21C^{HA}* followed by qPCR of putative *Mmp1* regulatory regions. We designed five primer pairs over a stretch of about 7000 bp upstream of the translational start site that contained

consensus Ets21C and/or AP-1 binding sites (Fig. 5, A). The primer pair that was located 7000 bp away from the translational start site served as a control pair, where we would not expect to find an enrichment of Ets21C. We also made sure that the amplicons covered the four putative AP-1 sites that, based on reporter studies, had previously been shown to regulate *Mmp1* expression (Uhlirova & Bohmann, 2006). Due to the very small amounts of DNA that were recovered after the ChIP, we have only performed one successful qPCR run, but these preliminary results are very promising. Two primer pairs that covered a region with several AP-1 and two Ets21C binding sites showed a 20 fold enrichment of Ets21C at these sites, compared to the control primer pair (Fig. 5, B and C). Although we have to repeat this experiment to reach meaningful conclusions, the results strongly hint towards binding of Ets21C at *Mmp1* regulatory regions. In addition, it will be important to extend these studies to the regulatory regions of the two other targets, *Pvf1* and *upd1* (see Fig. 4 and Fig. 5 of section 2.1). If Ets21C also binds directly here our model would be strengthened.

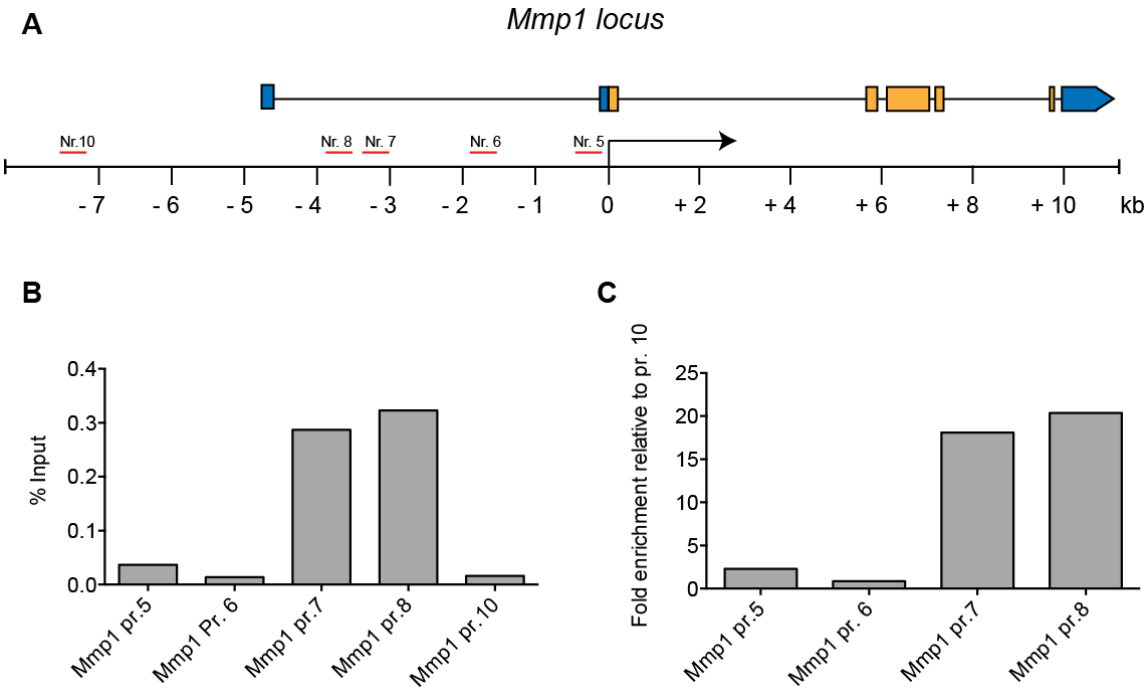

Figure 5: Enrichment of Ets21C at *Mmp1* regulatory regions. (A) Schematic overview of the *Mmp1* locus. Note that the region upstream of the translational start has been streched in length to better visualize the PCR amplicons (red lines Nr. 5 – Nr. 10). (B) and (C) qPCRs of Ets21C ChIP and input samples with the primer pairs indicated. Results are shown as % input (B) and as fold enrichment relative to the control primer pair Nr. 10 (C).

2.1.3 Ets21C activity is not regulated by phosphorylation on a consensus MAPK motif

A common theme among ETS proteins is the regulation of their activity via post-translational modifications. Those comprise phosphorylation, glycosylation, sumoylation, acetylation and ubiquitination. Phosphorylation is the most frequent modification found and in the majority of cases is executed by MAP kinases. The activities of two *Drosophila* ETS proteins, Pnt and Aop, crucially depend on phosphorylation by MAPK. We therefore wondered whether Ets21C activity was also dependent on phosphorylation. MAPKs phosphorylate threonine or serine residues that occur in the motif P/LXT/SP (X can be any amino acid). Ets21C contains a consensus MAPK phosphorylation motif (PVTP) close to the C-terminus. In addition, it contains a PNT domain that, besides other functions, is known to serve as sites for MAPK-mediated phosphorylation; in the case of human ETS-1 the PNT domain provides a docking site for ERK2 (Seidel, 2002). To test if Ets21C activity depends on phosphorylation of the potential MAPK motif identified, we generated a protein variant in which we replaced threonine 468 with alanine (Ets21C^{T468A}). As described earlier, overexpression of *Ets21C* in *Ras^{V12} dlg^{RNAi}* tumors leads to an enlargement of tumor size (Fig. 6, A). When we expressed the mutant *Ets21C^{T468A}*, tumors grew to the same size as when we expressed wild-type *Ets21C* (Fig. 6, A and B). Similar result were also obtained in wild-type eye imaginal discs. *Ets21C^{T468A}* caused the same phenotype as *Ets21C^{WT}* (Fig. 6, C and D). From these results we conclude that Ets21C function is not critically regulated by phosphorylation at this site. We can, however, not exclude that Ets21C is phosphorylated on a different, atypical MAPK sites or by another kinase that recognizes a different motif.

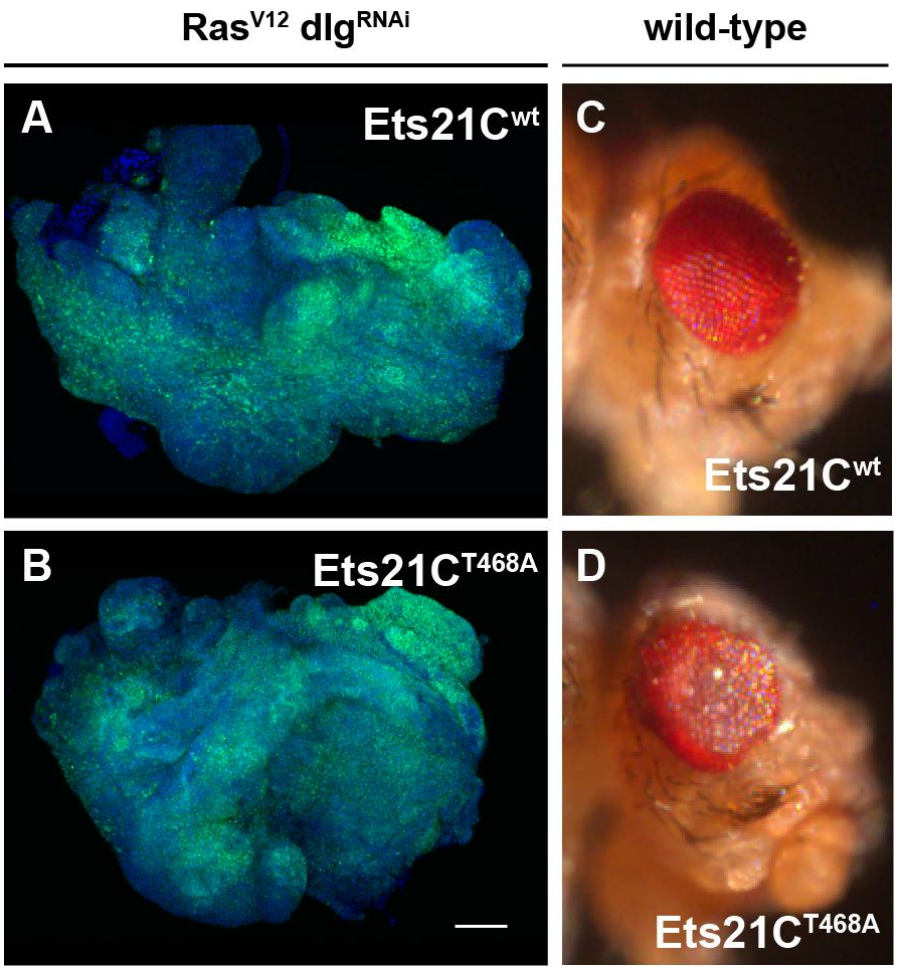

Figure 6: Ets21C is not phosphorylated at position 468. (A) and (B) Confocal images of *Ras^{V12} dlg^{RNAi}* tumors co-expressing *Ets21C^{wt}* (A) or *Ets21C^{T468A}*(B). Images of adult eyes expressing *Ets21C^{wt}* or *Ets21C^{T468A}*. Tumors express GFP (green) and are stained for DAPI (blue). (A) and (B) are composites of several images to display the whole tumor size. Scale bar: 100 µm.

2.1.4 Removing a part of Ets21C close to the N-terminus enhances its transcriptional activity

When we generated the protein variants that lack the ETS or the PNT domain (see manuscript Figure 5), we also generated a variant that is lacking a part close to the N-terminus (Ets21C$^{\Delta SOCS}$) that, based on SMART, has previously been annotated as a suppressor of cytokine signaling (SOCS) domain known from human SOCS4 and SOCS5. SOCS proteins are known to regulate JAK/STAT signaling (Stec & Zeidler, 2011). Because JAK/STAT signal-

ing is relevant to *Ras^{V12} dlg^{RNAi}* tumors, we aimed to analyse the function of the SOCS domain (Wu *et al*, 2010). However, at present the same region of the protein is only annotated as a region of low complexity and a direct alignment with the respective domains of SOCS4 and SOCS5 did show an obvious conservation (data not shown). Nevertheless, we still thought it might be interesting to see if this part of the protein is important for the function of Ets21C. Interestingly, the variant lacking the "SOCS" domain even more strongly induced target genes compared to full-length Ets21C (Fig. 7, D) and also enhanced tumor growth further (Fig. 7, A-C). The above results leave several possibilities open regarding the function of the "SOCS" domain, it could function as repressive domain, provide a platform for interactions with a transcriptional repressor or be subject to post-translational modifications. Further experiments will be necessary to distinguish between these possibilites.

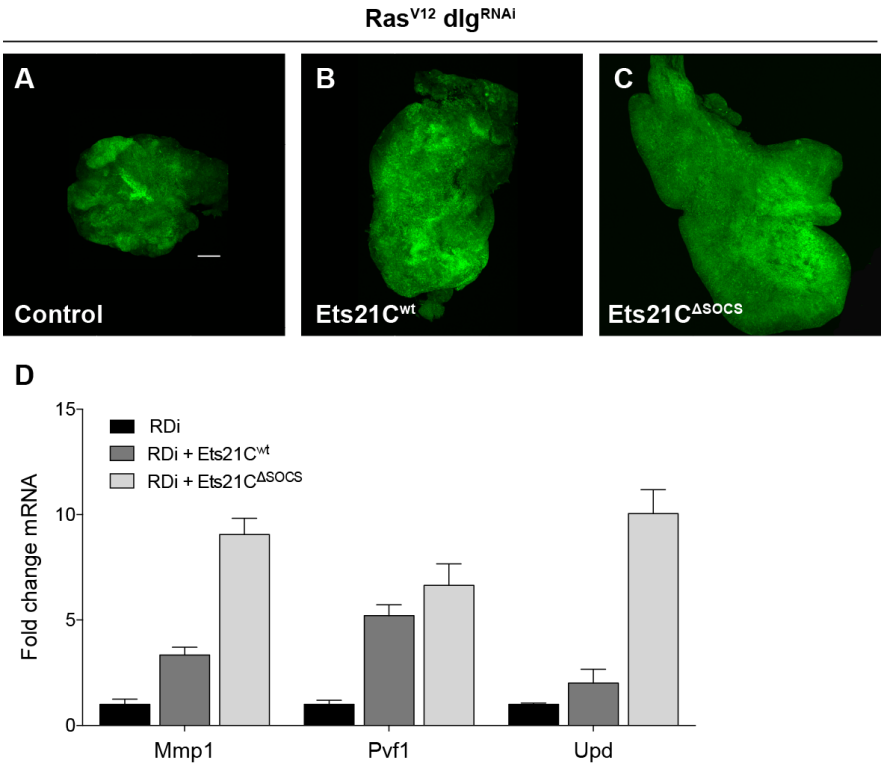

Figure 7: The N-terminal part of Ets21C restricts its activity. (A) - (C) Confocal images of control *Ras^{V12} dlg^{RNAi}* tumors (A) or tumors co-expressing *Ets21C^{wt}* (B) or *Ets21C$^{\Delta SOCS}$* (C). Ets21C$^{\Delta SOCS}$ caused larger tumors than Ets21C^{wt} and also increased expression of *Mmp1*, *Pvf1* and *upd1* as assessed by qPCR (D). Tumors express GFP (green). (B) and (C) are composites of several images to display the whole tumor size. Scale bar: 100 μm.

2.1.5 Mutagenesis of AP-1 binding sites in the Ets21C regulatory region

We and others have genetically shown that Ets21C expression is regulated by the JNK pathway, but no one has provided evidence for a direct binding of the JNK transcription factor AP-1 to the regulatory region of *Ets21C* (Boutros *et al*, 2002; Kulshammer *et al*, 2015). A careful investigation of this issue is especially important, as a very recent study proposed that *Ets21C* expression is regulated by EGFR/Ras signaling (Jin *et al*, 2015). AP-1 recognizes a core consensus motif of 5`- T(G/T)AGTCA(C/T) - 3` as determined by bacterial-one hybrid assays (Zhu *et al*, 2011). We identified four AP-1 consensus binding sites in the *Ets21C* regulatory region (Fig. 8, A). To test if these sites are required for Ets21C expression, we isolated the *Ets21C* gene region including upstream and downstream sequences up to the neighboring genes and deleted the predicted AP-1 binding sites (Fig. 8, A and B, further referred to as $Ets21C^{\Delta AP\text{-}1}$). We have previously generated an *Ets21C* null allele and found that growth of Ras^{V12} dlg^{RNAi} cells mutant for *Ets21C* is impaired (see Fig.1 section 2.1). To demonstrate that specific AP-1 sites govern *Ets21C* expression, we plan to express the wild-type *Ets21C* or $Ets21C^{\Delta AP\text{-}1}$ in Ras^{V12} dlg^{RNAi} $Ets21C^{-/-}$ cells. If *Ets21C* expression depends on the presence of these specific AP-1 sites, we would expect that only wild-type *Ets21C* rescues the observed growth defects, but not $Ets21C^{\Delta AP\text{-}1}$. Such a result would strongly hint towards binding of the *Ets21C* regulatory regions by AP-1. To further support this idea, we could try to identify the responsible AP-1 site, by deleting each of the four sites individually. A different, but complementary approach would be to perform chromatin immunoprecipitations (ChIP) of AP-1 either in Ras^{V12} dlg^{RNAi} tumors or wild-type cells with an active JNK pathway and test for an enrichment of *Ets21C* regulatory regions by qPCR.

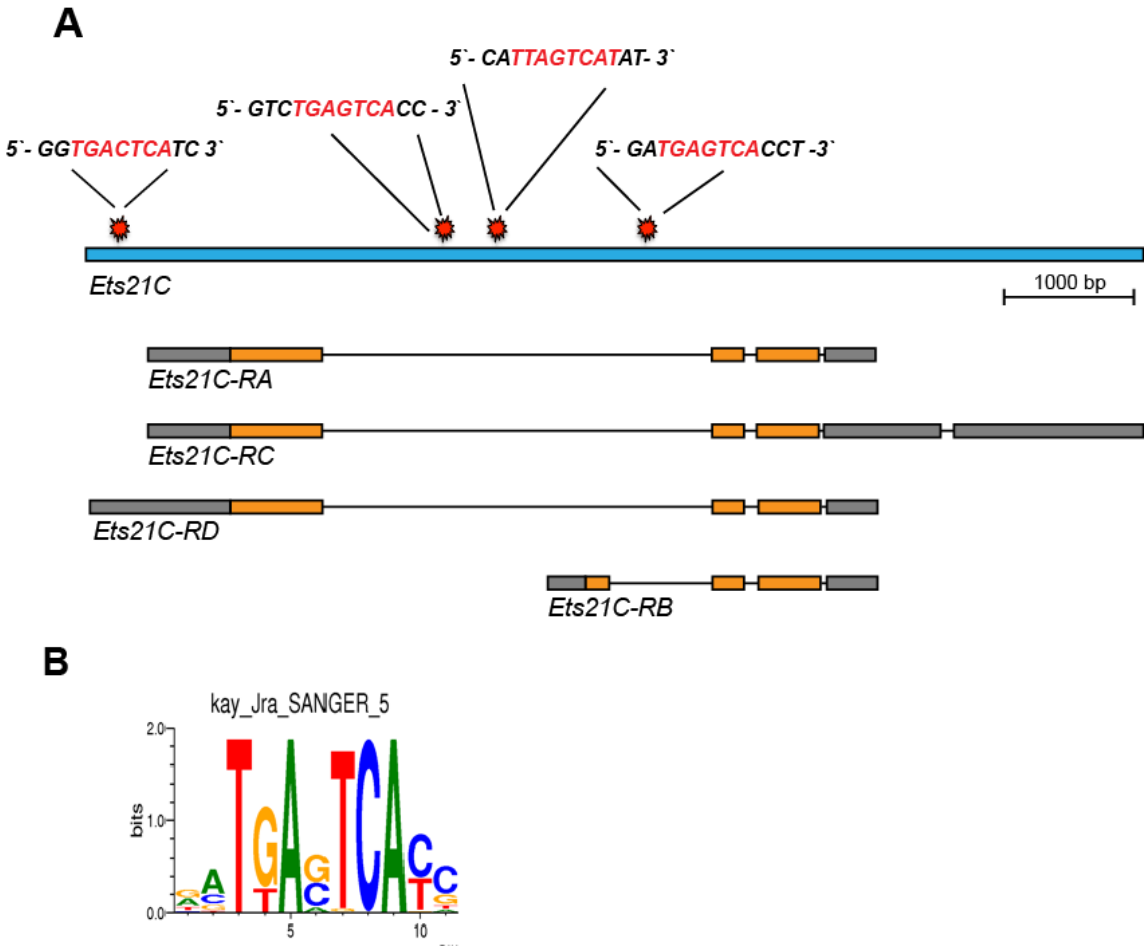

Figure 8: AP-1 binding sites in the Ets21C gene region. (A) Schematic representation of the *Ets21C* gene region. Red stars highlight consensus AP-1 binding motifs. (B) AP-1 binding motif as determined by bacterial one-hybrid assays.

2.1.6 Concluding remarks and future experiments

This study demonstrates the process of evaluating and functionally characterizing a candidate gene retrieved from an RNAi screen. By combining genetic, molecular biology and biochemical techniques, we have successfully unravelled Ets21C function and established a model explaining how Ets21C can induce and sustain tumor growth. Besides the experiments described in 2.1.5 to demonstrate a direct regulation of *Ets21C* expression by AP-1, we can think of further points that could be investigated and that would strengthen our model of Ets21C action:

(1) Is Ets21C required for the initial induction on of *Mmp1*, *Pvf1* and *upd1* expression or does it only reinforce and sustain AP-1-dependent transcription?
We have shown that a depletion of Ets21C reduces *Mmp1*, *Pvf1* and *upd1* expression levels as does a block of JNK signaling by expressing bsk^{DN} in Ras^{V12} dlg^{RNAi} tumors. However, we never directly compared the extent of transcript reduction between the two situations. As it is not possible to remove a gene product completely by RNAi, it would be better to measure *Mmp1*, *Pvf1* and *upd1* expression in $Ets21C^{-/-}$ mutant tumor cells and compare to expression levels of tumor cells that co-express bsk^{DN}. If target gene expression is entirely abolished in both cases, we could assume that Ets21C is necessary to initiate *Mmp1*, *Pvf1* and *upd1* expression.

(2) Do AP-1 and Ets21C co-occupy regulatory regions of target genes? Although we have found a physical interaction between AP-1 and Ets21C, we do not know if and how they bind to regulatory regions of target genes. To answer this question we would need to generate ChIP-seq or ChIP-qPCR data for both transcription factors and show that they bind to the same DNA sequences. ChIP analyses demand a vast amount of starting material, which is difficult to collect from *in vivo* samples. We discuss solutions to this issue in a subsequent section (2.2.3.3) about immunoprecipitations followed by mass spectroscopy, where we would face a similar challenge.

(3) Are both, Jun and Fos cooperating with Ets21C to drive target gene expression or only one of them? Despite having found a physical interaction between Ets21C and Jun and Fos, we do not know yet if Jun and Fos are both necessary to drive target gene expression. Since Jun and Fos can bind to each other, it is feasible that both associate with Ets21C by default, but only one of them is functionally important. We have tested such a scenario by co-expressing Ets21C and either an RNAi targeting *jun* or *fos*, but have obtained ambiguous results, most likely due to incomplete knockdown of the gene product (data not shown). To obtain more convincing data, we would need to generate Ras^{V12} dlg^{RNAi} tumors that overexpress Ets21C in a *jun* or *fos* mutant background. This is in principal possible, but will be genetically challenging. Dominant-negative alleles of Fos and Jun would be an alternative option as they might exert a stronger effect than RNAi, but are easier to combine with other transgenes than a mutant allele.

(4) Which target genes activated by Ets21C are causing cell death in a wild-type background? We have identified Ets21C target genes that can explain its effects on Ras^{V12} dlg^{RNAi} tumors, but we have not elucidated yet, which Ets21C targets are causing apoptosis in a wild-type background. As they are important for tumor growth, we have tested whether overexpression of Mmp1, Pvf1 or Upd1 would cause a similar phenotype as Ets21C in wild-type eye disc, but we did not observe comparable effects (data not shown). Another gene that is strongly upregulated upon *Ets21C* expression and downregulated by the $Ets21C^{RNAi}$ is *peptidoglycan recognition protein SA (PGRP-SA)*. PGRP-SA usually recognizes bacterial particles and induces an immune response by activating the Toll pathway (Michel *et al*, 2001). The JNK pathway has been proposed to activate immune signaling pathways (Delaney *et al*, 2006). In eye imaginal discs it has been shown that the JNK pathway is provoking cell death directly by activating pro-apoptotic factors, but also indirectly by activating the Toll pathway, which induces apoptosis via an independent mechanism (Wu *et al*, 2015). As *PGRP-SA* is induced by Ets21C, we reasoned that this could lead to Toll pathway activation and ultimately cause cell death. To test this hypothesis, we have expressed Ets21C in flies heterozygous mutant for *PGRP-SA*. This combination leads to a less severe Ets21C overexpression phenotype, which would support our hypothesis (data not shown). However, we need to perform additional experiments before any conclusions can be drawn about a functional relationship between Ets21C and PGRP-SA.

2.2 Evaluation of Alrm as a potential regulator of tumor growth

This part describes the characterization of *astrocytic leucin-rich repeat module* (*alrm, CG11910),* an additional suppressor that was retrieved from the initial RNAi screen. We also outline what follow up experiments could be done to further elucidate its function. We generated a deletion and an overexpression line for this gene and performed a few preliminary tests to determine how Alrm could affect tumor growth. Due to time constraints we decided to focus on analysing Ets21C and therefore stopped to work on Alrm.

2.2.1 Background

Alrm is a small gene lying in the intronic region of another gene, *Fur1*. The gene is usually expressed in a subtype of longitudinal glial cells that have recently been classified as *Drosophila* astrocytes, but its molecular function is unknown (Stork *et al*, 2014).
Interestingly, a former master student in the lab, George Busslinger, identified this gene in a screen for possible new components of the *Drosophila* TNF pathway. Egr is the *Drosophila* ortholog of mammalian TNF-α. Targeted expression of Egr in larval tissues activates the JNK pathway and causes apoptosis (Moreno *et al*, 2002; Igaki *et al*, 2002). Wengen (Wgn) was proposed to be the respective receptor for Egr. (Kanda *et al*, 2002). However, the evidence was inconclusive (see Section 2.3 for more information). In a yeast-two hybrid screen for additional Egr pathway components, using DTRAF2 as bait, Alrm was found as an interaction partner. DTRAF2 is an adaptor protein that likely links the downstream kinases Misshapen (Msn) to the upstream TNF receptor (Liu *et al*, 1999). Yet, expression of a dsRNA targeting *alrm* in eye imaginal discs that were mutant for *wgn* and overexpressed Egr could not rescue the small eye phenotype caused by Egr induced apoptosis. Since RNAi rarely removes the gene product completely, it is possible that small amounts of Alrm are still enough to transmit the Egr signal. Since depletion of *alrm* suppressed Ras^{V12} dlg^{RNAi} tumors, we aimed to investigate this phenotype more closely and to re-evaluate a role for Alrm in the activation of the JNK pathway.

2.2.2 Results

2.2.2.1 Alrm overexpression results in smaller tumors but does not affect normal tissue growth

Alrm has been shown to be specifically upregulated in neoplastic tumors (Master Thesis J. Toggweiler). As a knockdown of *alrm* lead to smaller tumors, we asked whether overexpression of *alrm* would increase tumor size. To this end, we generated flies overexpressing *alrm* cDNA under UAS control. Surprisingly, extra Alrm also resulted in smaller tumors (Fig. 9. A-C). This could be due to a dominant-negative effect of the overexpression. Such effects are often observed with overexpression constructs, especially if multiple proteins act in a complex and the overexpressed protein might engage in non-functional complexes with some of the other components.

Next, we asked whether the effects of knocking down or overexpressing *alrm* were specific for the tumors or whether it would also cause growth defects in a wild-type tissue. Wild-type eye imaginal discs depleted for *alrm* were growing normal and developed into a wild-type looking adult eye (Fig. 9, D and E). This was not unexpected as *alrm* expression is almost absent in wild-type discs (Master Thesis J. Toggweiler). Overexpression of Alrm also did not result in any obvious defects (Fig. 9, D and F). Taken together, these results suggest that *alrm* is not required for normal growth and development of eye imaginal disc tissue.

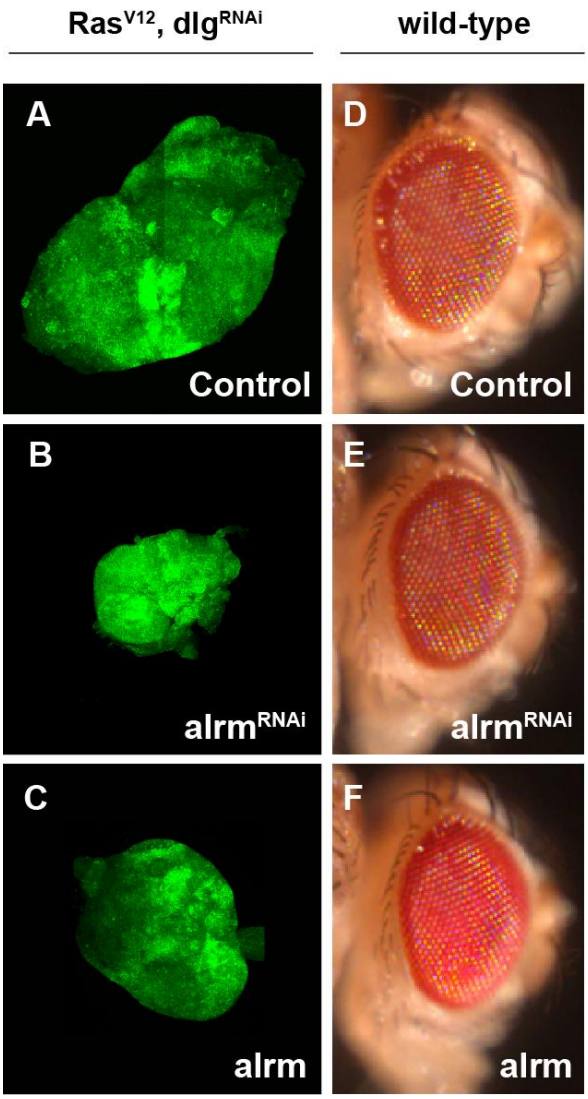

Figure 9: Phenotypes of an Alrm depletion or overexpression in neoplastic tumors and wild-type eye discs. (A) – (C) Confocal images of control *Ras^{V12} dlg^{RNAi}* tumors (A) or tumors co-expressing *alrm^{RNAi}* (B) or *alrm cDNA* (C). (D) – (F) Images of wild-type *Drosophila* eyes (D) or eyes expressing an *alrm^{RNAi}* (E) or alrm cDNA (F). Tumors express GFP (green). Depletion or overexpression of *Alrm* reduces tumor growth, but does not affect normal development. (A) is a composites of several images to display the whole tumor size.

2.2.2.2 Generating a deletion for *alrm* and independent RNAi lines

As RNAi might cause off-target effects, we generated an *alrm* mutant allele to confirm the phenotypes we observed with the RNAi line. For this, we used PiggyBac (PBac) insertion lines that contain FRT sites. Expression of Flp recombinase induces recombination between the FRT sites of two PiggyBacs in trans, deleting the genomic region in between (Parks *et al*, 2004). With this strategy, we deleted a 45 kB piece that contained the entire *alrm* gene region. Unfortunately, due to the positions of the PBac elements, we could not avoid to delete three other genes along with *alrm* (Fig. 10).

In addition, we designed four independent RNAi constructs to complement the RNAi we used in the original screen (Fig. 10).

Flies mutant for *alrm* and flies carrying the independent RNAi lines have not yet been tested in the tumor background.

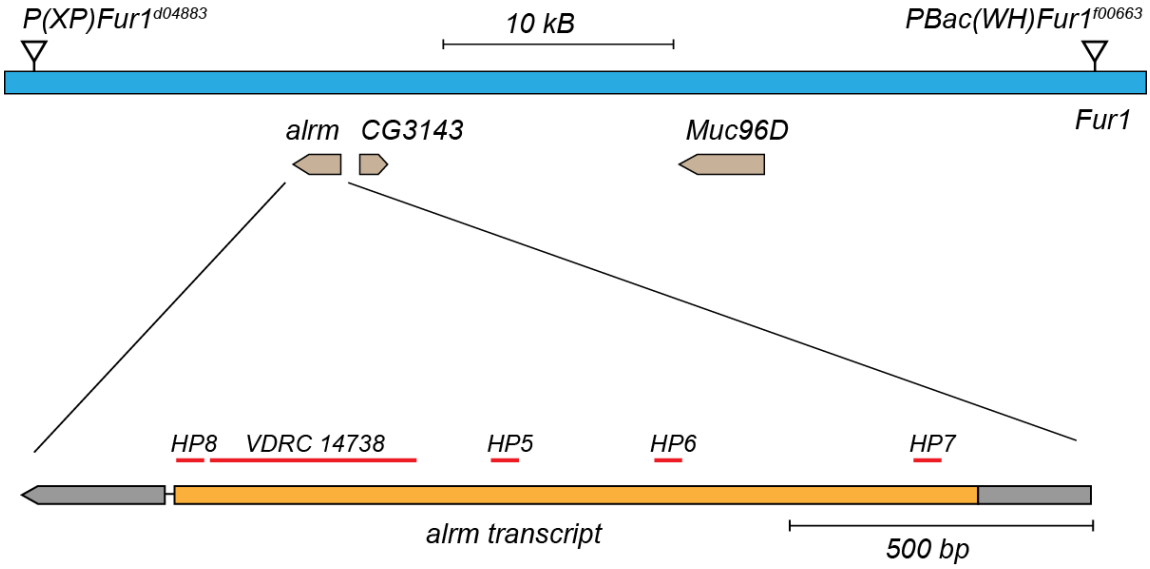

Figure 10: Overview of the genomic region surrounding *alrm* and a close up of the *alrm* transcript. Red bars indicate the target sites of the RNAi lines. Arrows mark the insertion sites of the PiggyBacs.

2.2.2.3 A depletion of *alrm* does not suppress the Egr small eye phenotype

Alrm has been found in a previous screen to interact with dTRAF2 and could therefore modify the activity of the JNK pathway. A common tool to test for effects on JNK signaling is the *GMR-egr* phenotype. Targeted expression of Egr in the *GMR*-expression domain causes apoptosis and an ablation of eye tissue leading to a very small adult eye. We therefore tested whether a knockdown of *alrm* would modify the GMR-egr phenotype, but did not see an increase in eye size (Fig. 11, A and B). As the GMR-egr phenotype can be variable, we quantified eye size by measuring the area of the eye, but we did not find a significant difference with or without the $alrm^{RNAi}$ (Fig. 11, C). These results suggest that *alrm* does not play a role in transducing the Egr signal to induce cell death genes.

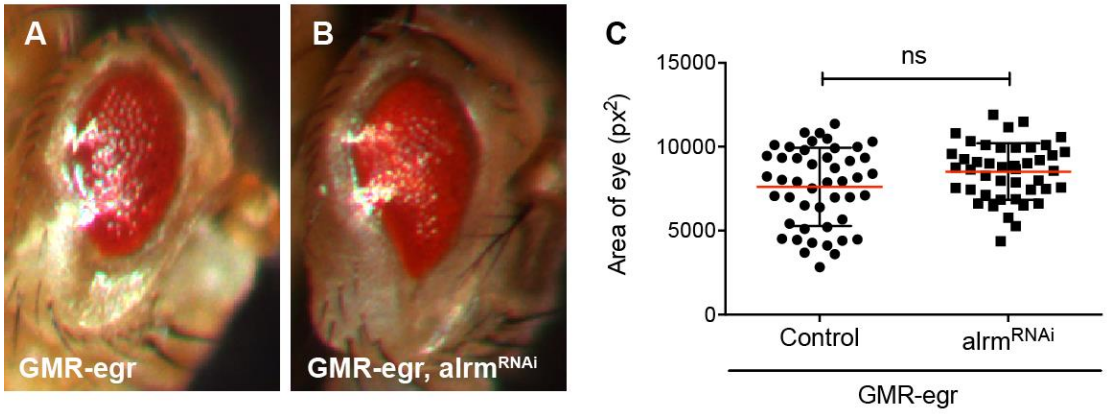

Figure 11: A knockdown of *alrm* does not suppress the Egr small eye phenotype. (A) and (B) Images of whole eyes expressing GMR-Gal4, UAS-egr (A) or GMR-Gal4, UAS-egr and $alrm^{RNAi}$ (B). (C) Quantification of eye size.

2.2.2.4 Depletion of *alrm* reduces Mmp1 and Ets21C expression levels

Although we did not observe an effect on the GMR-egr phenotype following *alrm* knockdown, we still wanted to test if JNK pathway activity was reduced in the tumor background. Alrm might not influence the expression of apoptosis inducers, but the expression of other genes that are activated through the JNK pathway and that support tumor growth. To this end, we monitored the expression of *Mmp1*, a known target gene of the JNK pathway, by qPCR in control tumors and tumors that co-expressed the $alrm^{RNAi}$. Upon Alrm depletion, *Mmp1* levels were reduced about 50% suggesting that Alrm influences JNK pathway activity (Fig. 12, A). The expression of *Ets21C*, another JNK target, was also reduced, but to a lesser extent than *Mmp1* (Fig.12, B).

In addition to the qPCR, we performed antibody stainings for Mmp1 in tumors that were depleted for Alrm and compared protein levels to control tumors. Similar to the qPCR we found a reduction of Mmp1 protein in tumors with an *Alrm* knockdown (Fig.12, C and D). However, as the Mmp1 distribution is patchy, it is not entirely clear if there is only less protein because the tumors are smaller or whether protein levels are indeed reduced. This issue needs further clarification, for example by quantifying the staining intensities with respect to the size of the tumors or by directly quantifying the amounts of protein with a western blot.

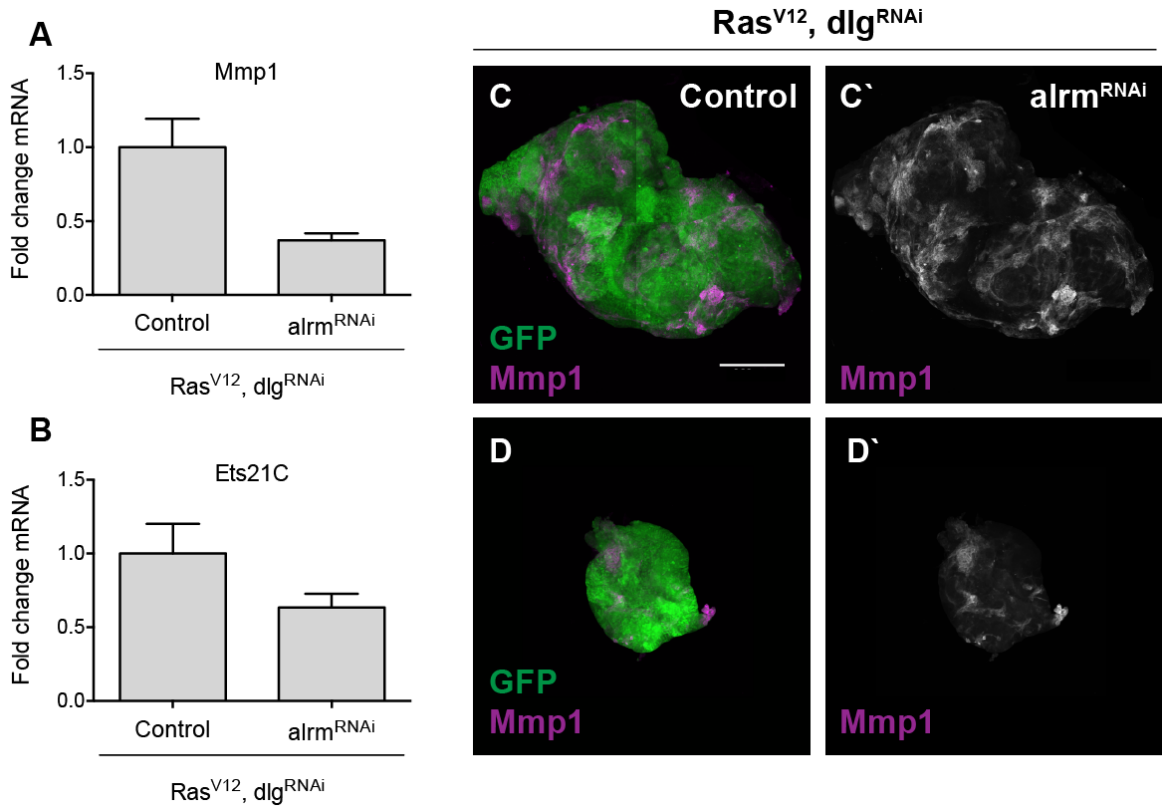

Figure 12: A knockdown of *alrm* seems to reduce the expression of JNK pathway target genes. (A) and (B) qPCR for *Mmp1* and *Ets21C* of control tumors and tumors expressing *alrm*^{RNAi} reveal a reduced expression of *Mmp1* and *Ets21C* in tumors depleted for Alrm. (C) and (D) Confocal images of control tumors and tumors expressing an *alrm*^{RNAi} that are stained for Mmp1. Mmp1 protein is still present in tumors depleted for Alrm. (C) is a composites of several images to display the whole tumor size. Scale bar: 100 µm.

2.2.3 Conclusions and future experiments

We have shown that Alrm is important for tumor growth, as depletion decreased tumor size (Master Thesis, Janine Toggweiler). Moreover, we made attempts to elucidate Alrm function and found a potential link with the JNK pathway, as $alrm^{RNAi}$ decreased the expression of the JNK target Mmp1. However, these results need to be confirmed and supplemented with additional data to uncover the role of Alrm in tumor growth. The following sections will give an outlook of what experiments could be done in the future to address this.

2.2.3.1 Using CRISPR/Cas9 to delete *alrm*

While this project was in progress, a new system for gene editing termed clustered regularly interspaced short palindromic respeat (CRISPR)/CRISPR-associated (Cas) has been adapted for use in *Drosophila* and makes targeted mutagenesis very simple (Bassett & Liu, 2014). Several techniques have been used and described to deliver Cas9 and the sgRNA in flies: 1.) co-injection of plasmids carrying Cas9 or the sgRNA into embryos (Gratz *et al*, 2013), 2.) co-injection of in vitro transcribed Cas9 mRNA and sgRNA (Bassett *et al*, 2013; Yu *et al*, 2013), 3.) injection of sgRNA plasmids into flies that stably express Cas9 in the germline (Sebo *et al*, 2014; Ren *et al*, 2013), and 4.) two transgenic fly strains are used: flies with germline Cas9 expression are crossed to flies with ubiquitous expression of the sgRNA (Kondo & Ueda, 2013). As the only limitation of targeting is the PAM sequence "NGG", virtually any gene can be targeted with the CRISPR/Cas9 system.

Generating a null-allele of *alrm* has been challenging, as the gene lies in the intron of another gene and the available PBac elements are located in such a way that a deletion of additional genes was inevitable. However, with the CRISPR/Cas9 system, it will be possible to introduce specific mutations only in the *alrm* gene. To check if suitable sequences for designing sgRNAs for *alrm* were available, we made use of the sgRNA design tool of the Drosophila RNAi screening center (DRSC, http://www.flyrnai.org/crispr2/). We found four potential sgRNA sequences in the *alrm* coding sequence (CDS) that are predicted to have no off-target effects (Fig. 13). We cloned these sgRNAs into vectors that stably integrate into the fly genome. Once transgenic lines have been established, they can be crossed to flies expressing

Cas9 in their germline. With this strategy, the generation of an *alrm* null allele should be straight forward. Besides generating a mutant allele, the CRISPR/Cas9 system could also be used to tag endogenous Alrm with, for example, GFP to investigate its localization and to monitor its expression.

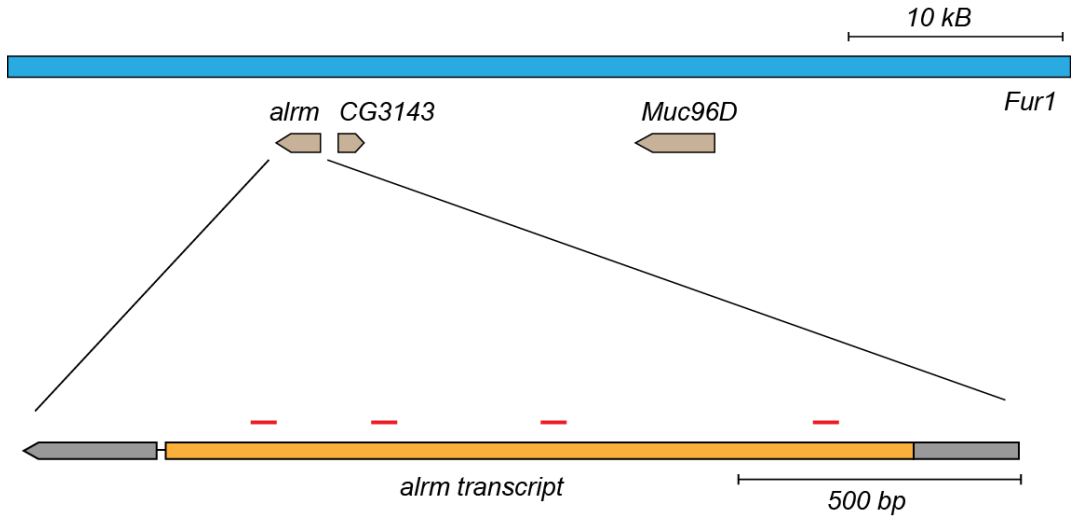

Figure 13: Schematic overview of the *alrm* gene region. The location of potential sgRNAs in the *alrm* coding sequence is indicated with red bars.

2.2.3.2 More detailed analysis of *alrm* mutant tumors

Once we have established *alrm* mutant flies and tested whether tumors homozygous mutant for *alrm* show growth defects, we will continue analysing *alrm* function. Growth of Ras^{V12} dlg^{RNAi} tumors is regulated by the PI3K and the MAPK pathways that are activated downstream of Ras signaling as well as the JNK pathway, which is induced by loss of polarity and leads to the activation of the JAK/STAT pathway (Igaki *et al*, 2006; Willecke *et al*, 2011; Wu *et al*, 2010). In addition, it has been shown that Hippo pathway activity is suppressed in cells with polarity defects leading to increased growth (Sun & Irvine, 2011). Based on results described in 4.2.2.4, we have evidence that a depletion of *alrm* might disturb JNK pathway activity as assesseed by expression of the JNK pathway target *Mmp1*, but Mmp1 protein levels were apparently similar to those in control tumors (see Fig. 12). To clarify this issue, we want to analyse *Mmp1* expression in *alrm* mutant tumor cells to be sure that *alrm* function is abol-

ished and to exclude off-target effects of the RNAi. Besides the JNK pathway, we also want to test the MAPK, PI3K, JAK/STAT and the Hippo pathways for changes in activity. To this end, we will monitor the expression of pathway target genes with qPCRs and immunostainings. With these experiments, we hope to better understand how a loss of *alrm* affects tumor growth.

2.2.3.3 Searching for interactors of Alrm – immunoprecipitation and mass spectrometry

Alrm contains several leucin-rich repeat (LLR) sequence motifs. Typically, LLRs consist of 20-29 amino acid residues with a conserved 11 residue motif (LxxLxLxx$^{N/}_{C}$xL). LLR sequences appear in proteins with distinct functions, but all of these proteins appear to be involved in protein-protein interactions and many play a role in signal transduction (Kobe, 2001). We were therefore intrigued by the idea that Alrm might serve as an adaptor protein for components of different signaling pathways. In order to find Alrm binding partners, we could precipitate Alrm protein and analyse protein complexes with mass spectrometry. A challenge will be to decide in which system we will perform the immunoprecipitations. The best system would be the Ras^{V12} dlg^{RNAi} tumors, however, to obtain enough material for an immunoprecipitation we will need to collect a vast number of tumors. Our laboratory has recently established a protocol for mass isolating and sorting imaginal discs (Marty *et al*, 2014). With this protocol, about 1000 imaginal discs can be isolated in less than three hours. A key requirement for sorting of the imaginal discs is the expression of a fluorescent protein in the tissue of interest. As our tumor cells express GFP they would be good candidates for sorting. However, due to the genetic set-up, only half of the progeny larvae from a cross develop tumors and crosses are quite laborious to prepare as a lot of virgin females are required to obtain enough progeny. Because of this, it might be rather challenging to collect the required numbers of larvae for the mass isolation and sorting. An alternative strategy would be to perform the immunoprecipitation from cell lines: in this case we could either express tagged Alrm in wild-type cells or engineer cells as such that they are mutant for *dlg* and express Ras^{V12} and Alrm. Using wild-type cells would be the simplest solution, yet we would first have to make sure that Alrm is evoking the same responses in wild-type cells as in Ras^{V12} dlg^{RNAi} tumors. Once the immunoprecipitation and mass spectrometry have been performed, we will analyze and search the identified interactors for components of the MAPK, PI3K,

JNK, JAK/STAT or Hippo pathways. These pathways have previously been shown to drive and sustain tumor growth (Igaki *et al*, 2006; Wu *et al*, 2010; Willecke *et al*, 2011; Sun & Irvine, 2011). Potential interaction partners will then be further analyzed and validated by co-immunoprecipitation and/or co-localization experiments and complemented with the experiments described in 4.2.3.2. By combining these approaches, we might elucidate the mechanisms by which loss of *alrm* affects tumor growth.

2.3 The *Drosophila* TNF receptor Grindelwald couples loss of cell polarity and neoplastic growth

Wengen (Wgn, CG6531) was the only easily identifiable member of the tumor necrosis factor receptor (TNFR) superfamily in *Drosophila*, but its role in *Drosophila* TNF signaling has been controversial for a long time. Kanda et al. (2002) have retrieved Wgn from a dominant modifier screen for downstream components of Egr signaling and reported that a dsRNA targeting *wgn* suppressed the Egr induced small eye phenotype. Furthermore, they found that full-length Wgn and Egr physically interact via their TNFR and TNF homology domain (Kanda *et al*, 2002). However, other groups were not able to confirm the interaction, but showed that Wengen interacts with DTRAF2 instead (Kauppila *et al*, 2003).

Michael Röthlisberger, a former master student in the Basler laboratory, had generated a *wgn* knockout (KO) allele by homologous recombination. Surprisingly, a *wgn* knockout could not suppress the Egr overexpression phenotype. This is unexpected, given the results of Kanda et al. (2002). Since neoplastic tumors depend on Egr signaling, we have also analysed Wgn in this background, but found that it is not required for tumor growth (Master thesis, J. Toggweiler). A finding that also contrasts with the results of Kanda et al. (2002) and Kauppila et al. (2003).

To solve this controversy, we were happy to assist with the investigations on Grindelwald (Grnd), a transmembrane protein identified in a genome-wide RNAi screen in Pierre Léopolds group. I reanalysed growth of Ras^{V12} dlg^{RNAi} tumors in a *wgn* knockout background and compared the effects to control tumors and tumors that were depleted for Grnd. In addition, I stained tumors for Mmp1, a protein that is expressed in response to JNK pathway activation. My results clearly demonstrated that Mmp1 expression is strongly reduced in tumors in which Grnd is knocked-down, but not in *wgn* mutant tumors.

These results are part of a study published in Nature:

Ditte S. Andersen, Julien Colombani, Valentina Palmerini, Krittalak Chakrabandhu, Emilie Boone, Michael Roethlisberger, Janine Toggweiler, Konrad Basler, Marina Mapelli, Anne-Odile Hueber & Pierre Leopold.

The Drosophila TNF receptor Grindelwald couples loss of polarity and neoplastic growth.

Nature 2015 522: 482-486.

LETTER

doi:10.1038/nature14298

The *Drosophila* TNF receptor Grindelwald couples loss of cell polarity and neoplastic growth

Ditte S. Andersen[1,2,3,4]*, Julien Colombani[1,2,3,4]*, Valentina Palmerini[5], Krittalak Chakrabandhu[1,2,3,6], Emilie Boone[1,2,3,4], Michael Röthlisberger[7], Janine Toggweiler[7], Konrad Basler[7], Marina Mapelli[5], Anne-Odile Hueber[1,2,3,6] & Pierre Léopold[1,2,3,4]

Disruption of epithelial polarity is a key event in the acquisition of neoplastic growth. JNK signalling is known to play an important part in driving the malignant progression of many epithelial tumours, although the link between loss of polarity and JNK signalling remains elusive. In a *Drosophila* genome-wide genetic screen designed to identify molecules implicated in neoplastic growth[1], we identified *grindelwald* (*grnd*), a gene encoding a transmembrane protein with homology to members of the tumour necrosis factor receptor (TNFR) superfamily. Here we show that Grnd mediates the pro-apoptotic functions of Eiger (Egr), the unique *Drosophila* TNF, and that overexpression of an active form of Grnd lacking the extracellular domain is sufficient to activate JNK signalling *in vivo*. Grnd also promotes the invasiveness of $Ras^{V12}/scrib^{-/-}$ tumours through Egr-dependent Matrix metalloprotease-1 (Mmp1) expression. Grnd localizes to the subapical membrane domain with the cell polarity determinant Crumbs (Crb) and couples Crb-induced loss of polarity with JNK activation and neoplastic growth through physical interaction with Veli (also known as Lin-7). Therefore, Grnd represents the first example of a TNFR that integrates signals from both Egr and apical polarity determinants to induce JNK-dependent cell death or tumour growth.

We recently carried out a genome-wide screen to identify molecules that are required for neoplastic growth[1]. The condition used for this screen was the disc-specific knockdown of *avalanche* (*rotund* (*rn*)>*avl*-RNAi; *avalanche* also known as *syntaxin 7*), a gene encoding a syntaxin that functions in the early step of endocytosis[2]. *rn*>*avl*-RNAi results in ectopic Wingless (Wg) expression, neoplastic disc overgrowth[2] (Fig. 1a, b), and a 2-day delay in larva-to-pupa transition[1]. We screened a collection of 10,100 transgenic RNA interference (RNAi) lines for their ability to rescue the pupariation delay and identified 121 candidate genes[1]. Interestingly, only eight candidate genes also rescued ectopic Wg expression and neoplastic overgrowth (Extended Data Fig. 1a). These included five lines targeting core components of the JNK pathway (Bendless, Tab2, Tak1, Hemipterous and Basket; Extended Data Fig. 1b). Using a *puckered* enhancer trap (*puc-lacZ*) as a readout for JNK activity, we confirmed that JNK signalling is highly upregulated in *rn*>*avl*-RNAi discs (Fig. 1a, b, right). One of the remaining lines targets *CG10176*, a gene encoding a transmembrane protein. Reducing expression of *CG10176* by using two different RNAi lines was as efficient as *tak1* silencing to restore normal Wg pattern and suppresses JNK signalling and neoplastic growth in the *rn*>*avl*-RNAi background (Fig. 1c, d and Extended Data Fig. 1c–e). Sequence analysis of *GC10176* identified a cysteine-rich domain (CRD) in the extracellular part with homology to vertebrate TNFRs (Fig. 1e and Extended Data Fig. 2) harbouring a glycosphingolipid-binding motif (GBM) characteristic of many TNFRs including Fas[3] (Fig. 1e and Extended Data Fig. 2). We named *CG10176 grindelwald* (*grnd*), after a village at the foot of Eiger, a Swiss mountain that lent its name to the unique *Drosophila* TNF, Egr. Immunostaining and subcellular fractionation of disc extracts confirmed that Grnd localizes to the membrane (Extended Data Fig. 1f–h). Moreover, co-immunoprecipitation experiments showed that both Grnd full-length and Grnd-intra, a form lacking its extracellular domain, directly associate with Traf2, the most upstream component of the JNK pathway (Fig. 1f–h). This interaction is disrupted by a single amino acid substitution within a conserved Traf6-binding motif[4] (human TRAF6 is the closest homologue to Traf2; Fig. 1f–h and Extended Data Fig. 3). Overexpression of Grnd-intra, but not full-length Grnd, is sufficient to induce JNK signalling, ectopic Wg expression and apoptosis (Fig. 1i–j and Extended Data Fig. 4a–c), and Grnd-intra-induced apoptosis is efficiently suppressed in a hep^{75} (JNKK) mutant background (Extended Data Fig. 4d, e), confirming that Grnd acts upstream of the JNK signalling cascade.

The *Drosophila* TNF Egr activates JNK signalling and triggers cell death or proliferation, depending on the cellular context[5]. We therefore tested whether Grnd is required for the small-eye phenotype generated by Egr-induced apoptosis in the retinal epithelium[6,7] (*GMR*>*egr*; Fig. 2a, b). As previously shown, inhibition of JNK signalling by reducing *tak1* (ref. 6) or *traf2* (ref. 8) expression, or by overexpressing *puckered*[7], blocks Egr-induced apoptosis and rescues the small-eye phenotype (Extended Data Fig. 5a–d). In contrast to a previous report[9], RNAi silencing of *wengen* (*wgn*), a gene encoding a presumptive receptor for Egr, does not rescue the small-eye phenotype (Extended Data Fig. 5e). Furthermore, the small-eye phenotype is not modified in a *wgn*-null mutant background (Fig. 2c and Extended Data Fig. 5h, m, n), confirming that Wgn is not required for Egr-induced apoptosis in the eye. By contrast, reducing *grnd* levels partially rescues the Egr-induced small-eye phenotype, producing a 'hanging-eye' phenotype (Fig. 2d) that is not further rescued in a *wgn*-knockout (wgn^{KO}) mutant background (Extended Data Fig. 5e–i). A similar phenotype was previously reported as a result of non-autonomous cell death induced by a diffusible form of Egr[10] (Extended Data Fig. 5k, l). This suggests that Grnd prevents Egr from diffusing outside of its expression domain. Co-immunoprecipitation experiments show that both full-length Grnd and Grnd-extra, a truncated form of Grnd lacking the cytoplasmic domain, associate with Egr through its TNF-homology domain (Fig. 2j, k). Although Grnd-extra can bind Egr, it cannot activate JNK signalling. Therefore, we reasoned that Grnd-extra expression might prevent both cell-autonomous and non-autonomous apoptosis by trapping Egr and preventing its diffusion and binding to endogenous Grnd. Indeed, *GMR*-Gal4-mediated expression of *grnd-extra* fully rescues the Egr small-eye phenotype (Fig. 2e and Extended Data Fig. 5j). To confirm that the removal of Grnd induces Egr-mediated non-autonomous cell death, we generated wing disc

[1]University of Nice-Sophia Antipolis, Institute of Biology Valrose, Parc Valrose, 06108 Nice, France. [2]CNRS, Institute of Biology Valrose, Parc Valrose, 06108 Nice, France. [3]INSERM, Institute of Biology Valrose, Parc Valrose, 06108 Nice, France. [4]Genetics and Physiology of Growth laboratory, Institute of Biology Valrose, Parc Valrose, 06108 Nice, France. [5]Department of Experimental Oncology, European Institute of Oncology, Via Adamello 16, 20139 Milan, Italy. [6]Death receptors Signalling and Cancer Therapy laboratory, Institute of Biology Valrose, Parc Valrose, 06108 Nice, France. [7]Institute of Molecular Life Sciences, University of Zurich, Winterthurerstrasse 190, 8057 Zurich, Switzerland.
*These authors contributed equally to this work.

©2015 Macmillan Publishers Limited. All rights reserved

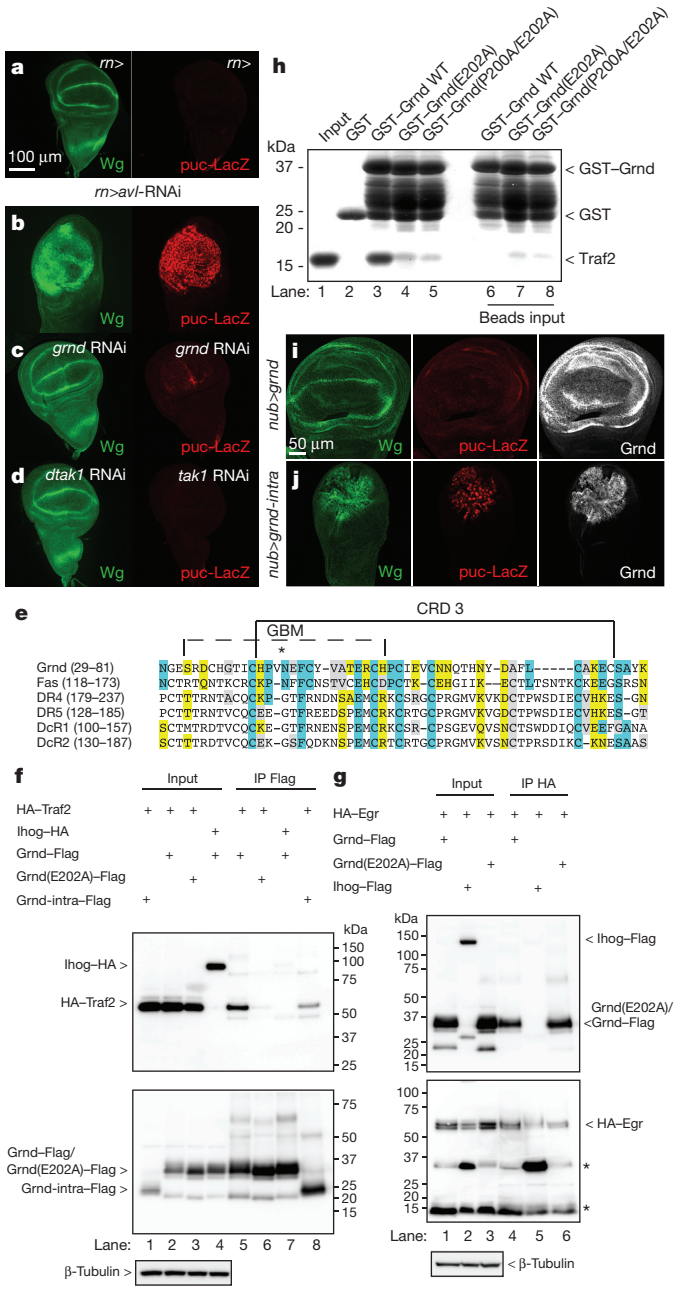

Figure 1 | Grnd is a novel member of the TNFR superfamily. a–d, Wing discs stained for Wg (left) or LacZ (right). **e**, Sequence alignment of Grnd and human TNFRs. Blue, identity; yellow, strong similarity to Grnd; grey, weak similarity to Grnd. **f**, **g**, Co-immunoprecipitation experiments from S2R^{+} cells co-expressing haemagglutinin (HA)–Traf2 or Ihog–HA (control), and either Grnd–Flag, Grnd-intra–Flag or Grnd(E202A)–Flag (**f**), or HA–Egr and either Grnd–Flag, Grnd(E202A)–Flag or Ihog–Flag (control) (**g**). Input loading is quantified using β-tubulin. **h**, Pull-down experiments of Traf2 with various truncated forms of glutathione *S*-transferase (GST)–Grnd. Commassie blue staining is used to visualize the bound species. WT, wild type. **i–j,** Wing discs stained for Wg (left), LacZ (middle) and Grnd (right).

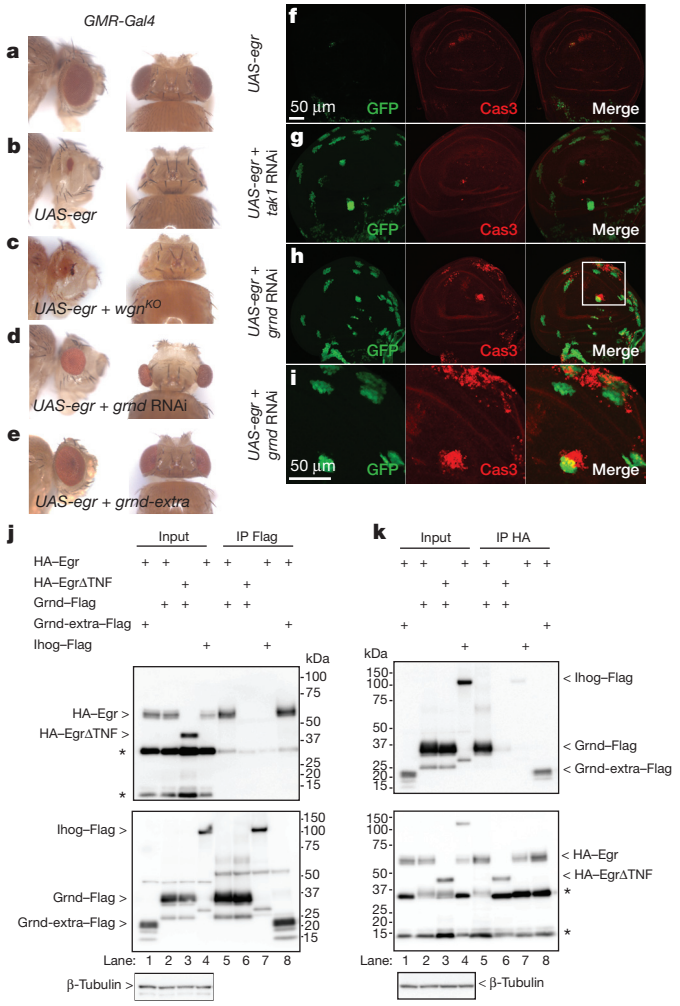

Figure 2 | Grnd is required for Egr-induced apoptosis. a–e, Light micrographs of *Drosophila* adult eyes of the indicated genotypes (all animals carry the *GMR-Gal4* driver). Original magnification, ×30. **f–i**, Wing discs carrying green fluorescent protein (GFP)-labelled clones (green) expressing *egr* (**f**), *egr* + *tak1* RNAi (**g**) or *egr* + *grnd* RNAi (**h**, **i**) and stained for Caspase 3 (Cas3; red). A close-up shows non-autonomous cell death around the *egr* + *grnd* RNAi clones. **j**, **k**, Co-immunoprecipitation (IP) experiments from S2R^{+} cells expressing HA–Egr or HA–EgrΔTNF (Egr lacking its TNF-homology domain; amino acids 278–415) and either Grnd–Flag, Grnd-extra–Flag or Ihog–Flag (control). Input loading is quantified using β-tubulin.

clones expressing *egr* alone, *egr* + *tak1* RNAi, or *egr* + *grnd* RNAi (Fig. 2f–i). As expected, reducing *tak1* levels in *egr*-expressing clones prevents their elimination by apoptosis (Fig. 2f, g). Similarly, reducing *grnd* levels prevents autonomous cell death, but also induces non-autonomous apoptosis (Fig. 2h, i). This suggests that Egr, like its mammalian counterpart TNF-α, can be processed into a diffusible form *in vivo* whose interaction with Grnd limits the potential to act at a distance. Flies carrying homozygous ($grnd^{Minos/Minos}$) or transheterozygous ($grnd^{Minos/Df}$) combinations of a transposon inserted in the *grnd* locus express no detectable levels of Grnd protein (Extended Data Fig. 6a, b) and are equally resistant to Egr-induced cell death (Extended Data Fig. 6e–j). In addition, $grnd^{Minos/Minos}$ mutant flies are viable and display no obvious phenotype (Extended Data Fig. 6c, d), suggesting that Grnd, like Egr, participates in a stress response to limit organismal damage. Collectively, our data demonstrate that Grnd is a new *Drosophila* TNF receptor that mediates most, if not all, Egr-induced apoptosis.

TNFs probably represent a danger signal produced in response to tissue damage to rid the organism of premalignant tissue or to facilitate wound healing. Disc clones mutant for the polarity gene *scribbled* (*scrib*) induce an Egr-dependent response resulting in the elimination of *scrib* mutant cells by JNK-mediated apoptosis[11,12]. To test the requirement for Grnd in this process, we compared *scrib*-RNAi and *scrib*-RNAi + *grnd*-RNAi clones obtained 72 h after heat shock induction. As expected, *scrib*-RNAi cells undergo apoptosis and detach from

©2015 Macmillan Publishers Limited. All rights reserved

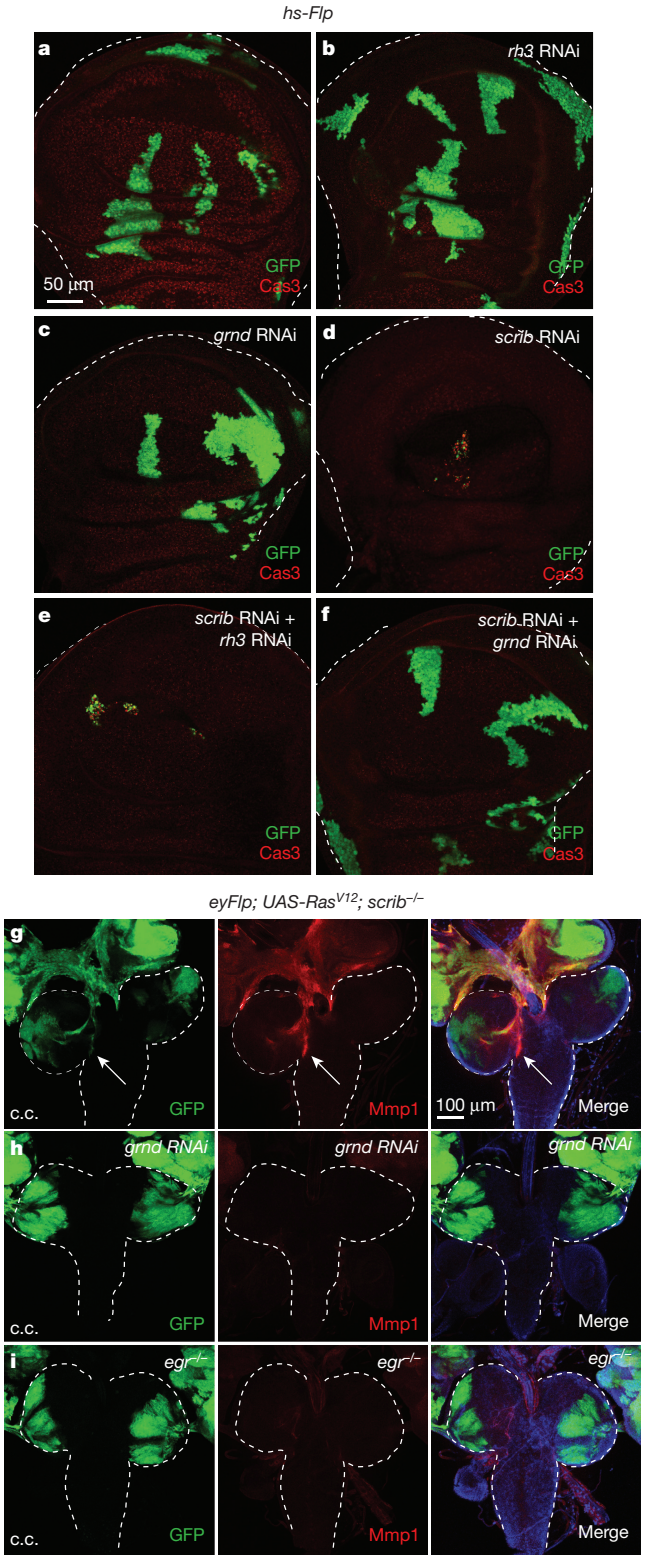

Figure 3 | Grnd is required for the Egr-induced invasiveness of $Ras^{V12}/scrib^{-/-}$ tumours. **a–f**, Wing discs dissected 5 days after egg deposition (AED) stained for Cas3 (red) and carrying GFP-labelled clones (green) of the indicated genotypes induced 2 days AED. **a**, **b**, **e**, Wild-type clones (**a**) and clones expressing the control *Rh3* RNAi (**b**) to exclude a Gal4 titration effect (**e**). **g–i,** Eye–brain complexes dissected 7 days AED carrying $Ras^{V12}/scrib^{-/-}$ (**g**) or $Ras^{V12}/scrib^{-/-}$ + *grnd* RNAi (**h**) clones (labelled by GFP), or $Ras^{V12}/scrib^{-/-}$ GFP-labelled clones in an *egr* mutant background (**i**) stained for Mmp1 (**g–i**, middle, red) and 4′,6-diamidino-2-phenylindole (DAPI; blue). $Ras^{V12}/scrib^{-/-}$ clones invade the ventral nerve cord (**g**, white arrow). c.c., cephalic complex.

the epithelium (Fig. 3a–d). By contrast, *scrib*-RNAi clones with reduced *grnd* expression survive (Fig. 3e, f), indicating that Grnd is required for Egr-dependent elimination of *scrib*-RNAi cells. Similar results were obtained by generating $scrib^{-/-}$ mutant clones in the eye disc (Extended Data Fig. 7a–d).

In both mammals and flies, TNFs are double-edged swords that also have the capacity to promote tumorigenesis in specific cellular contexts[5]. Indeed, $scrib^{-/-}$ eye disc cells expressing an activated form of *Ras* (Ras^{V12}) exhibit a dramatic tumour-like overgrowth and metastatic behaviour, a process that critically relies on Egr[13]. $Ras^{V12}/scrib^{-/-}$ metastatic cells show a strong accumulation of Grnd and Mmp1, and invade the ventral nerve cord[11,14,15] (Fig. 3g and Extended Data Figs 7e, 8a). Primary tumour cells reach peripheral tissues such as the fat body and the gut, where they form micrometastases expressing high levels of Grnd (Extended Data Fig. 7f, g). Reducing *grnd* levels in $Ras^{V12}/scrib^{-/-}$ clones is sufficient to restore normal levels of Mmp1 and abolish invasiveness in a way similar to that observed in an $egr^{-/-}$ background[13] (Fig. 3h, i and Extended Data Fig. 8a–c). Therefore, Grnd is required for the Egr-induced metastatic behaviour of $Ras^{V12}/scrib^{-/-}$ tumorous cells. Similarly, reducing *grnd*, but not *wgn* levels, strongly suppresses Mmp1 expression in Ras^{V12}/dlg-RNAi cells and limits tumour invasion (Extended Data Fig. 8d–g), indicating that Wgn does not have a major role in the progression of these tumours.

Perturbation of cell polarity is an early hallmark of tumour progression in epithelial cells. In contrast to small patches of polarity-deficient cells, for example, $scrib^{-/-}$ clones, organ compartments or animals fully composed of polarity-deficient cells become refractory to Egr-induced cell death and develop epithelial tumours. The formation of these tumours requires JNK/MAPK signalling, but not Egr[13,16], suggesting Egr-independent coupling between loss of polarity and JNK/MAPK-dependent tumour growth. In line with these observations, we noticed that, in contrast to Grnd, Egr is not required to drive neoplastic growth in *rn>avl*-RNAi conditions (Extended Data Fig. 9a, b). This suggests that, in addition to its role in promoting Egr-dependent functions, Grnd couples loss of polarity with JNK-dependent growth independently of Egr. Disc immunostainings revealed that Grnd co-localizes with the apical determinant Crb in the marginal zone, apical to the adherens junction protein E-cadherin (E-cad) and the atypical protein kinase C (aPKC; Fig. 4a and Extended Data Fig. 9c, d). In *avl*-RNAi discs, Grnd and Crb accumulate in a wider apical domain[2] (Extended Data Fig. 9e, g). Apical accumulation of Crb is proposed to be partly responsible for the neoplastic growth induced by *avl* knockdown, since overexpression of Crb or a membrane-bound cytoplasmic tail of Crb (Crb-intra) mimics the *avl*-RNAi phenotype[2] (Extended Data Fig. 9f). We therefore examined whether Grnd might couple the activity of the Crb complex with JNK-mediated neoplastic growth. Indeed, reducing *grnd* levels, but not *wgn*, in *rn>crb-intra* discs suppresses neoplastic growth as efficiently as inhibiting the activity of the JNK pathway (Fig. 4c–f and Extended Data Fig. 9h, i). Notably, Yki activation is not rescued in these conditions (Extended Data Fig. 9j–l), illustrating the ability of Crb-intra to promote growth independently of Grnd by inhibiting Hippo signalling through its FERM-binding motif (FBM)[17,18]. Indeed, neoplastic growth and polarity defects induced by a form of Crb-intra lacking its FBM (CrbΔFBM-intra) are both rescued by Grnd silencing (Fig. 4i, j). As expected, the size of *rn>crbΔFBM-intra;grnd*-RNAi discs is reduced compared to the size of *rn>crb-intra; grnd*-RNAi discs (compare Fig. 4e, f with Fig. 4j).

Crb, Stardust (Sdt; PALS1 in humans), and Pals1-associated tight junction protein (Patj) make up the core Crb complex[19], which recruits the adaptor protein Veli (MALS1–3 in humans)[20–22]. In agreement with previous yeast two-hybrid data[23], we find that Grnd binds directly and specifically to the PDZ domain of Veli through a membrane-proximal stretch of 28 amino acids in its intracellular domain (Extended Data Fig. 10a–e). Grnd localization is unaffected in

©2015 Macmillan Publishers Limited. All rights reserved

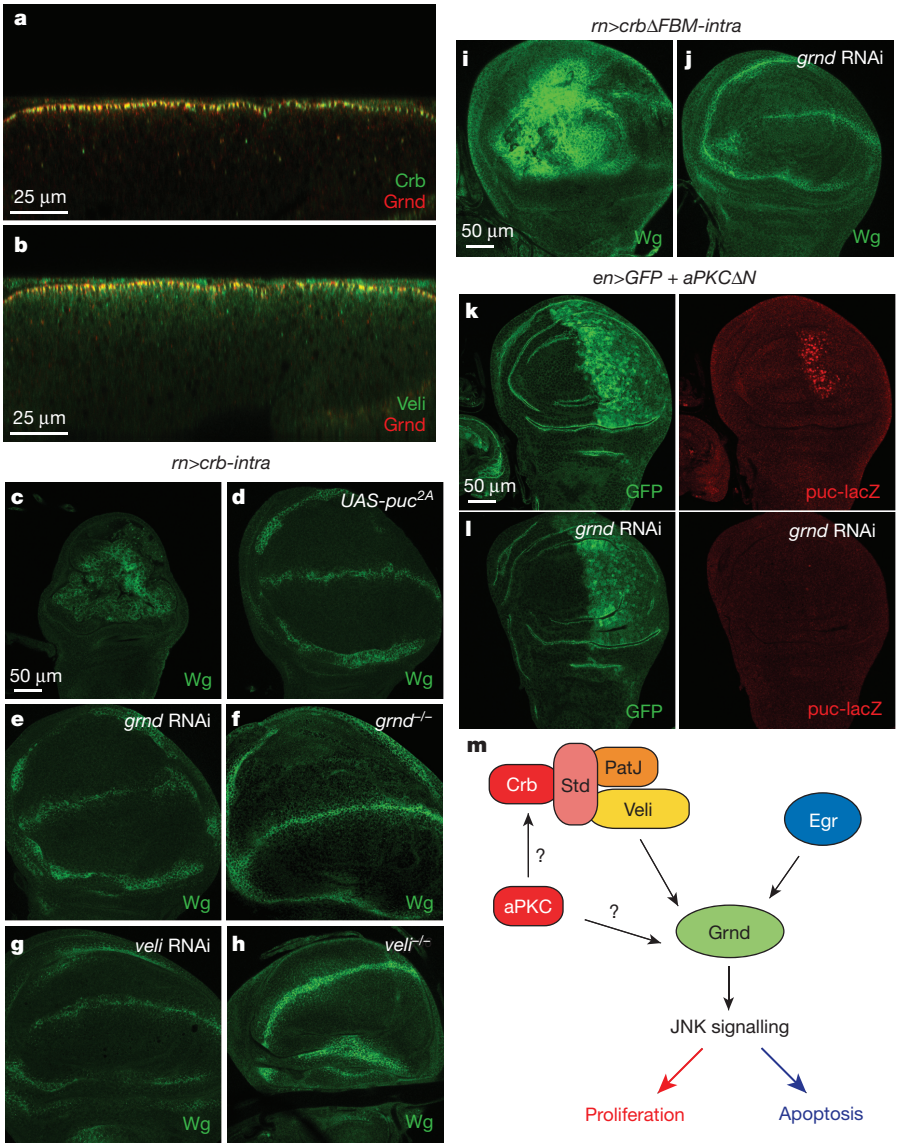

Figure 4 | *grnd* is required downstream of the apical Crb polarity complex for JNK-dependent neoplastic growth. **a, b**, Transverse sections of wild-type discs stained for Grnd (red), Crb (**a**, green) or Veli (**b**, green). **c–h**, Discs expressing *crb-intra* alone (**c**), or combined with the indicated genotypes (**d–h**), dissected 6 days AED, stained for Wg (green). **i, j**, Discs expressing Crb-intra lacking its FBM (*crbΔFBM-intra*) alone (**i**) or with *grnd* RNAi (**j**) stained for Wg (in green). **k, l**, Discs from *puc-LacZ* animals expressing activated aPKC (aPKCΔN)[26] in the posterior domain alone (**k**) or together with *grnd* RNAi (**l**). **m**, A model for Grnd function.

$crb^{-/-}$ and *veli* RNAi mutant clones (Extended Data Fig. 10f–h). However, reducing *veli* expression rescues the patterning defects and disc morphology of *rn>crb-intra* mutant cells (Fig. 4g, h), suggesting that Grnd couples Crb activity with JNK signalling through its interaction with Veli. Interestingly, aPKC-dependent activation of JNK signalling[16] also depends on Grnd (Fig. 4k, l). aPKC is capable of directly binding and phosphorylating Crb, which is important for Crb function[24]. This suggests that aPKC, either directly or through Crb phosphorylation, activates Grnd-dependent JNK signalling in response to perturbation of apico-basal polarity.

Our data are consistent with a model whereby Grnd integrates signals from Egr, the unique fly TNF, and apical polarity determinants to induce JNK-dependent neoplastic growth or apoptosis in a context-dependent manner (Fig. 4m). Recent work reveals a correlation between mammalian Crb3 expression and tumorigenic potential in mouse kidney epithelial cells[25]. The conserved nature of the Grnd receptor suggests that specific TNFRs might carry out similar functions in vertebrates, in which the link between apical cell polarity and tumour progression remains elusive.

Online Content Methods, along with any additional Extended Data display items and Source Data, are available in the online version of the paper; references unique to these sections appear only in the online paper.

Received 25 September 2013; accepted 9 February 2015.
Published online 15 April 2015.

1. Colombani, J., Andersen, D. S. & Leopold, P. Secreted peptide Dilp8 coordinates *Drosophila* tissue growth with developmental timing. *Science* **336,** 582–585 (2012).
2. Lu, H. & Bilder, D. Endocytic control of epithelial polarity and proliferation in *Drosophila*. *Nature Cell Biol.* **7,** 1232–1239 (2005).
3. Chakrabandhu, K. *et al.* The extracellular glycosphingolipid-binding motif of Fas defines its internalization route, mode and outcome of signals upon activation by ligand. *Cell Death Differ.* **15,** 1824–1837 (2008).
4. Ye, H. *et al.* Distinct molecular mechanism for initiating TRAF6 signalling. *Nature* **418,** 443–447 (2002).
5. Vidal, M. The dark side of fly TNF: an ancient developmental proof reading mechanism turned into tumor promoter. *Cell Cycle* **9,** 3851–3856 (2010).
6. Igaki, T. *et al.* Eiger, a TNF superfamily ligand that triggers the *Drosophila* JNK pathway. *EMBO J.* **21,** 3009–3018 (2002).

©2015 Macmillan Publishers Limited. All rights reserved

7. Moreno, E., Yan, M. & Basler, K. Evolution of TNF signaling mechanisms: JNK-dependent apoptosis triggered by Eiger, the *Drosophila* homolog of the TNF superfamily. *Curr. Biol.* **12,** 1263–1268 (2002).
8. Xue, L. *et al.* Tumor suppressor CYLD regulates JNK-induced cell death in *Drosophila*. *Dev. Cell* **13,** 446–454 (2007).
9. Kanda, H., Igaki, T., Kanuka, H., Yagi, T. & Miura, M. Wengen, a member of the *Drosophila* tumor necrosis factor receptor superfamily, is required for Eiger signaling. *J. Biol. Chem.* **277,** 28372–28375 (2002).
10. Narasimamurthy, R. *et al.* Structure–function analysis of Eiger, the *Drosophila* TNF homolog. *Cell Res.* **19,** 392–394 (2009).
11. Brumby, A. M. & Richardson, H. E. *scribble* mutants cooperate with oncogenic Ras or Notch to cause neoplastic overgrowth in *Drosophila*. *EMBO J.* **22,** 5769–5779 (2003).
12. Igaki, T., Pastor-Pareja, J. C., Aonuma, H., Miura, M. & Xu, T. Intrinsic tumor suppression and epithelial maintenance by endocytic activation of Eiger/TNF signaling in *Drosophila*. *Dev. Cell* **16,** 458–465 (2009).
13. Cordero, J. B. *et al.* Oncogenic Ras diverts a host TNF tumor suppressor activity into tumor promoter. *Dev. Cell* **18,** 999–1011 (2010).
14. Pagliarini, R. A. & Xu, T. A genetic screen in *Drosophila* for metastatic behavior. *Science* **302,** 1227–1231 (2003).
15. Uhlirova, M. & Bohmann, D. JNK- and Fos-regulated Mmp1 expression cooperates with Ras to induce invasive tumors in *Drosophila*. *EMBO J.* **25,** 5294–5304 (2006).
16. Sun, G. & Irvine, K. D. Regulation of Hippo signaling by Jun kinase signaling during compensatory cell proliferation and regeneration, and in neoplastic tumors. *Dev. Biol.* **350,** 139–151 (2011).
17. Ling, C. *et al.* The apical transmembrane protein Crumbs functions as a tumor suppressor that regulates Hippo signaling by binding to Expanded. *Proc. Natl Acad. Sci. USA* **107,** 10532–10537 (2010).
18. Robinson, B. S., Huang, J., Hong, Y. & Moberg, K. H. Crumbs regulates Salvador/Warts/Hippo signaling in *Drosophila* via the FERM-domain protein Expanded. *Curr. Biol.* **20,** 582–590 (2010).
19. Bulgakova, N. A. & Knust, E. The Crumbs complex: from epithelial-cell polarity to retinal degeneration. *J. Cell Sci.* **122,** 2587–2596 (2009).
20. Bachmann, A., Grawe, F., Johnson, K. & Knust, E. *Drosophila* Lin-7 is a component of the Crumbs complex in epithelia and photoreceptor cells and prevents light-induced retinal degeneration. *Eur. J. Cell Biol.* **87,** 123–136 (2008).
21. Bachmann, A. *et al.* Cell type-specific recruitment of *Drosophila* Lin-7 to distinct MAGUK-based protein complexes defines novel roles for Sdt and Dlg-S97. *J. Cell Sci.* **117,** 1899–1909 (2004).
22. Olsen, O. *et al.* Renal defects associated with improper polarization of the CRB and DLG polarity complexes in MALS-3 knockout mice. *J. Cell Biol.* **179,** 151–164 (2007).
23. Giot, L. *et al.* A protein interaction map of *Drosophila melanogaster*. *Science* **302,** 1727–1736 (2003).
24. Sotillos, S., Diaz-Meco, M. T., Caminero, E., Moscat, J. & Campuzano, S. DaPKC-dependent phosphorylation of Crumbs is required for epithelial cell polarity in *Drosophila*. *J. Cell Biol.* **166,** 549–557 (2004).
25. Karp, C. M. *et al.* Role of the polarity determinant crumbs in suppressing mammalian epithelial tumor progression. *Cancer Res.* **68,** 4105–4115 (2008).
26. Betschinger, J., Mechtler, K. & Knoblich, J. A. The Par complex directs asymmetric cell division by phosphorylating the cytoskeletal protein Lgl. *Nature* **422,** 326–330 (2003).

Acknowledgements We thank G. Jarretou for technical assistance, the Vienna *Drosophila* RNAi Centers, the *Drosophila* Genetics Resource Center, the Bloomington Stock Center, N. Caridi and S. Pasqualato for technical assistance and P.L. laboratory members for comments on the manuscript. This work was supported by the CNRS, INSERM, Agence Nationale de la Recherche, Fondation pour la Recherche Médicale, Association pour la Recherche contre le Cancer (grant no. PJA20131200042 to J.C.), European Research Council (Advanced grant no. 268813 to P.L.), Marie Curie Life Long Training (grant no. 252373 to D.S.A.), the Labex Signalife program (grant ANR-11-LABX-0028-01 to P.L.), the Italian Association for Cancer Research (AIRC IG-12877) and the Italian Ministry of Health (GR-2008-1134103) to M.M.

Author Contributions D.S.A., J.C., K.C., A.-O.H., K.B., M.M. and P.L. designed the research; D.S.A., J.C., K.C., V.P., E.B., M.R. and J.T. performed experiments; D.S.A., J.C., K.C., E.B., A.-O.H., K.B., V.P., M.M. and P.L. analysed the data; D.S.A., J.C. and P.L. wrote the manuscript.

Author Information Reprints and permissions information is available at www.nature.com/reprints. The authors declare no competing financial interests. Readers are welcome to comment on the online version of the paper. Correspondence and requests for materials should be addressed to J.C. (julien.colombani@unice.fr) or P.L. (leopold@unice.fr).

©2015 Macmillan Publishers Limited. All rights reserved

3 Concluding remarks on *Drosophila* tumor models

Defects in signal transduction and cell-cell communication induced by loss of function of tumor suppressor genes or gain of function of oncogenes are key in transforming a healthy cell into a malignant derivative. Studies in *Drosophila* have been seminal in understanding the function of many oncogenes and tumor suppressor genes and in dissecting the complex regulations of signaling pathways; and the fly continues to reveal important concepts, as shown in this thesis and as discussed in sections 1.1.2. Despite the tremendous contributions to our understanding of basic cancer biology, *Drosophila* has only marginally been involved in finding clinically relevant cancer therapeutics. The Cagan laboratory has been one of the few groups that has tested therapeutic compounds in a *Drosophila* model of thyroid cancer and an identified kinase inhibitor has been subsequently advanced into clinical trials for treatment of thyroid cancer (Vidal, 2005). A factor limiting the utility of *Drosophila* for cancer research is clearly the complexity of many tumors that might go beyond what can be modelled in *Drosophila* and a lack of comparable organs. The underlying biology of each tissue affects the efficacy of a specific drug, as its application can lead to completely different outcomes in cancers originated from different tissues even if the genetic lesions are similar. Nevertheless, the Cagan lab has proven that *Drosophila* can be useful in identifying new drugs, but the cancer optimally presents a simple genetic profile such as dependency on one single oncogene. Finding an efficient screening system might be a second obstacle in identifying small molecule compounds in *Drosophila*: ideally a phenotype should be amenable for quick analysis to facilitate evaluation of compounds. Such a system has been set up by the Brumby and Richardson groups to screen compounds in Ras^{V12} $scrib^{-/-}$ tumors and could be adapted for use in other tumor models as well (Willoughby *et al*, 2012). With such a platform at hand the role of *Drosophila* tumor models might be advanced from only contributing the understanding of basic cancer biology to also identifying relevant therapeutic compounds.

4 Appendix

4.1 Loss of function and gain of function phenotypes of other *Drosophila* ETS genes in a wild-type background

As discussed in the introductory section 1.2.2, only a few of the *Drosophila* ETS proteins have been linked to growth and development of eye or wings. To assess the role for other *Drosophila* ETS proteins in these tissues, we knocked down and ectopically expressed them in the developing eye and wing by means of eye disc and wing disc specific Gal4 drivers (eye: *GMR-Gal4* (posterior to the morphogenetic furrow), *eyFlp-act>>Gal4* (entire eye disc); wing: *nubbin (nub)-Gal4* (wing pouch) and *hedgehog* (*hh*)-*Gal4* (posterior compartment). Table 2 summarizes the phenotypes observed and detailed descriptions for each gene are found in sections 4.1.1. – 4.1.8. Although a function for Ets21C is described already in earlier sections of this thesis and Pnt and Aop have been studied in detail by other groups, they were also included in the analysis for comparisons.

Table 2: Overview of phenotypes caused by a depletion or overexpression of *Drosophila* ETS genes in the developing wing and eye tissue.

	Phenotypes			
	Knockdown		**Overexpression**	
	Eyes	**Wings**	**Eyes**	**Wings**
pnt	much smaller, rough	normal	lethal	normal
aop	much smaller or lethal	normal	smaller and rough	smaller, abnormal veins
Ets21C	slightly larger	missing parts of veins	much smaller	smaller, blisters
Ets98B	smaller	smaller, vein defects	rough eye or lethal	lethal
Ets96B	normal	slightly smaller	normal	normal
Ets65A	normal	normal	normal	normal
Ets97D	slightly larger	normal	slightly smaller, rounder	smaller
E74	normal	smaller ,extra veins	n.d.	n.d.

4.1.1 Pointed

From previous studies, Pointed (Pnt) is known to play an important role as transcription factor of the MAP kinase pathway (Brunner *et al*, 1994). In agreement with its described function, a knockdown of *pnt* in the developing eye lead to severe reductions in size and defects in morphology (Fig. 14, A, D, E and H). Ectopic expression in the eye even resulted in pupal lethality (Fig. 14, A-C and E-G). Interestingly, a knockdown in wing imaginal discs does not cause any defects, suggesting that Pnt function is dispensable for wing development (Fig. 14, I-L). Effects of overexpressing Pnt in the wing still need to be determined.

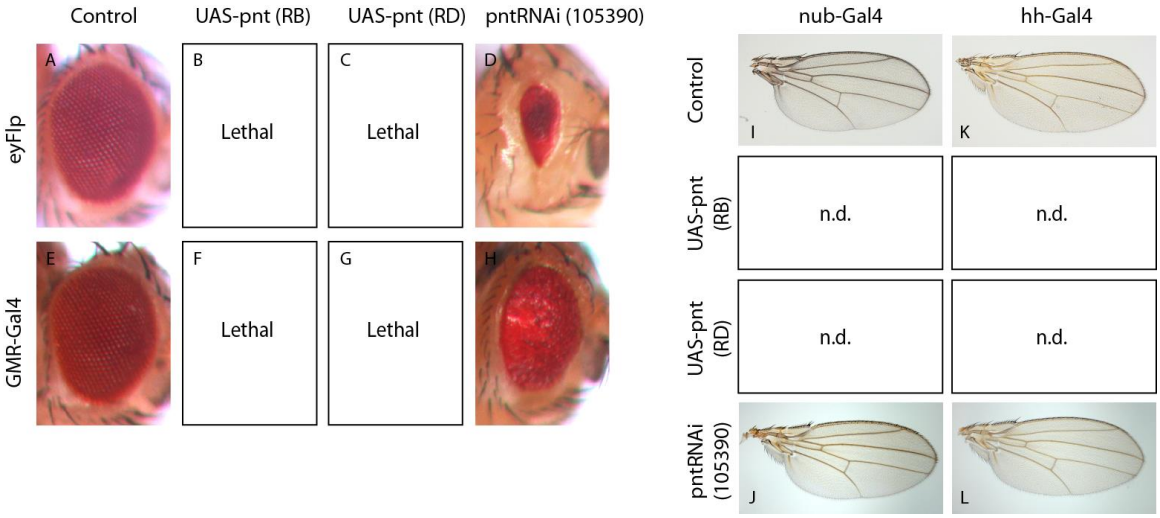

Figure 14: Eye and wing phenotypes resulting from depleting or ectopically expressing Pnt in imaginal tissue. Images of adult eyes (A-H) and wings (I-L) are shown.

4.1.2 Anterior open

In contrast to Pnt, Anterior open (Aop) represses the transcription of MAPK targets and is inactivated if the pathway is active (Brunner *et al*, 1994; O'Neill *et al*, 1994). We would therefore expect similar defects from a missexpression or downregulation as observed for *pnt*. Depletion in eye discs also resulted in a rough eye phenotype and overexpression is lethal (Fig. 15, A-H). Defects observed in wing discs are only mild, Aop overexpression leads to

wing vein defects (Fig. 15, I-N). A depletion of Aop does not affect wing patterning, but might reduce size slightly (Fig. 15, I, K-M, O and P).

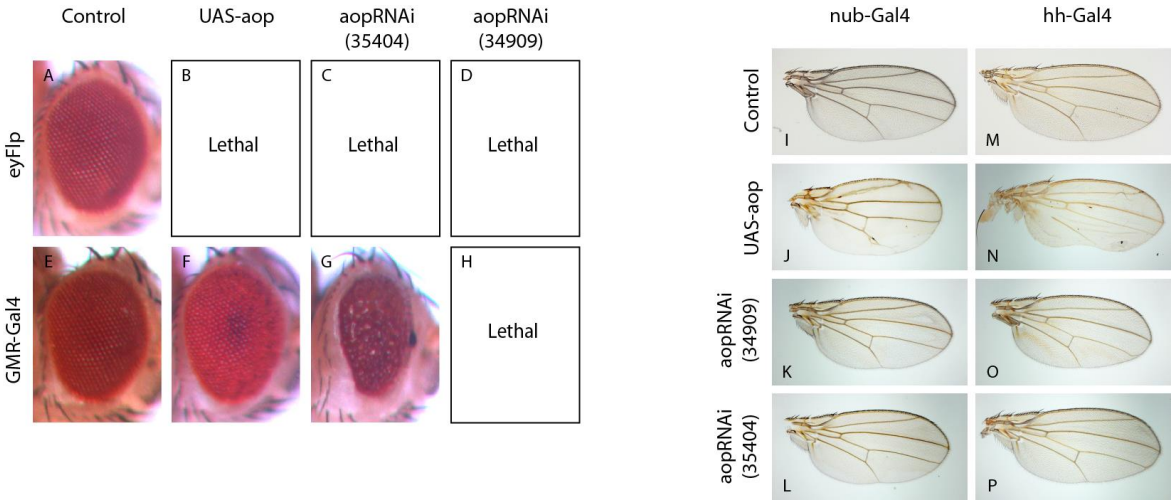

Figure 15: Eye and wing phenotypes resulting from depleting or ectopically expressing Aop in imaginal tissue. Images of adult eyes (A-H) and wings (I-P) are shown.

4.1.3 Ets21C

Ets21C has been poorly characterized so far. It has only been found up-regulated in response to bacterial infection or tissue damage. We recently found that Ets21C seems to positively regulate growth of neoplastic tumors in *Drosophila* (this thesis). Interestingly, in a wild-type background opposite phenotypes were observed. Overexpression of Ets21C causes very small eyes or pupal lethality and also small wings that do not properly unfold and show defective veins and blisters (Fig. 16, A, B, E, F, I, J, M and N). A knockdown of Ets21C in eye tissue leads to slightly larger (Line 51225) or normal (Line 106153) eyes (Fig. 16, A, C-E, G and H). Depletion of the gene product in wings leads to different phenotypes. With line 51225 wings seem to be slightly larger as well and miss parts of longitudinal veins L2 or L4 as well as L5 (Fig. 16, I, K, M and O). Line 106153, however, seems to cause smaller or normally sized wings without patterning defects (Fig. 16, I, L, M and P).

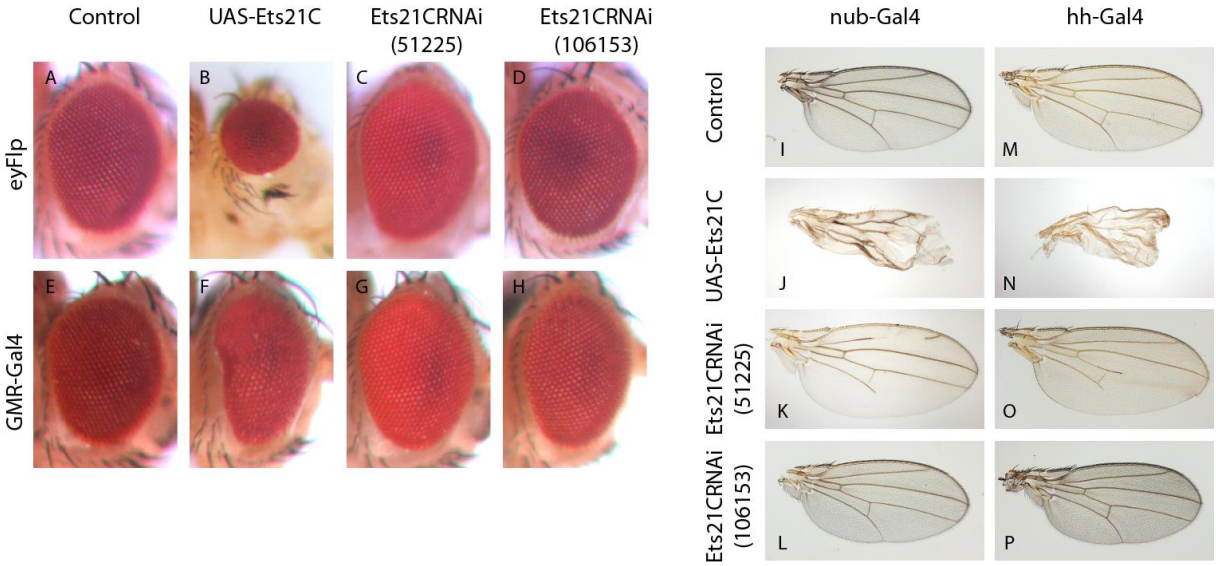

Figure 16: Effects of Ets21C depletion or ectopic expression in eye and wing tissue. Images of adult eyes (A-H) and wings (I-P) are shown.

4.1.4 E74

E74 mutants have difficulties to complete metamorphosis and usually die as pupae (Fletcher et al., 1995). A depletion of E74 in the developing eye does not affect eye size and morphology (Fig. 17, A-D). In contrast, a knockdown of *E74* in the wing imaginal disc resulted in reduced wing size and extra veins (Fig. 17, E-H).

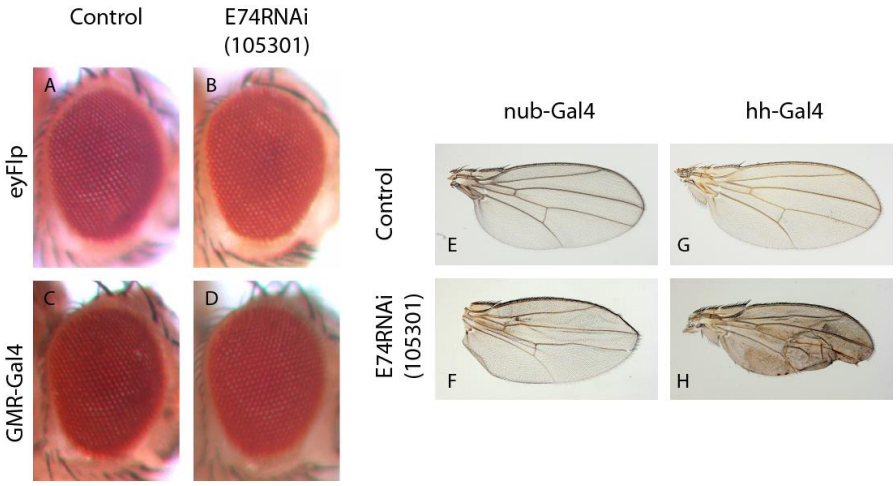

Figure 17: Effects of E74 depletion in eye and wing tissue. Images of adult eyes (A-D) and wings (E-H) are shown.

4.1.5 Ets98B

Overexpression of Ets98B with GMR-Gal4 led to abnormal development of the ommatidia resulting in a rough eye phenotype (Fig. 18, E and F). Ectopic expression in the entire eye disc even led to pupal lethality (Fig. 18, G and H). A knockdown of *Ets98B* in eye tissue resulted in very different phenotypes depending on the driver and the RNAi line. In combination with *eyFlp*, line 10932 resulted in smaller eyes that were only composed of cells that did not express the RNAi as they were colored white or light orange (Fig., 18, compare A and C). The cells that expressed the RNAi would be of dark red color, suggesting that these cells have died (Fig. 18, C). This phenotype was not observed with the second RNAi line (107292) (Fig. 18, D) Also, a knockdown of *Ets98B* with *GMR-Gal4* did not affect eye development, except for line 107292 that seemed to enlarge eye size slightly (Fig. 18, G and H). In wing imaginal discs, ectopic expression of Ets98B led to pupal lethality (Fig. 18, J and N). Downregulation of Ets98B in the wing pouch or the posterior compartment resulted in smaller and not correctly unfolded wings with patterning defects such as thicker or missing veins (Fig. 18, I, K, L-M, O and P).

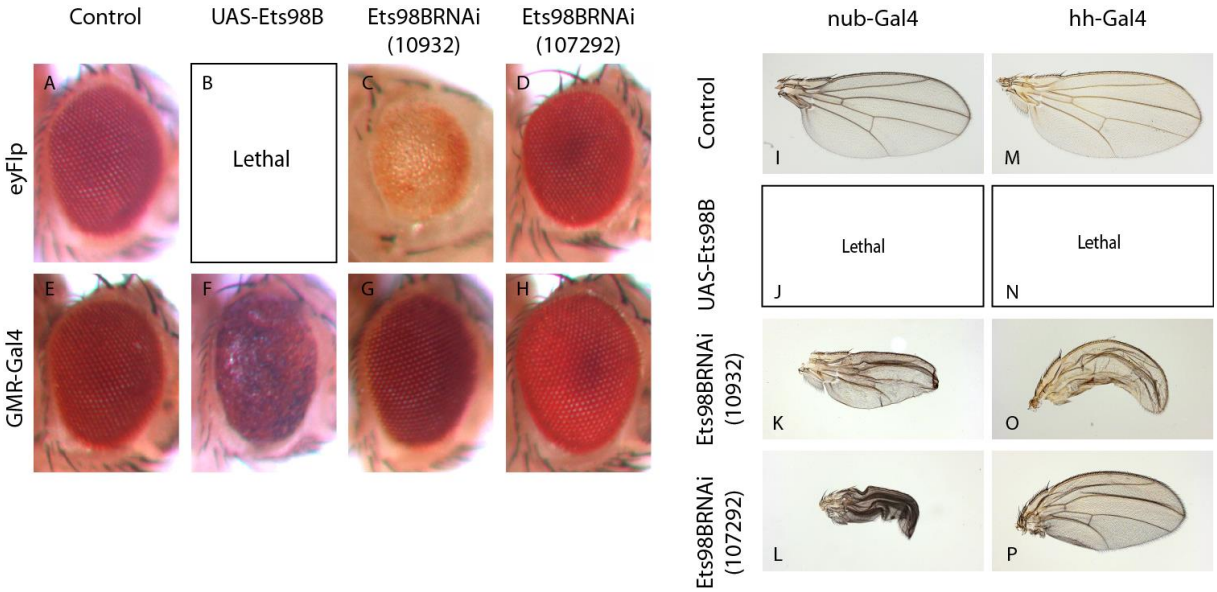

Figure 18: Effects of Ets98B depletion or ectopic expression in eye and wing tissue. Images of adult eyes (A-H) and wings (I-P) are shown.

4.1.6 Ets96B

Ets96B has not been functionally characterized so far. Overexpression in the whole eye disc caused slightly enlarged eyes (Fig. 19, A and B). Wings did not seem to be affected (Fig. 19, G, H, J and K). A a knockdown of *Ets96B* led to a slight reduction in eye and wing size (Fig. 19, A, C and F, G, I-J and L). This could, however, also been due to normal size variablity within the population.

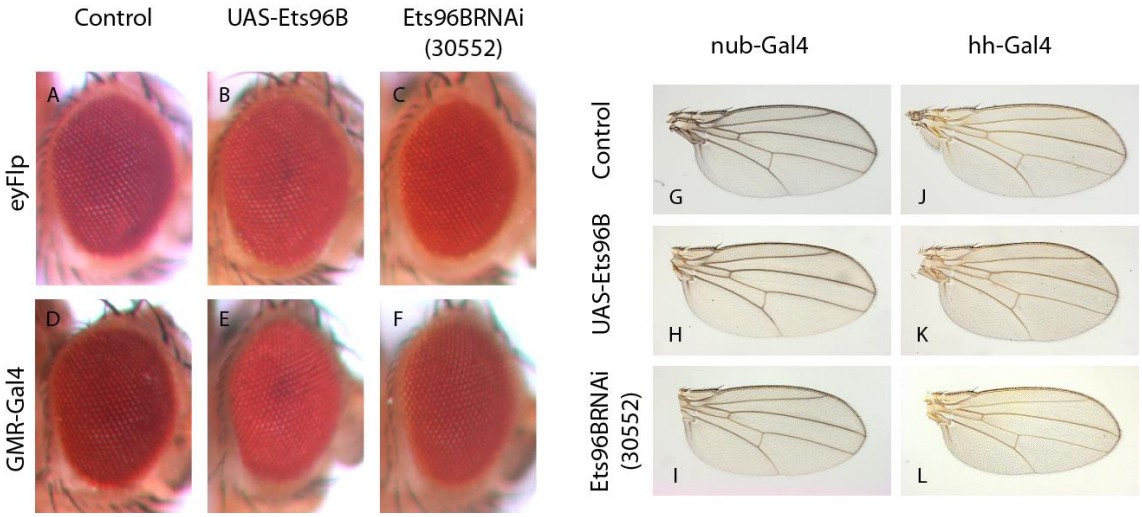

Figure 19: Effects of Ets96B depletion or ectopic expression in eye and wing tissue. Images of adult eyes (A-F) and wings (G-L) are shown.

4.1.7 Ets65A

Ets65A has been identified by Chen et al., 1992, but its function remained unknown. Wing and eye size as well as morphology were normal upon overexpression and knockdown (Fig. 20, A-B, D-H, I and L). Only a depletion in the whole eye or ectopic expression in the posterior compartment resulted in smaller eyes or wings (Fig. 20, C and K).

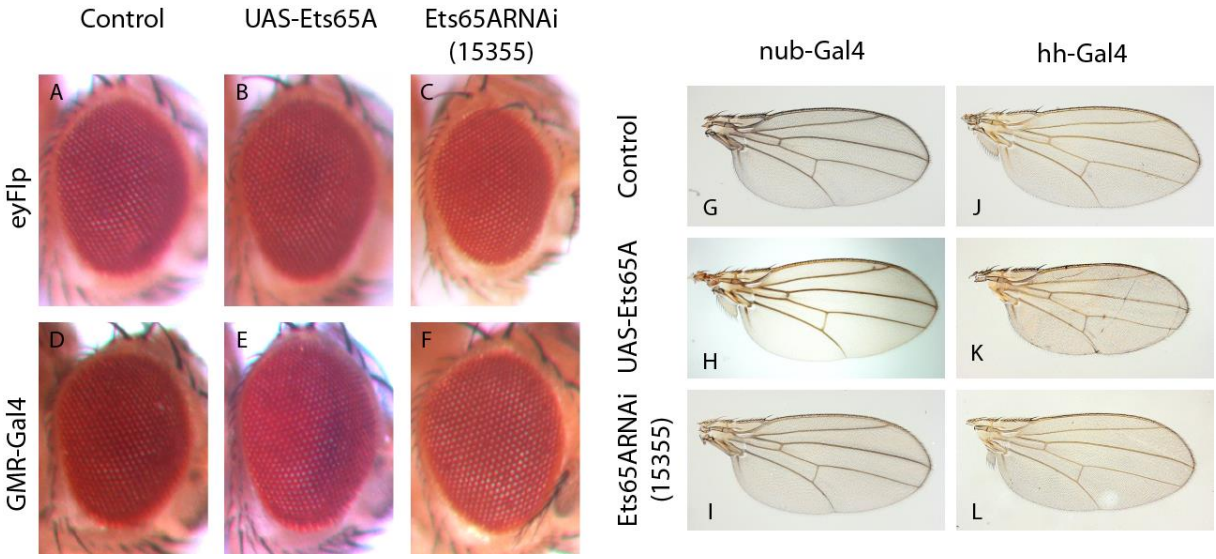

Figure 20: Effects of Ets65A depletion or ectopic expression in eye and wing tissue. Images of adult eyes (A-F) and wings (G-L) are shown.

4.1.8 Ets97D

Ets97D is required for the proper formation of the oocyte (Gajewski & Schulz, 1995; Schulz *et al*, 1993). Its function in the development of the adult eyes and wings, however, has not been studied yet. Overexpression of Ets97D neither affected eye or wing size nor morphology (Fig. 21, A, B, E, F, I, J, M and N). A knockdown of Ets97D with *GMR-Gal4* also had no apparent effect (Fig. 21, G and H). Depletion of the gene product in the whole eye, however, reduced eye size and lead to a more roundish shape (Fig. 21, C and D). A similar effect was observed in wings (Fig. 21, I, K-M, O and P). Particularly the knockdown in the wing pouch with line 108936 led to a dramatic reduction in size and defects in wing unfolding (Fig. 21, L). This phenotype is very similar to the one observed with an RNAi line targeting Ets98B (compare Fig. 18, L and P to Fig. 21, L and P).

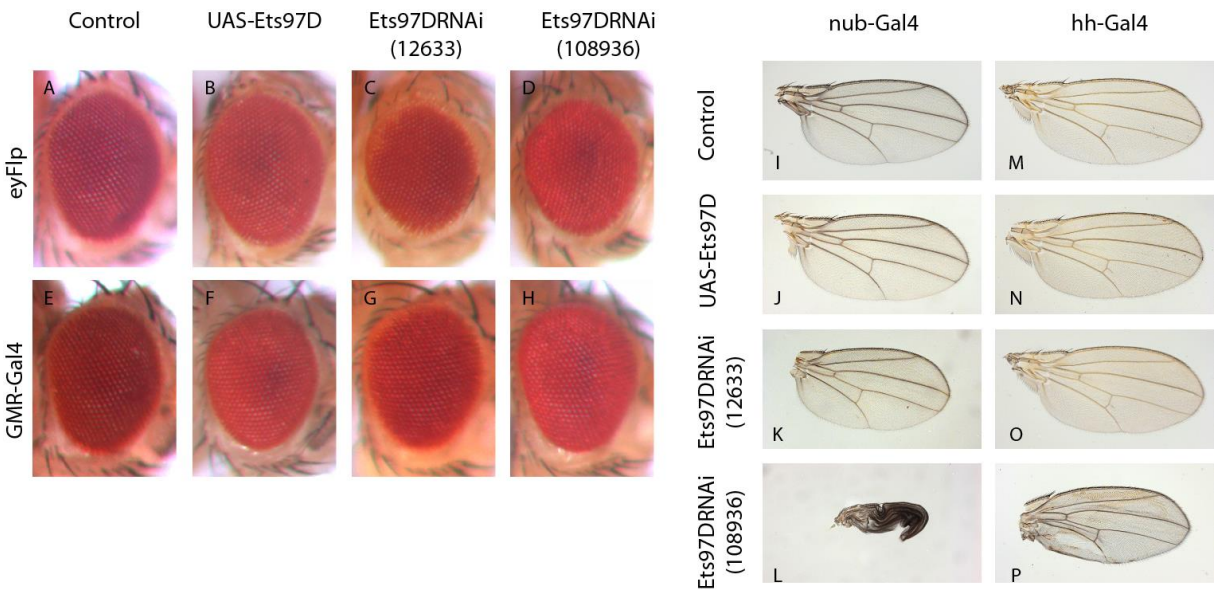

Figure 21: Effects of Ets97D depletion or ectopic expression in eye and wing tissue. Images of adult eyes (A-H) and wings (I-P) are shown. Note the extensive wing size reduction upon knockdown with line 108936 (L).

4.1.9 Conclusions

Based on the roles of Pnt and Aop during eye development and the interesting phenotype of Ets21C overexpression in eyes (see Ets21C Manuscript Sup. Fig. 2), we tested other members of the *Drosophila* ETS gene family for a role in eye and wing development. Two members, Ets96b and Ets65A do not seem to affect eye or wing development as neither depletion nor overexpression of the gene product caused an apparent phenotype. However, a depletion of Ets98B, Ets97D and E74 resulted in defective wings, suggesting an involvement of these genes in wing growth and patterning. A depletion of Ets98B also caused a rough eye phenotype and smaller eyes, but these phenotypes varied a lot depending on the driver and RNAi line used. The similarity between the *Ets97D* and *Ets98B* knockdown phenotype in wings is striking and demands further investigations to test if the two proteins act in a common pathway or whether the identical phenotypes were caused by RNAi off-target effects. The phenotypes of Ets98B and Ets97D were only similar with RNAi, but not if the proteins were overexpressed in wing or eye tissue. Ets97D did not cause any effect, but Ets98B overexpression exerted a strong effect on wing or eye tissue as it caused lethality or a rough eye phenotype.

Here, it would be interesting to perform further experiments to understand how Ets98B over-expression affects eye and wing development.

4.2 Methods

Fly husbandry

Flies were grown under standard conditions at 25°C. Fly stocks used in sections 2.1.1 – 2.1.5, 2.2 and Appendix 4.1 are listed in a separate appendix (4.3).

Generation of the *alrm* deletion

Alrm was removed with an *in trans* recombination of flanking PiggyBac (PBac) elements according to the strategy of Parks et al. (Parks *et al*, 2004) (see Fig. 10). PBac elements *XP (-) Fur1^{d04883}* and *WH (+) Fur1^{f00663}* were combined with *hsp70-flp* on the X-chromosome and then brought together in trans. *yw, hsFlp; XP Fur1^{d04883}/WH Fur1^{f00663}* progeny were heat-shocked two days AEL for 1h at 37°C. The heat-shock was repeated the next two days. Single adult males were crossed to balancer chromosomes and progeny were screened for positive recombination. Both PBac elements initially carry a *mini-white* gene, restoring red eye color in flies mutant for the *white* (*w*) gene. Successful recombination between XP elements in minus direction and WH elements in plus direction, removes the *mini-white* sequences of both PBac elements, resulting in flies with white eyes. We therefore could easily screen flies for white eye color. Isogenic stocks were established from three independent white eyed males and successful recombination was confirmed by PCR with primers *XP 5` plus* and *WH 5` minus* according to Parks et al. (Parks *et al*, 2004). A product is only yielded if recombination was successful as the region between the primer binding sites is otherwise too long.

Cloning and generation of transgenes

Ets21C phosphomutant

A plasmid with the open-reading frame of the *Ets21C* A isoform was obtained from FlyORF and the modification of the phosphorylation site was introduced with a simple PCR. As the putative phosphorylation sites lies very close to the C-terminus, we designed a 37 nt long primer *5`- TCTAGACTAGTTGAATGCATTTGTGGTGGGTGCGACC – 3`* that contained a

substitution of the threonine codon of amino acid 468 with alanine, the remaining sequence including stop codon and an XbaI cut site. In addition to the XbaI site, we introduced an Acc65I site a the start of the coding sequence for subcloning into pUAST.attB.

Ets21C$^{\Delta SOCS}$

To delete the SOCS domain, we performed an overlapping PCR that removed amino acids 57-110 of Ets21C. The truncated protein version was cloned into pUAST.attB via 5` Acc65I and 3` XbaI cut sites that had been attached in the PCR.

Alrm overexpression

To generate the alrm overexpression construct, we amplified the *alrm* sequence from genomic DNA and attached 5` Acc65I and 3` XbaI cut sites for subcloning into pUAST.attB.

Independent alrm RNAi lines

Dharmacon algorithm was used to design the RNAi target site of 21-mer oligos. We choose four different target sites in the *alrm* coding sequence that were not overlapping with the sequence of the VDRC RNAi line 14738 for further processing. Target sites were converted into 71 nt long oligos using http://flybuzz.berkeley.edu/cgi-bin/constructHairpin.cgi and a 5` NheI and 3` EcoRI site was attached. After an annealing step, oligos were inserted into pNE3.2 via NheI and EcoRI sites. pNE3 vector was obtained from B. Haley and is a derivative of *pUAST-attB* (Haley *et al*, 2008; Bischof *et al*, 2007).
Sequences of the oligos used:

HP5: *5`- ctagcagtattgggaaacgttcagggttatagttatattcaagcatattacccgaaggtttcccaatgcg - 3`*
HP6: *5`- ctagcagtaaatttctcttggagttttaatagttatattcaagcatataaaaactcctagagaaatttgcg - 3*
HP7: *5`- ctagcagtcgtgattggtggcagtgataatagttatattcaagcatataatcactgcgaccaatcacggcg - 3*
HP8: *5`- ctagcagttcgcatgttgcaggagatgtatagttatattcaagcatattcatctcctccaacatgcgagcg -3*

All constructs were inserted via the ΦC31 integrase system into landing site *ZH-86Fb*.

Deletion of AP-1 sites

Putative AP-1 sites in the *Ets21C* genomic region (see Fig. 8) were deleted with overlapping PCRs according. An *Ets21C* Bacterial artificial chromosome (Bac) (CH322-41A08) served as template for the PCR. With this strategy we have generated two mutant fragments, the first contained three deleted AP-1 sites and the second the remainig AP-1 site. The fragments with the deleted sites were then exchanged in two steps with the wild-type sequence via ClaI and XbaI and XbaI and Pfl23II sites. The entire *Ets21C* genomic region including upstream and downstream sequences up to the next neighboring genes has previously been amplified from the *Ets21C* Bac and has been subcloned into pGEMeasy-T vector (Promega). Once the wild-type sequence had been exchanged for the mutant one, the entire fragment was swapped into a pattB vector via 5` NotI and 3` Acc65I sites that had been attached in the initial PCR to amplify the Ets21C gene region. The same was done with the wild-type fragment.

Immunofluorescence

Fixation and immunostainings of *Drosophila* eye imaginal discs and tumors were performed according to standard protocols. Primary antibody used in this study was: anti-Mmp1 (1/200, 3B8D12, Developmental studies hybridoma bank (DSHB)). Alexa fluor 594 (1/500, Molecular Probes) was used as label for the secondary antibody. Imaginal discs were mounted in VectaShield (Vector Laboratories). Images were taken with a Zeiss Lsm710 confocal microscope and processed with ImageJ and Adobe Photoshop.

Quantification of adult eye size

Images of adult eyes were taken with an Axioplan camera. Eye area was mesured in ImageJ by manually outlining borders of the eye and using the „measure and label“ function of the „Analyze“ plugin of ImageJ to count the number of pixels included in the outlined area (Abràmofff *et al*, 2005).

RNA isolation and real-time PCR

For RNA isolations, larvae were dissected in Ringers plus 0.05% Tween-20 and tumors were collected in an 1.5 ml Eppendorf tube. Tumors were centrifuged for 10 min at 4°C and pellets were snap freezed in liquid nitrogen, stored at -80°C or processed further. For each experiment total RNA was isolated from 30 tumors or 45 wild-type eye discs with the indicated genotypes using the NucleoSpin RNA kit (Machery Nagel). Following an additional Dnase digest for 1h at 37°C (DNA-free^{TM} kit, Ambion), 500 ng of total RNA was used for cDNA synthesis with the transcriptor High Fidelity cDNA Synthesis Kit (Roche) using oligo-dT primers. Quantitative PCR reactions were performed in triplicates using the MESA Green qPCR Mastermix Plus for SYBR Assay (Eurogentec) and an ABI Prism SDS 7900 HT (Applied Biosystems). All measurements of transcript levels were normalized to *actin-5C*, *alpha-tubulin* and *TATA box binding protein (TBP)*. Primers were designed with Roche Universal Probe Library or with Primer3plus. When ever possible an intron-spanning assay was chosen. Primers used were: Ets21C: F: caacgacgacgaaccaaat, R: gttcgcgttggacgaatc, Mmp1: F: gaaggctcggacaacgagt, R: gtcgttggactggtgatcg, actin: F: gcccatctacgagggttatgc, R: aatcgcgaccagccagatc, alpha-tubulin at 84C: F: gccagatgccgtctgacaa, R: agtctcgctgaagaaggtgttga, TATA binding protein: F: cgcgcatcatccaaaagc, R: gccgaccatgttttgaatcttaa

Quantitative PCR reactions based on DNA isolated from ChIP experiments described below were performed according to the same protocol as RNA based reactions, but only in duplicates. Reactions were run on input chromatin and ChIP specific DNA. Reactions with no DNA served as negative control. Differences in cycle thresholds (cts) were normalized to a control primer pair and fold enrichment was calculated based on the ΔΔct method. Primers used were:

Mmp1_5: F: gaacagagcgaatggaaagg, R: ctgttggaaagtgggattgg,
Mmp1_6: F: tcgctgacgataaggtggat, R: ctcttcgcagaaatcccaac,
Mmp1_7: F: atgaatctgcggtctggatt, R: ttcggtgaaacatacactttcc
Mmp1_8: F: ggcaccaccccattaatatc, R: attgctcaggccgattactg
Mmp1_10: F: tcggaatcccctgagtaatg, R: attcatttgccttgcacgtt

Chromatin immunoprecipitation (ChIP)

ChIP was done on 150 Ras^{V12} dlg^{RNAi} tumors expressing HA-tagged Ets21C. Tumors were dissected in pools of 50 tumors and fixed in 1% formaldehyde and PBS-Tween 20 (0.1%) for 10 min at room temperature. Crosslinking was stopped with 125 mM glycine for 5 min at room temperature and tumors were washed twice with PBS-Tween 20 (0.1%) plus protease inhibitors (Mini EDTA free, Roche). After a centrifugation step at 5000 g, the supernatant was removed and 250 µl lysis buffer was added (5mMPIPES at pH8.0, 85mMKCl, 0.5% NP-40, protease inhibitors). The sample was snap frozen in liquid nitrogen and stored at -80°C until further processing.

The ChIP was performed as described in (Schertel *et al*, 2015) with the following modifications: For sonication the following parameters were used (duty cycle 10%, intensity, 5; cycle/burst, 200; time, 45s) to obtain fragments of an average size of 500 bp. Three sonication reactions were pooled to obtain material from 150 tumors for the IP. 2% of the chromatin was kept as input at 4°C until reverse crosslinking and elution steps. The two final wash steps after incubation of antibody-chromatin complexes with beads were done with additional 0.25% SDS. Finally, DNA was eluted in 20 µl H_2O and stored at -20°C until further use. The antibody used was Rabbit anti-HA Chip grade (ab9110, Abcam).

4.3 Fly stocks

The following section lists fly stocks that have been used or generated during this thesis. Stocks used in section 4.2 and section 4.3 are listed separately in the manuscripts.

General fly stocks

yw; Sp/CyO; MKRS/TM6b
yw; Sp/SM5; MKRS/TM6b
yw; Sp/CyO; TM2/TM6b *BK9*

Sections 4.1.1 – 4.1.5 l additional experiments on Ets21C

eyFlp; act>y+>Gal4, UAS-GFP/CyO, tub-Gal80;UAS-Ras^{V12}/TM6b
eyFlp; Sp/CyO; act>CD2>Gal4, UAS-GFP/TM6b
eyFlp; UAS-Ras^{V12}, UAS-dlg^{RNAi}/CyO, tub-Gal80; act>CD2>Gal4, UAS-GFP/TM6b
yw; UAS-dlg^{RNAi} , UAS-Ets21C$^{RNAi\ 51225}$/CyO; MKRS/TM6b
yw; UAS-dlg^{RNAi}/CyO; UAS-Ets21C^{HA}/TM6b
Ets21C RNAi*:* VDRC 51225 (II)
dlg RNAi: VDRC 41134 (II)
yw; Sp/CyO; UAS-Ets21C$^{HA\ (86Fb)}$/TM6b FlyORF
yw; Sp/CyO; UAS-Ets21C$^{T468A\ (86Fb)}$/TM6b
yw; Sp/CyO; UAS-Ets21C$^{\Delta SOCS\ (86Fb)}$/TM6b
yw; Sp/CyO; UAS-Ets21C$^{wt\ (86Fb)}$/TM6b

Section 4.2 evaluation of alrm

eyFlp; Sp/CyO; act>CD2>Gal4, UAS-GFP/TM6b
eyFlp; UAS-Ras^{V12}, UAS-dlg^{RNAi}/CyO, tub-Gal80; act>CD2>Gal4, UAS-GFP/TM6b
alrm RNAi: VDRC 14738 (II)
y w; Sp/CyO; UAS-alrm/TM6b

w; GMR-Gal4; +/+

y wFlp; Sp/CyO; UAS-Egr^{86Fb}/TM6b

y w; Sp/CyO; alrm$^{RNAi\ (HP5)}$/TM6b

y w; Sp/CyO; alrm$^{RNAi\ (HP6)}$/TM6b

y w; Sp/CyO; alrm$^{RNAi\ (HP7)}$/TM6b

y w; Sp/CyO; alrm$^{RNAi\ (HP8)}$/TM6b

y w; Sp/CyO; alrm$^{\Delta d04883\text{-}f00663}$/TM6b

Appendix 7.2 Loss and gain of function of other Drosophila ETS genes during development

ey Flp; Sp/CyO; act>CD2>Gal4, UAS-GFP/TM6b

y w Flp; nub-Gal4; +/+

y wFlp; Sp/CyO; hh-Gal4/TM6b

w; GMR-Gal4; +/+

pointed RNAi: VDRC 105390 (II)

ywFlp; ; UAS-PntRB$^{(86Fb)}$/TM3 FlyORF

ywFlp; ; UAS-PntRD$^{(86Fb)}$/TM3 FlyORF

aop RNAi: BL 35404

aop RNAi: BL 34909

y w; Sp/CyO; UAS-aop$^{(86Fb)}$/TM6b FlyORF

E74 RNAi: VDRC 105301 (II)

Ets21C RNAi: VDRC 51225 (II)

Ets21C RNAi: VDRC 106153 (II)

y w; Sp/CyO; UAS-Ets21C$^{HA\ (86Fb)}$/TM6b

Ets98B RNAi: VDRC 10932 (II)

Ets98B RNAi: VDRC 107292 (II)

yw; Sp/CyO; UAS-98B^{86Fb}

Ets96B RNAi: VDRC 30552 (I)

y w; ; UAS-96B^{86Fb}/TM3 FlyORF

Ets65A RNAi: VDRC 15355 (I)

yw; Sp/CyO; UAS-65A$^{(86Fb)}$/TM6b FlyORF

Ets97D RNAi: VDRC 12633 (III)

Ets97D RNAi: VDRC 108936 (II)

y w; ; UAS-97D^{86Fb}/TM3 FlyORF

4.4 Plasmid list

This table lists plasmids that have been used or generated in this thesis.

Name	Construct	Cloning details
pJT01	pUASTattB – Ets21CT468A	Ets21C ORF into pUAST via Acc65I, XbaI, site directed muta T468A
pJT02	pUASTattB – Ets21CΔEts	Ets21C ORF into pUAST via Acc65I, XbaI, deletion of aa 254-339.
pJT03	pUASTattB – Ets21CΔPnt	Ets21C ORF into pUAST via Acc65I, XbaI, deletion of aa 143-214.
pJT04	pUASTattB – Ets21CΔSOCS	Ets21C ORF into pUAST via Acc65I, XbaI, deletion of aa 57-110.
pJT05	pUASTattB – Ets21Cwt	Ets21C ORF into pUAST without HA-tag
pJT06	pGEM-easyT – genomic Ets21C^{WT}	PCR of Ets21C genomic region (10kB) from BAC into pGEM-easyT
pJT07	pGEM-easyT – genomic Ets21C$^{\Delta AP\text{-}1\ (1\text{-}3)}$	PCR of Ets21C genomic region (ca. 4kB) from BAC to delete AP-1 sites 1-3 into pGEM-easyT
pJT08	pGEM-easyT – genomic Ets21C$^{\Delta AP\text{-}1\ (4)}$	PCR of Ets21C genomic region (ca. 2kB) from BAC to delete AP-1 site 4 into pGEM-easyT
pJT09	pGEM-easyT – genomic Ets21$^{wt_\Delta AP\text{-}1\ (1\text{-}3)}$	pJT07 swapped into pJT06 via ClaI and XbaI
pJT10	pGEM-easyT – genomic Ets21C $^{\Delta AP\text{-}1all}$	pJT08 swapped into pJT10 via XbaI and Pfl23II sites
pJT11	pattB genomic Ets21C^{wt}	Genomic Ets21C^{wt} swapped into pattB via NotI and Acc65I
pJT12	pattB genomic Ets21C$^{\Delta AP\text{-}1all}$	Genomic Ets21C$^{\Delta AP\text{-}1(1\text{-}4)}$ in pJT10 swapped into pattB via NotI and Acc65I
pJT13	pUAST-alrm	PCR of alrm CDS cloned into pUAST via Acc65I and XbaI
pJT14	pNE3.2_Ets21C^{HP1}	Ets21C oligo HP1 cloned into pNE3.2 via NheI and EcoRI
pJT15	pNE3.2_Ets21C^{HP2}	Ets21C oligo HP2 cloned into pNE3.2 via NheI and EcoRI
pJT16	pNE3.2_Ets21C^{HP3}	Ets21C oligo HP3 cloned into pNE3.2 via NheI and EcoRI
pJT17	pNE3.2_Ets21C^{HP4}	Ets21C oligo HP4 cloned into pNE3.2 via NheI and EcoRI
pJT18	pNE3.2_alrm^{HP5}	Alrm oligo HP5 cloned into pNE3.2 via NheI and EcoRI

pJT19	pNE3.2_alrm^{HP6}	Alrm oligo HP6 cloned into pNE3.2 via NheI and EcoRI
pJT20	pNE3.2_alrm^{HP7}	Alrm oligo HP7 cloned into pNE3.2 via NheI and EcoRI
pJT21	pNE3.2_alrm^{HP8}	Alrm oligo HP8 cloned into pNE3.2 via NheI and EcoRI
pJT22	pUAST – HA Ets21CWT	5` NheI site added to Ets21CWT and swapped into pRN155.
pJT23	pUAST– HA Ets21CΔEts	5` NheI site added to Ets21CΔEts and swapped into pRN155.
pJT24	pUAST– HA Ets21CΔPnt	5` NheI site added to Ets21CΔPnt and swapped into pRN155.
pJT25	pUAST – HA Ets21CΔSOCS	5` NheI site added to Ets21CΔSOCS and swapped into pRN155.
pRN159	pUAST – HAFos	Fos CDS between NheI and XbaI sites, generated by R. Narasimamurthy
pRN151	pUAST – JunFLAG	generated by R. Narasimamurthy
pRN36	pUAST – dTak1	generated by R. Narasimamurthy
	tub-Gal4	obtained from A. Franz
	pUAST – GFP	obtained from D. Zimmerli

4.5 Primer list

The following primers have been used for genotyping, cloning or sequencing.

Nr.	Name	Sequence 5`- 3`	Restriction sites
JT001	Ets21CAcc65I	gggtaccatggccattctacagaatagc	Acc65I
JT002	Ets21CXbaI2	cgaatctagatcagttgaatgcatttgtgg	XbaI
JT003	CG11910mRNA	taccatggcggtactctggt	
JT004	CG11910mRNA rev	ccggctatagcttcatcttcat	
JT005	CG11910Acc65I	cgggtaccatggcggtactctggtgg	Acc65I
JT006	CG11910XbaI	cgtctagactatagcttcatcttcatctcc	XbaI
JT007	Ets21CmRNA	gcttaatggccattctacagaatag	
JT008	Ets21CmRNA	tcagttgaatgcatttgtggtg	
JT009	hsp70	ctgccaagaagtaattattgaatac	
JT010	SV40	ctgtaggtagtttgtccaattatgtc	
JT011	CG11910_seq	atcgattgccagccaaatttagg	
JT012	CG11910_seq2	ggaaatcagttgaagcagctg	
JT013	CG11910_seq2	gtttcttgaacaatccctctgg	
JT014	CG11910_seq3	ccaatgtgagcagtctggattt	
JT015	Ets21C mRNA	gcaggaacatcccagcttaatg	
JT016	Ras85D_Exon1	cacgtttcacgtcactttcg	
JT017	Ras85D_Exon2 (CDS)	ctcgattgtggggtcgtact	
JT018	VDRC41134_IR	cgcgaattccacacaccacccgacccaag	
JT019	VDRC41134_IR	cgctctagaccattttaatcgcccgctcgt	
JT020	VDRC51225_IR	cgcgaattcgctcaggcgcagggaggaga	
JT021	VDRC51225_IR	cgctctagacctggtcgtagtttcccgcagaag	
JT022	VDRC_hsp70	gaggcgcttcgtctacggagcgac	
JT023	Ets21C_B	atgagcgtcagcgtggac	
JT024	Ets21C_B	tcagttgaatgcatttgtggtgg	
JT025	VDRC41134_IR	cgcgaattccacacaccacccgacccaag	
JT026	VDRC41134_IR	cttgggtcgggtggtgtgtggaattcgcg	
JT027	41134_IR	aagcgagagtacgaggtgga	
JT028	Hsp70_rev	gtattcaataattacttcttggcag	
JT029	Ets21CGen_NotI	gcggccgcaatgtttcaaccagcag	NotI

JT030	Ets21CGen_NotI2	gcggccgctacaatggaatg	NotI
JT031	pLacZ fwd	cagctggcgtaatagcgaaga	
JT032	pLacZ rev	cttcctgtagccagctttcatc	
JT033	Ets21CGen_XbaI	cgtcgaggttctagatctgtacc	XbaI
JT034	Ets21C_Ex1 fwd	gtactactacgacaagaacatcatgac	
JT035	Ets21C_3`UTR	gagacctcgtatggaataaaggac	
JT036	Ets21C_Ex1End_2	tcctcctccgcctccactt	
JT037	Ets21C_Ex2	atccgtaccagctgctga	
JT038	Ets21C_Ex1 rev	cggcgtggtgattgtaggaa	
JT039	sEts21C_Ex4 fwd	ccaagtggaaagctcatgg	
JT040	sEts21C_Ex4_fwd2	acagggccaaagtgaagtga	
JT041	sEts21C_Ex4_fwd3	gcagcagtagctccacca	
JT042	sEts21C_Ex3 fwd	aacaatccaatcgggtcaaa	
JT043	sEts21C_Ex2 fwd	tctcctctcgctcgctct	
JT044	sEts21C_Ex1End rev	atcaggtgctccgtgtagg	
JT045	T7 fwd	taatacgactcactataggg	
JT046	SP6 rev	tatttaggtgacactatag	
JT047	attB rev	atg atg gac cag atg ggt gag g	
JT048	Mut. Ets21C fwd	ggtcgcacccaccacaaatg	
JT049	Mut. Ets21C rev	catttgtggtgggtgcgacc	
JT050	Ets21C_Ex4 rev	agactaagccataagaggacatagg	
JT051	Ets21C_Ex3 rev	ggctaaaagacacagttccca	
JT052	Ets21C_Ex4_cds fwd	cgacaggtttcccaaggat	
JT053	pLacZ rev	tcttcgctattacgccagctg	
JT054	attB fwd	cctcacccatctggtccatcat	
JT055	Bac 41A08 fwd	gggcaggcacataaatctgg	
JT056	Bac 41A08 rev	agagctcccttgatgtcacc	
JT057	Ets21C_SOCS_rev	gtgtcgccagcgggagcgtctccttcgcttccag	
JT058	Ets21C_SOCS_fwd	ctggaagcgaaggagacgctcccgctggcgacac	
JT059	Ets21C_Pnt_fwd	gccatctcctcgaaggaactagcttataccacgccaccg	
JT060	Ets21C_Pnt_rev	cggtggcgtggtataagctagttccttcgaggagatggc	
JT061	Ets21C_Ets_fwd	caaggctcagggggccaaaatggccgcatgccaggctc	
JT062	Ets21C_Ets_rev	gagcctggcatgcggccattttggccccctgagccttg	
JT063	Ets21C_Ets_fwd2	gacttccacggtctgatgggacttccacggtctgatgg	
JT064	Ets21C_Ets_rev2	ccatcagaccgtggaagtcccatcagaccgtggaagtc	
JT065	Ets21C_Ets_fwd3	aggctcagggggccaaatccgccgcatgccaggctca	
JT066	Ets21C_Ets_rev3	tgagcctggcatgcggcggatttggccccctgagcct	

JT067	Ets21C_Pnt fwd_new	gccatctcctcgaaggaacagcttataccacgcc	
JT068	Ets21C_Pnt rev_new	ggcgtggtataagctgttccttcgaggagatggc	
JT069	Ets21C_Ets fwd_3 new	aggctcagggggccaaatcgccgcatgccaggctca	
JT070	Ets21C_Ets rev_3 new	tgagcctggcatgcggcgatttggccccctgagcct	
JT071	pGEM Oligo_ rev	gtaagcttgtaagcaatttctgttag	
JT072	pGEM Oligo_rev_2	tacggcagttagaaattgtaagc	
JT073	VDRC_6212 Fos fwd	cgcgaattcctggagaagcggggcgagag	
JT074	VDRC_6212 Fos rev	cgctctagaatgcccgtaatcgtgccgttg	
JT075	AP-1Mut_det rev	tggcctagtccgtatgagtcac	
JT076	AP-1Mut_det fwd	atcggcggatgagtcacct	
JT077	BacA08 inwards fwd	caagtaggcatggcatggac	
JT078	BacA08out rev	cgaagaaaacgggcatcagt	
JT079	AP-1Mut_seq fwd	ctgtggcaggaagagcaagt	
JT080	AP-1Mut_seq rev	tgcgtttattggtagcctgc	
JT081	AP-1Mut_seq rev2	tggatgatggaaccagaaaag	
JT082	AP-1Pos_det_rev	cctagtccgtaccgtccattg	
JT083	AP-1Mut_last fwd	agacttttgcgaccatgagc	
JT084	AP-1Mut_last rev	ggcgtggtgattgtaggaac	
JT085	XmajI PCR fwd	tcgcaggtaaattagcaaggc	
JT086	AP-1 new PCR 1fwd	tcgcagcatcgttcacaaaa	
JT087	Pfl23II_PCR rev	tctcggtgttcagcaccac	
JT088	Ets21Cp_Acc65I	ggtaccatggccattctacagaatagc	Acc65I
JT089	Ets21CphosMutA_Stop_XbaI	tctagatcagttgaatgcatttgtggtgggtgcgacc	XbaI
JT090	Ets21CphosMutG_Stop_XbaI	tctagatcagttgaatgcatttgtggtgggtccgacc	XbaI
JT091	Ets21CphosMutA_XbaI	ggtcactcccaccacaaatgcattcaactga	XbaI
JT092	Ets21CphosMutG_XbaI	ggtcggacccaccacaaatgcattcaactctaga	XbaI
JT093	Ets21CphosMutA_Stop_XbaIN	tctagactagttgaatgcatttgtggtgggtgcgacc	XbaI
JT094	Ets21CphosMutA_HA_BssHII	gcgcgcggtcactcccaccacaaatgcattcaactga	BssHII
JT095	Ets21C_cds rev2	agacgctccggttggagt	
JT096	A08_fragment rev	actgtgatagtcgccctgct	
JT097	white 2 fwd	tttgtgacctgttcggagtg	
JT098	Ets21CwtXbaI2 rev	ctctagactagttgaatgcatttgtgg	XbaI
JT099	Ets21C Ex3 fwd2	gcggatgagtcaccttgatt	
JT100	Bac_phosMutA_fwd	ccggtcgcacccaccacaaatg	
JT101	Bac_phosMutA_rev	catttgtggtgggtgcgaccgg	
JT102	Ets21CwtXbaI3 rev	gtactctagactagttgaatgcatttgtgg	XbaI
JT103	BacA08_geno rev	ccgttccaaatgtctggtct	

JT104	Fos rev out	atgtactgcgtttgctgctg	
JT105	Fos fwd out	catcggcaacaacatgaact	
JT106	Ets21C_gene_NotI fwd	gcggccgcacctttgccaaatatcgga	NotI
JT107	Ets21C_gene_Acc65I rev	ggtaccgccaccaaactcccgaaaa	Acc65I
JT108	Ets21C_gene_NotI	gcggccgctggaatgtttcaaccagcaga	NotI
JT109	Ets21C_gene_Acc65I rev	agcagcacacgtcaacaatc	Acc65I
JT110	Ets21C_gene_NotI2	gcggccgctttcaaccagcagatactaa	NotI
JT111	Fos_RA_end fwd	gcaccttcaacttcgactcc	
JT112	Ets21C_HAXbaI	gatctctagacgtgacgtaagctagcacta	XbaI
JT113	Ets21C_NheI	attctgctagcatggccattctacagaatag	NheI

5 Bibliography

Abràmofff MD, Magalhães PJ & Ram SJ (2005) Image processing with ImageJ. *Biophotonics Int.* **11:** 36–43

Alipov G, Nakayama T, Ito M, Kawai K, Naito S, Nakashima M, Niino D & Sekine I (2005) Overexpression of Ets-1 proto-oncogene in latent and clinical prostatic carcinomas. *Histopathology* **46:** 202–208

Andersen DS, Colombani J, Palmerini V, Chakrabandhu K, Boone E, Röthlisberger M, Toggweiler J, Basler K, Mapelli M, Hueber A-O & Léopold P (2015) The Drosophila TNF receptor Grindelwald couples loss of cell polarity and neoplastic growth. *Nature* **522:** 482–486

Baldus CD, Liyanarachchi S, Mrózek K, Auer H, Tanner SM, Guimond M, Ruppert AS, Mohamed N, Davuluri R V, Caligiuri MA, Bloomfield CD & de la Chapelle A (2004) Acute myeloid leukemia with complex karyotypes and abnormal chromosome 21: Amplification discloses overexpression of APP, ETS2, and ERG genes. *Proc. Natl. Acad. Sci. U. S. A.* **101:** 3915–20

Bassett AR & Liu J-L (2014) CRISPR/Cas9 and genome editing in Drosophila. *J. Genet. Genomics* **41:** 7–19

Bassett AR, Tibbit C, Ponting CP & Liu J-L (2013) Highly Efficient Targeted Mutagenesis of Drosophila with the CRISPR/Cas9 System. *Cell Rep.* **4:** 220–228

Benz CC, O'Hagan RC, Richter B, Scott GK, Chang CH, Xiong X, Chew K, Ljung BM, Edgerton S, Thor A & Hassell J a (1997) HER2/Neu and the Ets transcription activator PEA3 are coordinately upregulated in human breast cancer. *Oncogene* **15:** 1513–25

Bilder D (2000) Cooperative Regulation of Cell Polarity and Growth by Drosophila Tumor Suppressors. *Science (80-.).* **289:** 113–116

Bilder D & Perrimon N (2000) Localization of apical epithelial determinants by the basolateral PDZ protein Scribble. *Nature* **403:** 676–80

Bischof J, Maeda RK, Hediger M, Karch F & Basler K (2007) An optimized transgenesis system for Drosophila using germ-line-specific phiC31 integrases. *Proc. Natl. Acad. Sci. U. S. A.* **104:** 3312–7

Boutros M, Agaisse H & Perrimon N (2002) Sequential activation of signaling pathways during innate immune responses in Drosophila. *Dev. Cell* **3:** 711–22

Brand AH & Perrimon N (1993) Targeted gene expression as a means of altering cell fates and generating dominant phenotypes. *Development* **118:** 401–15

Brumby AM & Richardson HE (2003) scribble mutants cooperate with oncogenic Ras or Notch to cause neoplastic overgrowth in Drosophila. *EMBO J.* **22:** 5769–79

Brumby AM & Richardson HE (2005) Using Drosophila melanogaster to map human cancer pathways. *Nat. Rev. Cancer* **5:** 626–39

Brunner D, Dücker K, Oellers N, Hafen E, Scholzi H & Klambt C (1994) The ETS domain protein Pointed-P2 is a target of MAP kinase in the Sevenless signal transduction pathway. *Nature* **370:** 386–389

Cangemi R, Mensah A, Albertini V, Jain A, Mello-Grand M, Chiorino G, Catapano C V & Carbone GM (2008) Reduced expression and tumor suppressor function of the ETS transcription factor ESE-3 in prostate cancer. *Oncogene* **27:** 2877–2885

Chambers MC, Lightfield KL & Schneider DS (2012) How the fly balances its ability to combat different pathogens. *PLoS Pathog.* **8:** e1002970

Chen T, Bunting M, Karim FD & Thummel CS (1992) Isolation and characterization of five Drosophila genes that encode an ets-related DNA binding domain. *Dev. Biol.* **151:** 176–91

Colombani J, Andersen DS & Leopold P (2012) Secreted Peptide Dilp8 Coordinates Drosophila Tissue Growth with Developmental Timing. *Science (80-.).* **336:** 582–585

Cooper CDO, Newman J a & Gileadi O (2014) Recent advances in the structural molecular biology of Ets transcription factors: interactions, interfaces and inhibition. *Biochem. Soc. Trans.* **42:** 130–8

Cordero JB, Macagno JP, Stefanatos RK, Strathdee KE, Cagan RL & Vidal M (2010) Oncogenic Ras Diverts a Host TNF Tumor Suppressor Activity into Tumor Promoter. *Dev. Cell* **18:** 999–1011

Dar AC, Das TK, Shokat KM & Cagan RL (2012) Chemical genetic discovery of targets and anti-targets for cancer polypharmacology. *Nature* **486:** 80–84

Delaney JR, Stöven S, Uvell H, Anderson K V, Engström Y & Mlodzik M (2006) Cooperative control of Drosophila immune responses by the JNK and NF-κB signaling pathways. *EMBO J.* **25:** 3068–3077

Dittmer J (2003) The biology of the Ets1 proto-oncogene. *Mol. Cancer* **2:** 29

Doggett K, Grusche F a, Richardson HE & Brumby AM (2011) Loss of the Drosophila cell polarity regulator Scribbled promotes epithelial tissue overgrowth and cooperation with oncogenic Ras-Raf through impaired Hippo pathway signaling. *BMC Dev. Biol.* **11:** 57

Enomoto M, Kizawa D, Ohsawa S & Igaki T (2015) JNK signaling is converted from anti- to pro-tumor pathway by Ras-mediated switch of Warts activity. *Dev. Biol.* **403:** 162–171

Fernández BG, Gaspar P, Brás-Pereira C, Jezowska B, Rebelo SR & Janody F (2011) Actin-Capping Protein and the Hippo pathway regulate F-actin and tissue growth in Drosophila.Fernández, B. G., Gaspar, P., Brás-Pereira, C., Jezowska, B., Rebelo, S. R., & Janody, F. (2011). Actin-Capping Protein and the Hippo pathway regulate F-actin and. *Development* **138:** 2337–46

Ferres-Marco D, Gutierrez-Garcia I, Vallejo DM, Bolivar J, Gutierrez-Aviño FJ & Dominguez M (2006) Epigenetic silencers and Notch collaborate to promote malignant tumours by Rb silencing. *Nature* **439:** 430–436

Fletcher JC & Thummel CS (1995) The Drosophila E74 gene is required for the proper stage- and tissue-specific transcription of ecdysone-regulated genes at the onset of metamorphosis. *Development* **121:** 1411–1421

Gabay L, Scholz H, Golembo M, Klaes A, Shilo BZ & Klämbt C (1996) EGF receptor signaling induces pointed P1 transcription and inactivates Yan protein in the Drosophila embryonic ventral ectoderm. *Development* **122:** 3355–3362

Gajewski KM & Schulz RA (1995) Requirement of the ETS domain transcription factor D-ELG for egg chamber patterning and development during Drosophila oogenesis. *Oncogene* **11:** 1033–40.

Galang CK, Muller WJ, Foos G, Oshima RG & Hauser CA (2004) Changes in the expression of many Ets family transcription factors and of potential target genes in normal mammary tissue and tumors. *J. Biol. Chem.* **279:** 11281–11292

García-Aragoncillo E, Carrillo J, Lalli E, Agra N, Gómez-López G, Pestaña A & Alonso J (2008) DAX1, a direct target of EWS/FLI1 oncoprotein, is a principal regulator of cell-cycle progression in Ewing's tumor cells. *Oncogene* **27:** 6034–6043

Garelli A, Gontijo AM, Miguela V, Caparros E & Dominguez M (2012) Imaginal Discs Secrete Insulin-Like Peptide 8 to Mediate Plasticity of Growth and Maturation. *Science (80-.).* **336:** 579–582

Gateff E (1978) Malignant neoplasms of genetic origin in Drosophila melanogaster. *Science (80-.).* **200:** 1448–1459

Gateff E (1994) Tumor suppressor and overgrowth suppressor genes of Drosophila melanogaster: developmental aspects. *Int. J. Dev. Biol.* **38:** 565–90

Gladstone M, Frederick B, Zheng D, Edwards A, Yoon P, Stickel S, DeLaney T, Chan DC, Raben D & Su TT (2012) A translation inhibitor identified in a Drosophila screen enhances the effect of ionizing radiation and taxol in mammalian models of cancer. *Dis. Model. Mech.* **5:** 342–350

Goberdhan DCI, Paricio N, Goodman EC, Mlodzik M & Wilson C (1999) by antagonizing the Chico / PI3-kinase signaling pathway Drosophila tumor suppressor PTEN controls cell size and number by antagonizing the Chico / PI3-kinase signaling pathway. *Genes Dev.***:** 3244–3258

Golub TR, Barker GF, Lovett M & Gilliland DG (1994) Fusion of PDGF receptor β to a novel ets-like gene, tel, in chronic myelomonocytic leukemia with t(5;12) chromosomal translocation. *Cell* **77:** 307–316

Golub TR, Goga A, Barker GF, Afar DE, McLaughlin J, Bohlander SK, Rowley JD, Witte ON & Gilliland DG (1996) Oligomerization of the ABL tyrosine kinase by the Ets protein TEL in human leukemia. *Mol. Cell. Biol.* **16:** 4107–16

Gratz SJ, Cummings AM, Nguyen JN, Hamm DC, Donohue LK, Harrison MM, Wildonger J & O'connor-Giles KM (2013) Genome engineering of Drosophila with the CRISPR RNA-guided Cas9 nuclease. *Genetics* **194:** 1029–1035

Gu X, Zerbini LF, Otu HH, Bhasin M, Yang Q, Joseph MG, Grall F, Onatunde T, Correa RG & Libermann T a (2007) Reduced PDEF expression increases invasion and expression of mesenchymal genes in prostate cancer cells. *Cancer Res.* **67:** 4219–26

Haley B, Hendrix D, Trang V & Levine M (2008) A simplified miRNA-based gene silencing method for Drosophila melanogaster. *Dev. Biol.* **321:** 482–490

Hanahan D & Weinberg RA (2000) The Hallmarks of Cancer. *Cell* **100:** 57–70

Hanahan D & Weinberg RA (2011) Hallmarks of Cancer: The Next Generation. *Cell* **144:** 646–674

Harvey KF, Zhang X & Thomas DM (2013) The Hippo pathway and human cancer. *Nat. Rev. Cancer* **13:** 246–257

Hiebert SW, Sun W, Davis JN, Golub T, Shurtleff S, Buijs A, Downing JR, Grosveld G, Roussell MF, Gilliland DG, Lenny N & Meyers S (1996) The t(12;21) translocation converts AML-1B from an activator to a repressor of transcription. *Mol. Cell. Biol.* **16:** 1349–1355

Hollenhorst PC, Jones DA & Graves BJ (2004) Expression profiles frame the promoter specificity dilemma of the ETS family of transcription factors. *Nucleic Acids Res.* **32:** 5693–702

Hollenhorst PC, McIntosh LP & Graves BJ (2011) Genomic and biochemical insights into the specificity of ETS transcription factors. *Annu. Rev. Biochem.* **80:** 437–71

Hollenhorst PC, Shah AA, Hopkins C & Graves BJ (2007) Genome-wide analyses reveal properties of redundant and specific promoter occupancy within the ETS gene family. *Genes & Dev.* **21:** 1882–1894

Hsouna A, Watson DK & Hsu T (2004) Developmental expression pattern of D-ets4, the Drosophila homologue of human Pdef. *Gene Expr. Patterns* **5:** 285–289

Hsu T & Schulz R a (2000) Sequence and functional properties of Ets genes in the model organism Drosophila. *Oncogene* **19:** 6409–16

Igaki T, Kanda H, Yamamoto-Goto Y, Kanuka H, Kuranaga E, Aigaki T & Miura M (2002) Eiger, a TNF superfamily ligand that triggers the Drosophila JNK pathway. *EMBO J.* **21:** 3009–18

Igaki T, Pagliarini R a & Xu T (2006) Loss of cell polarity drives tumor growth and invasion through JNK activation in Drosophila. *Curr. Biol.* **16:** 1139–46

Jiang C, Lamblin a F, Steller H & Thummel CS (2000) A steroid-triggered transcriptional hierarchy controls salivary gland cell death during Drosophila metamorphosis. *Mol. Cell* **5:** 445–455

Jin Y, Ha N, Forés M, Xiang J, Gläßer C, Maldera J, Jiménez G & Edgar B a. (2015) EGFR/Ras Signaling Controls Drosophila Intestinal Stem Cell Proliferation via Capicua-Regulated Genes. *PLOS Genet.* **11:** e1005634

Justice RW, Zilian O, Woods DF, Noll M & Bryant PJ (1995) The Drosophila tumor suppressor gene warts encodes a homolog of human myotonic dystrophy kinase and is required for the control of cell shape and proliferation. *Genes Dev.* **9:** 534–546

Kanda H, Igaki T, Kanuka H, Yagi T & Miura M (2002) Wengen, a member of the Drosophila tumor necrosis factor receptor superfamily, is required for Eiger signaling. *J. Biol. Chem.* **277:** 28372–5

Kar A & Gutierrez-Hartmann A (2013) Molecular mechanisms of ETS transcription factor-mediated tumorigenesis. *Crit. Rev. Biochem. Mol. Biol.* **48:** 522–543

Kauppila S, Maaty WSA, Chen P, Tomar RS, Eby MT, Chapo J, Chew S, Rathore N, Zachariah S, Sinha SK, Abrams JM & Chaudhary PM (2003) Eiger and its receptor, Wengen, comprise a TNF-like system in Drosophila. *Oncogene* **22:** 4860–4867

Kim C a., Phillips ML, Kim W, Gingery M, Tran HH, Robinson M a., Faham S & Bowie JU (2001) Polymerization of the SAM domain of TEL in leukemogenesis and transcriptional repression. *EMBO J.* **20:** 4173–4182

Kim S, Denny CT & Wisdom R (2006) Cooperative DNA binding with AP-1 proteins is required for transformation by EWS-Ets fusion proteins. *Mol. Cell. Biol.* **26:** 2467–78

Kinsey M, Smith R, Iyer AK, McCabe ERB & Lessnick SL (2009) EWS/FLI and its downstream target NR0B1 interact directly to modulate transcription and oncogenesis in Ewing's sarcoma. *Cancer Res.* **69:** 9047–9055

Klämbt C (1993) The Drosophila gene pointed encodes two ETS-like proteins which are involved in the development of the midline glial cells. *Development* **117:** 163–176

Kobe B (2001) The leucine-rich repeat as a protein recognition motif. *Curr. Opin. Struct. Biol.* **11:** 725–732

Kondo S & Ueda R (2013) Highly Improved Gene Targeting by Germline-Specific Cas9 Expression in Drosophila. *Genetics* **195:** 715–721

Kulshammer E, Mundorf J, Kilinc M, Frommolt P, Wagle P & Uhlirova M (2015) Interplay among Drosophila transcription factors Ets21c, Fos and Ftz-F1 drives JNK-mediated tumor malignancy. *Dis. Model. Mech.* **8:** 1279–1293

Kulshammer E & Uhlirova M (2013) The actin cross-linker Filamin/Cheerio mediates tumor malignancy downstream of JNK signaling. *J. Cell Sci.* **126:** 927–938

Lacronique V, Boureux A, Valle VD, Poirel H, Quang CT, Mauchauffé M, Berthou C, Lessard M, Berger R, Ghysdael J & Bernard OA (1997) A TEL-JAK2 fusion protein with constitutive kinase activity in human leukemia. *Science* **278:** 1309–12

Lai S-L & Lee T (2006) Genetic mosaic with dual binary transcriptional systems in Drosophila. *Nat. Neurosci.* **9:** 703–709

Lai ZC & Rubin GM (1992) Negative control of photoreceptor development in Drosophila by the product of the yan gene, an ETS domain protein. *Cell* **70:** 609–620

Lee T & Luo L (1999) Mosaic analysis with a repressible cell marker for studies of gene function in neuronal morphogenesis. *Neuron* **22:** 451–61

Leprince D, Gegonne A, Coll J, de Taisne C, Schneeberger A, Lagrou C & Stehelin D (1983) A putative second cell-derived oncogene of the avian leukaemia retrovirus E26. *Nature* **306:** 395–397

Liu H, Su YC, Becker E, Treisman J & Skolnik EY (1999) A Drosophila TNF-receptor-associated factor (TRAF) binds the ste20 kinase Misshapen and activates Jun kinase. *Curr. Biol.* **9:** 101–4

Lu H & Bilder D (2005) Endocytic control of epithelial polarity and proliferation in Drosophila. *Nat. Cell Biol.* **7:** 1232–1239

Maira SM, Wurtz JM & Wasylyk B (1996) Net (ERP/SAP2) one of the Ras-inducible TCFs, has a novel inhibitory domain with resemblance to the helix-loop-helix motif. *EMBO J.* **15:** 5849–65

Marcucci G, Baldus CD, Ruppert AS, Radmacher MD, Mrózek K, Whitman SP, Kolitz JE, Edwards CG, Vardiman JW, Powell BL, Baer MR, Moore JO, Perrotti D, Caligiuri M a., Carroll AJ, Larson R a., De La Chapelle A & Bloomfield CD (2005) Overexpression of the ETS-related gene, ERG, predicts a worse outcome in acute myeloid leukemia with normal karyotype: A Cancer and Leukemia Group B study. *J. Clin. Oncol.* **23:** 9234–9242

Marty F, Rockel-Bauer C, Simigdala N, Brunner E & Basler K (2014) Large-scale imaginal disc sorting: A protocol for ‘omics’-approaches. *Methods* **68:** 260–264

Metzger RJ & Krasnow MA (1999) Genetic Control of Branching Morphogenesis. *Science (80-.).* **284:** 1635

Michel T, Reichhart J, Hoffmann JA & Royet J (2001) Drosophila Toll is activated by Gram-positive bacteria through a circulating peptidoglycan recognition protein. *Nature* **414:** 756–759

Mochmann LH, Bock J, Ortiz-Tánchez J, Schlee C, Bohne A, Neumann K, Hofmann WK, Thiel E & Baldus CD (2011) Genome-wide screen reveals WNT11, a non-canonical WNT gene, as a direct target of ETS transcription factor ERG. *Oncogene* **30:** 2044–56

Moreno E, Yan M & Basler K (2002) Evolution of TNF signaling mechanisms: JNK-dependent apoptosis triggered by Eiger, the Drosophila homolog of the TNF superfamily. *Curr. Biol.* **12:** 1263–8

Neto-Silva RM, Wells BS & Johnston L a (2009) Mechanisms of Growth and Homeostasis in the Drosophila Wing. *Annu. Rev. Cell Dev. Biol.* **25:** 197–220

Noselli S (1998) JNK signaling and morphogenesis in Drosophila. *Trends Genet.* **14:** 33–38

Nunn MF, Seeburg PH, Moscovici C & Duesberg PH (1983) Tripartite structure of the avian erythroblastosis virus E26 transforming gene. *Nature* **306:** 391–395

O'Neill EM, Rebay I, Tjian R & Rubin GM (1994) The activities of two Ets-related transcription factors required for Drosophila eye development are modulated by the Ras/MAPK pathway. *Cell* **78:** 137–147

Pagliarini R a (2003) A Genetic Screen in Drosophila for Metastatic Behavior. *Science (80-.).* **302:** 1227–1231

Papadopoulos P, Ridge S a, Boucher C a, Stocking C & Wiedemann LM (1995) The Novel Activation of ABL by Fusion to an ets-related Gene, TEL The Novel Activation of ABL by Fusion to an ete-related Gene, TEL1. *Cancer Res.***:** 34–38

Parisi F, Stefanatos RK, Strathdee K, Yu Y & Vidal M (2014) Transformed epithelia trigger non-tissue-autonomous tumor suppressor response by adipocytes via activation of Toll and Eiger/TNF signaling. *Cell Rep.* **6:** 855–67

Parks AL, Cook KR, Belvin M, Dompe N a, Fawcett R, Huppert K, Tan LR, Winter CG, Bogart KP, Deal JE, Deal-Herr ME, Grant D, Marcinko M, Miyazaki WY, Robertson S, Shaw KJ, Tabios M, Vysotskaia V, Zhao L, Andrade RS, et al (2004) Systematic generation of high-resolution deletion coverage of the Drosophila melanogaster genome. *Nat. Genet.* **36:** 288–92

Pastor-Pareja JC, Wu M & Xu T (2008) An innate immune response of blood cells to tumors and tissue damage in Drosophila. *Dis. Model. Mech.* **1:** 144–54; discussion 153

Pribyl LJ, Watson DK, McWilliams MJ, Ascione R & Papas TS (1988) The Drosophila ets-2 gene: Molecular structure, chromosomal localization, and developmental expression. *Dev. Biol.* **127:** 45–53

Pribyl LJ, Watson DK, Schulz RA & Papas TS (1991) D-elg, a member of the Drosophila ets gene family: sequence, expression and evolutionary comparison. **6:** 1175–1183

Qiao F & Bowie JU (2005) The Many Faces of SAM. *Sci. Signal.* **2005:** re7–re7

Qiao F, Song H, Kim C a., Sawaya MR, Hunter JB, Gingery M, Rebay I, Courey AJ & Bowie JU (2004) Derepression by depolymerization: Structural insights into the regulation of Yan by Mae. *Cell* **118:** 163–173

Radyuk SN, Michalak K, Klichko VI, Benes J & Orr WC (2010) Peroxiredoxin 5 modulates immune response in Drosophila. *Biochim. Biophys. Acta* **1800:** 1153–63

Read RD (2005) A Drosophila Model of Multiple Endocrine Neoplasia Type 2. *Genetics* **171:** 1057–1081

Rebay I & Rubin GM (1995) Yan functions as a general inhibitor of differentiation and is negatively regulated by activation of the Ras1/MAPK pathway. *Cell* **81:** 857–866

Ren X, Sun J, Housden BE, Hu Y, Roesel C, Lin S, Liu L-P, Yang Z, Mao D, Sun L, Wu Q, Ji J-Y, Xi J, Mohr SE, Xu J, Perrimon N & Ni J-Q (2013) Optimized gene editing technology for Drosophila melanogaster using germ line-specific Cas9. *Proc. Natl. Acad. Sci.* **110:** 19012–19017

Riggi N & Stamenkovic I (2007) The Biology of Ewing sarcoma. *Cancer Lett.* **254:** 1–10

Romana SP, Mauchauffé M, Le Coniat M, Chumakov I, Le Paslier D, Berger R & Bernard O a (1995) The t(12;21) of acute lymphoblastic leukemia results in a tel-AML1 gene fusion. *Blood* **85:** 3662–3670

Rostad K, Mannelqvist M, Halvorsen OJ, Øyan AM, Bø TH, Stordrange L, Olsen S, Haukaas SA, Lin B, Hood L, Jonassen I, Akslen LA & Kalland KH (2007) ERG upregulation and related ETS transcription factors in prostate cancer. *Int. J. Oncol.* **30:** 19–32

Salomon RN & Jackson FR (2008) Tumors of the testis and midgut in aging flies. *Fly (Austin).* **2:** 265–268

Sansores-Garcia L, Bossuyt W, Wada K-I, Yonemura S, Tao C, Sasaki H & Halder G (2011) Modulating F-actin organization induces organ growth by affecting the Hippo pathway. *EMBO J.* **30:** 2325–2335

Schertel C, Albarca M, Rockel-Bauer C, Kelley NW, Bischof J, Hens K, van Nimwegen E, Basler K & Deplancke B (2015) A large-scale, in vivo transcription factor screen defines bivalent chromatin as a key property of regulatory factors mediating Drosophila wing development. *Genome Res.* **25:** 514–523

Schulz R a, The SM, Hogue D a, Galewsky S & Guo Q (1993) Ets oncogene-related gene Elg functions in Drosophila oogenesis. *Proc. Natl. Acad. Sci.* **90:** 10076–10080

Scott GK, Daniel JC, Xiong X, Maki R a., Kabat D & Benz CC (1994) Binding of an ETS-related protein within the DNase I hypersensitive site of the HER2/neu promoter in human breast cancer cells. *J. Biol. Chem.* **269:** 19848–19858

Sebo ZL, Lee HB, Peng Y & Guo Y (2014) A simplified and efficient germline-specific CRISPR/Cas9 system for *Drosophila* genomic engineering. *Fly (Austin).* **8:** 52–57

Seidel JJ (2002) An ERK2 docking site in the Pointed domain distinguishes a subset of ETS transcription factors. *Genes Dev.* **16:** 127–137

Seth A & Watson DK (2005) ETS transcription factors and their emerging roles in human cancer. *Eur. J. Cancer* **41:** 2462–2478

Sharrocks a D (2001) The ETS-domain transcription factor family. *Nat. Rev. Mol. Cell Biol.* **2:** 827–37

Sharrocks AD, Yang SH & Galanis A (2000) Docking domains and substrate-specificity determination for MAP kinases. *Trends Biochem. Sci.* **25:** 448–453

Stec WJ & Zeidler MP (2011) Drosophila SOCS Proteins. *J. Signal Transduct.* **2011:** 894510

Stork T, Sheehan A, Tasdemir-Yilmaz OE & Freeman MR (2014) Neuron-Glia interactions through the heartless fgf receptor signaling pathway mediate morphogenesis of drosophila astrocytes. *Neuron* **83:** 388–403

Sun C, Dobi A, Mohamed A, Li H, Thangapazham RL, Furusato B, Shaheduzzaman S, Tan S-H, Vaidyanathan G, Whitman E, Hawksworth DJ, Chen Y, Nau M, Patel V, Vahey M, Gutkind JS, Sreenath T, Petrovics G, Sesterhenn I a, McLeod DG, et al (2008) TMPRSS2-ERG fusion, a common genomic alteration in prostate cancer activates C-MYC and abrogates prostate epithelial differentiation. *Oncogene* **27:** 5348–53

Sun G & Irvine KD (2011) Regulation of Hippo signaling by Jun kinase signaling during compensatory cell proliferation and regeneration, and in neoplastic tumors. *Dev. Biol.* **350:** 139–51

Swann JB & Smyth MJ (2007) Immune surveillance of tumors. *J. Clin. Invest.* **117:** 1137–1146

Thompson BJ, Mathieu J, Sung H-H, Loeser E, Rørth P & Cohen SM (2005) Tumor Suppressor Properties of the ESCRT-II Complex Component Vps25 in Drosophila. *Dev. Cell* **9:** 711–720

Tomlins S a, Laxman B, Varambally S, Cao X, Yu J, Helgeson BE, Cao Q, Prensner JR, Rubin M a, Shah RB, Mehra R & Chinnaiyan AM (2008) Role of the TMPRSS2-ERG Gene Fusion in Prostate Cancer. *Neoplasia* **10:** 177–IN9

Turner DP, Findlay VJ, Moussa O & Watson DK (2007) Defining ETS transcription regulatory networks and their contribution to breast cancer progression. *J. Cell. Biochem.* **102:** 549–59

Udan RS, Kango-Singh M, Nolo R, Tao C & Halder G (2003) Hippo promotes proliferation arrest and apoptosis in the Salvador/Warts pathway. *Nat. Cell Biol.* **5:** 914–920

Uhlirova M & Bohmann D (2006) JNK- and Fos-regulated Mmp1 expression cooperates with Ras to induce invasive tumors in Drosophila. *EMBO J.* **25:** 5294–304

Vidal M (2005) ZD6474 Suppresses Oncogenic RET Isoforms in a Drosophila Model for Type 2 Multiple Endocrine Neoplasia Syndromes and Papillary Thyroid Carcinoma. *Cancer Res.* **65:** 3538–3541

Wada K-I, Itoga K, Okano T, Yonemura S & Sasaki H (2011) Hippo pathway regulation by cell morphology and stress fibers. *Development* **138:** 3907–3914

Wasylyk C, Bradford AP, Gutierrez-Hartmann A & Wasylyk B (1997) Conserved mechanisms of Ras regulation of evolutionary related transcription factors, Ets1 and Pointed P2. *Oncogene* **14:** 899–913

Willecke M, Toggweiler J & Basler K (2011) Loss of PI3K blocks cell-cycle progression in a Drosophila tumor model. *Oncogene* **30:** 4067–74

Willoughby LF, Schlosser T, Manning S a., Parisot JP, Street IP, Richardson HE, Humbert PO & Brumby a. M (2012) An in vivo large-scale chemical screening platform using Drosophila for anti-cancer drug discovery. *Dis. Model. Mech.* **529:** 521–529

Woods DF & Bryant PJ (1991) The discs-large tumor suppressor gene of Drosophila encodes a guanylate kinase homolog localized at septate junctions. *Cell* **66:** 451–464

Wu C, Chen C, Dai J, Zhang F, Chen Y, Pastor-pareja C, Xue L & Li W (2015) Toll pathway modulates TNF-induced JNK-dependent cell death in Drosophila.

Wu M, Pastor-Pareja JC & Xu T (2010) Interaction between Ras(V12) and scribbled clones induces tumour growth and invasion. *Nature* **463:** 545–8

Yordy JS & Muise-Helmericks RC (2000) Signal transduction and the Ets family of transcription factors. *Oncogene* **19:** 6503–13

Yu Z, Ren M, Wang Z, Zhang B, Rong YS, Jiao R & Gao G (2013) Highly Efficient Genome Modifications Mediated by CRISPR/Cas9 in Drosophila. *Genetics* **195:** 289–291

Zhang Z, Verheyden JM, Hassell J a. & Sun X (2009) FGF-Regulated Etv Genes Are Essential for Repressing Shh Expression in Mouse Limb Buds. *Dev. Cell* **16:** 607–613

Zhu LJ, Christensen RG, Kazemian M, Hull CJ, Enuameh MS, Basciotta MD, Brasefield J a, Zhu C, Asriyan Y, Lapointe DS, Sinha S, Wolfe S a & Brodsky MH (2011) FlyFactorSurvey: a database of Drosophila transcription factor binding specificities determined using the bacterial one-hybrid system. *Nucleic Acids Res.* **39:** D111–D117

Acknowledgements

First and foremost I would like to thank Konrad Basler for his constant scientific support and the freedom to design and carry out this project. His enthusiasm and ingenious scientific thinking was an invaluable help.

Many thanks go to my PhD committee members Ian Frew and Stefan Luschnig for stimulating discussions and valuable suggestions during my committee meetings.

I also thank the members of the Brunner, Lehner and Luschnig groups for discussions, input and ideas during the joint lab meetings.

Further thanks goes to Julian Colombani and Pierre Léopold for letting me assist with the Grindelwald project.

I am grateful to all the past and present members of the Basler group for the scientific support and great atmosphere in the lab, for board game nights, skiweekends, beach volleyball games or after-work beers.

Special thanks go to:

- Maria Willecke for setting up the tumor model and my master thesis project, which built the framework for this thesis. I also very much appreciated her advice and the discussions about our projects.
- George Hausmann for the many discussions about experiments and comments and corrections of scientific texts.
- Claudio Cantu for valuable advice and discussions of experiments.
- Marc Debrunner for embryo injections.
- Eliane Escher for sequencing support and help with cloning.
- Martin Moser for support with qPCRs.

- Claudia Rockel for being such a great desk neighbor, for our little “career chats” and for help with ChIP experiments.
- Alexandra Franz for introducing me to the cell culture and constantly supplying me with cells when needed.
- Dario Zimmerli for the many scientific discussions, for flipping fly stocks when I was on holidays and for our beach volleyball games during summer and snowboarding in winter.

My studies and this thesis would not have been possible without the constant moral and emotional support of my family and friends. It is great to have you around.
Thank you, Stefan, for your love, support, and patience if I sometimes was too absorbed with my work.

Curriculum vitae

NAME	TOGGWEILER
VORNAME	Janine
GEBOREN AM	2. Mai 1985 in Zürich
HEIMATORT	Mönchaltorf
NATIONALITÄT	Schweizerin

SCHULBILDUNG

1998 – 2004	Kantonsschule Züricher Oberland Wetzikon
2004	Matura, Typus A mit Latein

AUSBILDUNG

2005 – 2009	Bachelorstudium in Biologie an der Universität Zürich (CH) Nebenfach Biochemie
2009 – 2011	Masterstudium in Molekular – und Zellbiologie an der Universität Zürich (CH)
2010 – 2011	Masterarbeit in Molekular – und Zellbiologie an der Universität Zürich am Institute of Molecular Life Sciences unter der Leitung von Prof. Dr. Konrad Basler: „ Identification and characterization of genes involved in neoplastic growth in *Drosophila*“
2011	Master of Science in Molecular – and Cellular Biology
2011 – 2016	Doktorandin am Institute of Molecular Life Sciences an der Universität Zürich unter der Leitung von Prof. Dr. Konrad Basler

PUBLIKATIONEN

Willecke, M, **Toggweiler, J.** and Basler, K. (2011) Loss of PI3K blocks cell cycle progression in a *Drosophila* tumor model. **Oncogene**, *30*, 4067-4074.

Andersen, D.S, Colombiani, J, Palmerini, V., Chakrabadhu, K., Boone, E., Röthlisberger, M., **Toggweiler, J**., Basler, K., Mapelli, M., Hueber, AO and Léopold, P. (2015). The *Drosophila* TNF receptor grindelwald couples loss of polarity and neoplastic growth. **Nature** 522, 482-486.